POLITECNICO
MILANO 1863

SCUOLA DI INGEGNERIA INDUSTRIALE
E DELL'INFORMAZIONE

# Electrical Reserve Sizing: A Comparative Analysis of Methodological Approaches

Tesi di Laurea Magistrale in
Energy Engineering - Ingegneria Energetica

Author: **Alessandra Colpani**

Student ID: 260209
Advisor: Prof. Marco Merlo
Co-advisors: Silvia Corigliano, Matteo Spiller
Academic Year: 2025-26

# Abstract

In the last decade, the methods used by Transmission System Operators (TSOs) to size electrical reserves have changed substantially, driven by the growing penetration of renewable generation in the energy mix. The transition has not been uniform: differences in generation mix, regulatory framework, and energy market structure have led synchronous areas to develop their own approaches, and today a wide variety of methods coexist.

Comparing these methods directly is not straightforward, as each has been developed on a specific system. This thesis addresses this gap by developing a Comparative Reserve Sizing Framework. Eight reserve sizing methods, drawn from both TSO practice and academic research, are applied under identical input conditions to a common set of operating scenarios derived from a real power system dataset.

The results show that the choice of method has substantial consequences. In the reference system considered, the spread between the lowest and highest reserve estimates is significant across all reserve categories: primary reserve ranges from approximately 400 MW to 1013 MW, while the secondary plus tertiary reserve spans from approximately 424 MW to over 1700 MW depending on the method. Within probabilistic approaches, methods that retain the dimensioning incident as a binding floor tend to produce higher requirements than those that derive the reserve purely from the imbalance distribution, with the magnitude of this difference depending on the size of the dimensioning incident relative to the system. Methods also differ in how they respond to changing operating conditions: both system load and renewable penetration affect the reserve requirements of probabilistic methods, with load being the dominant driver, while deterministic methods produce fixed requirements regardless of system state.

**Keywords:** electrical reserves, reserve sizing, TSO practice review, methodological comparison, balancing reserves, energy transition

# Abstract in lingua italiana

Nell'ultimo decennio i metodi di dimensionamento delle riserve di bilanciamento hanno subito una trasformazione significativa, trainata dalla crescente penetrazione delle fonti rinnovabili. La transizione non è avvenuta in modo omogeneo: il mix generativo, il quadro normativo e la struttura del mercato elettrico hanno spinto ciascuna area sincrona a sviluppare il proprio approccio, e oggi la pratica operativa varia considerevolmente da un sistema all'altro.

Confrontare questi metodi non è immediato, poiché ognuno è stato sviluppato e validato su un sistema specifico. Questa tesi affronta questa lacuna sviluppando un Comparative Reserve Sizing Framework. Otto metodi di dimensionamento delle riserve, tratti sia dalla pratica operativa dei TSO sia dalla letteratura accademica, vengono applicati in condizioni di ingresso identiche ad un insieme comune di scenari operativi derivati da un sistema elettrico reale.

I risultati mostrano che la scelta del metodo ha conseguenze rilevanti. Nel sistema di riferimento considerato, lo scarto tra le stime più basse e più alte è significativo in tutte le categorie di riserva: la riserva primaria varia da circa 400 MW a 1013 MW, mentre la riserva secondaria più terziaria si estende da circa 424 MW a oltre 1700 MW a seconda del metodo. All'interno degli approcci probabilistici, i metodi che mantengono l'incidente di dimensionamento come vincolo fisso tendono a produrre requisiti più elevati rispetto a quelli che derivano la riserva dalla distribuzione statistica degli sbilanciamenti, con una differenza che dipende dalla dimensione dell'incidente di dimensionamento rispetto alla taglia del sistema. I metodi si differenziano inoltre nella capacità di adattarsi alle condizioni operative: sia il livello di carico sia la penetrazione rinnovabile influenzano i requisiti dei metodi probabilistici, con il carico come driver dominante, mentre i metodi deterministici producono un requisito costante indipendentemente dallo stato del sistema.

**Parole chiave:** riserve elettriche, dimensionamento delle riserve, pratiche TSO, confronto metodologico, riserve di bilanciamento, transizione energetica

# Contents

# List of Symbols

| Variable | Description | Unit |
|---|---|---|
| $a$ | Empirical coefficient in UCTE aFRR formula | MW |
| $A^{\mathrm{VRD}}$ | Semi-amplitude of the VRD sawtooth wave | MW |
| $b$ | Empirical coefficient in UCTE aFRR formula | MW |
| $CF_r$ | Capacity factor of renewable technology $r$ | – |
| $k$ | Number of clusters in $k$-means clustering | – |
| $K_i$ | Frequency bias factor of LFC block $i$ | MW/Hz |
| $DI$ | Dimensioning incident | MW |
| $\Delta f$ | Frequency deviation from nominal | Hz |
| $\Delta P_{tie}$ | Deviation of net interchange from scheduled value | MW |
| $\Delta P_i$ | Active power change of LFC block $i$ | MW |
| $PC_p$ | $p$-th percentile of a distribution | – |
| $P_D$ | Accepted deficit probability | – |
| $L_l$ | Load of node $l$ in current scenario | MW |
| $L_{\max}$ | Maximum load of the control area | MW |
| $P_a$ | Nominal power of asset $a$ | MW |
| $P_{\mathrm{mean},i}$ | Mean produced power of technology $i$ in current scenario | MW |
| $P_{\mathrm{nom}}$ | Nominal power per unit | MW |
| $P_r$ | Installed capacity of renewable technology $r$ | MW |
| $P_{\mathrm{system}}$ | Total system nominal load capacity | MW |
| $p_{\mathrm{tf},a}$ | Trip probability of asset $a$ over horizon $t_{\mathrm{tf}}$ | – |
| $R_{\bar{t}}^{\mathrm{imb}}$ | Total system imbalance signal at time $\bar{t}$ | MW |
| $R_{\bar{t}}^{\Delta\mathrm{imb}}$ | Residual imbalance (imbalance minus 15-min running mean) | MW |
| $R_{\bar{t}}^{\mathrm{trip}}$ | Tripping contribution to imbalance at time $\bar{t}$ | MW |
| $R_{\bar{t}}^{\Delta f}$ | Forecast error contribution to imbalance at time $\bar{t}$ | MW |
| $R_{\bar{t}}^{\mathrm{VRD}}$ | VRD contribution to imbalance at time $\bar{t}$ | MW |

| Variable | Description | Unit |
|---|---|---|
| $\Delta R_t^{\mathrm{imb}}$ | 1-minute change in the Monte Carlo imbalance signal | MW/min |
| $R^{\mathrm{FCR}}$ | FCR requirement (Giglio et al.) | MW |
| $R^{\mathrm{aFRR}}$ | aFRR requirement (Giglio et al.) | MW |
| $R^{\mathrm{mFRR}}$ | mFRR requirement (Giglio et al.) | MW |
| $R^{\mathrm{RR}}$ | RR requirement (Giglio et al.) | MW |
| $R_{\mathrm{FR}}^{\mathrm{FCR}}$ | FCR requirement (France methodology) | MW |
| $R_{\mathrm{FR}}^{\mathrm{aFRR}}$ | aFRR requirement (France methodology) | MW |
| $R_{\mathrm{FR}}^{\mathrm{mFRR}}$ | mFRR requirement (France methodology) | MW |
| $R_{\mathrm{NO}}^{\mathrm{FCR}}$ | FCR requirement (Nordic methodology) | MW |
| $R_{\mathrm{NO}}^{\mathrm{aFRR}}$ | aFRR requirement (Nordic methodology) | MW |
| $R_{\mathrm{NO}}^{\mathrm{mFRR}}$ | mFRR requirement (Nordic methodology) | MW |
| $R_{\mathrm{NO}}^{\mathrm{FRR}}$ | Total FRR requirement (Nordic methodology) | MW |
| $R_{\mathrm{ER}}^{\mathrm{PFR}}$ | Primary frequency response requirement (ERCOT) | MW |
| $R_{\mathrm{ER}}^{\mathrm{RegUp}}$ | Regulation Up requirement (ERCOT) | MW |
| $R_{\mathrm{ER}}^{\mathrm{RegDown}}$ | Regulation Down requirement (ERCOT) | MW |
| $R_{\mathrm{ER}}^{\mathrm{RRS}}$ | Responsive Reserve Service requirement (ERCOT) | MW |
| $R_{\mathrm{ER}}^{\mathrm{ECRS}}$ | ERCOT Contingency Reserve Service requirement | MW |
| $R_{\mathrm{ER}}^{\mathrm{NonSpin}}$ | Non-Spinning Reserve requirement (ERCOT) | MW |
| $R_{\mathrm{UC}}^{\mathrm{FCR}}$ | FCR requirement (UCTE methodology) | MW |
| $R_{\mathrm{UC}}^{\mathrm{aFRR}}$ | aFRR requirement (UCTE methodology) | MW |
| $R_{\mathrm{UC}}^{\mathrm{mFRR}}$ | mFRR requirement (UCTE methodology) | MW |
| $R_{\mathrm{ZI}}^{\mathrm{aFRR}}$ | aFRR requirement (Zima methodology) | MW |
| $R_{\mathrm{ZI}}^{\mathrm{mFRR}}$ | mFRR requirement (Zima methodology) | MW |
| $R_{\mathrm{ZI}}^{\mathrm{RR}}$ | RR requirement (Zima methodology) | MW |
| $R_{\mathrm{NS}}^{\mathrm{aFRR}}$ | aFRR requirement (n-sigma methodology) | MW |
| $R_{\mathrm{NS}}^{\mathrm{mFRR}}$ | mFRR requirement (n-sigma methodology) | MW |
| $R_{\mathrm{NS}}^{\mathrm{RR}}$ | RR requirement (n-sigma methodology) | MW |
| $\Delta R_{\mathrm{NS}}^{\mathrm{wind}}$ | Wind-induced incremental reserve (n-sigma method) | MW |
| $n_{\mathrm{aFRR}}$ | Reliability factor for aFRR sizing (n-sigma method) | – |
| $n_{\mathrm{mFRR}}$ | Reliability factor for mFRR sizing (n-sigma method) | – |
| $n_{\mathrm{RR}}$ | Reliability factor for RR sizing (n-sigma method) | – |
| $n$ | Generic reliability factor | – |

## List of Symbols

| Variable | Description | Unit |
|---|---|---|
| $n_{\text{mod}}$ | Number of units online for a given technology | – |
| $X_{CR}$ | Reserve requirement at deficit probability $P_D$ (Zima method) | MW |
| $\bar{t}$ | Monte Carlo time step | min |
| $t_{\text{OFF}}$ | Trip persistence duration | min |
| $t_{\text{tf}}$ | Activation horizon (secondary: 15 min; tertiary: 60 min) | min |
| $t_{\text{VRD}}$ | Market interval duration | min |
| $u_{a,\bar{t}}$ | Binary trip indicator for asset $a$ at time $\bar{t}$ | – |
| $Z$ | Uniformly distributed random variable for trip sampling | – |
| $VRD$ | Variation of residual demand | MW |
| $\mathbf{x}$ | System state vector | – |
| $\Delta E_{30}$ | Deviation of 1-min average from 30-min moving average | MW |
| $\Delta E_{bo}$ | Open-loop control deviation (RTE methodology) | MW |
| $\Delta E_{\text{ST}}$ | Short-term imbalance band (Nordic methodology) | MW |
| $\lambda_a$ | Annual failure rate of asset $a$ | trips/yr |
| $\mu_a^{\text{trip}}$ | Trip probability of asset $a$ per Monte Carlo time step | – |
| $\sigma_i^{\%}$ | Forecast error coefficient of technology $i$ | % |
| $\sigma_l$ | Normalised forecast error standard deviation of load $l$ | – |
| $\sigma_r$ | Normalised forecast error standard deviation of technology $r$ | – |
| $\sigma_L$ | Load forecast error coefficient | % |
| $\sigma_{\text{load}}$ | Total load standard deviation | MW |
| $\sigma_{\text{lfe}}$ | Load forecast error standard deviation component | MW |
| $\sigma_{\text{lsv}}$ | Spontaneous load variation standard deviation component | MW |
| $\sigma_{\text{net}}$ | Combined net demand forecast error standard deviation | MW |
| $\sigma_{\text{ter}}$ | Combined tertiary horizon standard deviation (Zima method) | MW |
| $\sigma_{\Delta f}$ | Total forecast uncertainty standard deviation | MW |
| $WCSS$ | Within-cluster sum of squares | – |
| $w_t$ | Weight of operating scenario $t$ (hours per year) | h/yr |
| $\Omega_G$ | Set of conventional generating units | – |
| $\Omega_{MC}$ | Monte Carlo time domain | – |
| $\Omega_R$ | Set of renewable generation technologies | – |
| $\Omega_S$ | Set of storage units | – |

# List of Acronyms

| Acronym | Definition |
|---|---|
| ACE | Area Control Error |
| ACER | Agency for the Cooperation of Energy Regulators |
| AEMO | Australian Energy Market Operator |
| aFRR | Automatic Frequency Restoration Reserve |
| AGC | Automatic Generation Control |
| ARERA | Autorità di Regolazione per Energia Reti e Ambiente |
| ATC | Available Transmission Capacity |
| BA | Balancing Authority |
| BAL | Balancing Reliability Standard (NERC) |
| BESS | Battery Energy Storage System |
| BNetzA | Bundesnetzagentur |
| BRP | Balance Responsible Party |
| BSP | Balancing Service Provider |
| CAISO | California Independent System Operator |
| CCGT | Combined Cycle Gas Turbine |
| CE | Continental Europe |
| CHP | Combined Heat and Power |
| CRE | Commission de Régulation de l’Énergie |
| CREG | Commission de Régulation de l’Électricité et du Gaz |
| CREOS | CREOS Luxembourg S.A. |
| DI | Dimensioning Incident |
| DFCM | Dynamic Frequency Control Model |
| DKW | Denmark West (bidding zone) |
| DRP | Disturbance Recovery Period |
| EB GL | Electricity Balancing Guideline |

| Acronym | Definition |
|---|---|
| ECRS | ERCOT Contingency Reserve Service |
| EENS | Expected Energy Not Served |
| ENTSO-E | European Network of Transmission System Operators for Electricity |
| ERCOT | Electric Reliability Council of Texas |
| ERO | Electric Reliability Organization |
| ESS | Essential System Services |
| EWIC | East-West Interconnector |
| FASS | Future Arrangements for System Services |
| FCAS | Frequency Control Ancillary Services |
| FCR | Frequency Containment Reserve |
| FCR-D | Frequency Containment Reserve for Disturbance |
| FCR-N | Frequency Containment Reserve for Normal operation |
| FERC | Federal Energy Regulatory Commission |
| FFR | Fast Frequency Response |
| FRR | Frequency Restoration Reserve |
| GCC | Grid Control Cooperation |
| HVDC | High-Voltage Direct Current |
| IEA | International Energy Agency |
| IE/NI | Ireland and Northern Ireland |
| IFRO | Interconnection Frequency Response Obligation |
| IGCC | Imbalance Netting |
| ISO | Independent System Operator |
| ISO-NE | Independent System Operator New England |
| LFC | Load Frequency Control |
| LFCBOA | LFC Block Operational Agreement |
| LOR | Lack of Reserve (LOR1/LOR2/LOR3: escalating shortage levels) |
| LREG | Regulating Lower (NEM) |
| MARI | Manually Activated Reserves Initiative |
| mFRR | Manual Frequency Restoration Reserve |
| MILP | Mixed Integer Linear Programming |
| MISO | Midcontinent Independent System Operator |
| NEM | National Electricity Market |

## List of Acronyms

| Acronym | Definition |
|---|---|
| NEMDE | NEM Dispatch Engine |
| NER | National Electricity Rules |
| NERC | North American Electric Reliability Corporation |
| NOFB | Normal Operating Frequency Band |
| NYISO | New York Independent System Operator |
| OCGT | Open Cycle Gas Turbine |
| PFR | Primary Frequency Response |
| PICASSO | Platform for International Coordination of Automated Frequency Restoration and Sta |
| PJM | PJM Interconnection |
| POR | Primary Operating Reserve |
| PSP | Pumped Storage Plant |
| RERT | Reliability and Emergency Reserve Trader |
| RES | Renewable Energy Sources |
| RoCoF | Rate of Change of Frequency |
| RR | Replacement Reserve |
| RRD | Regulating Lower Direction (WEM) |
| RREG | Regulating Raise (NEM) |
| RRS | Responsive Reserve Service |
| RSG | Reserve Sharing Group |
| RTE | Réseau de Transport d'Électricité |
| RTO | Regional Transmission Organization |
| SAM | Synchronous Area Monitor |
| SAFA | Synchronous Area Framework Agreement |
| SAOA | Synchronous Area Operational Agreement |
| SCED | Security-Constrained Economic Dispatch |
| SEMO | Single Electricity Market Operator |
| SO GL | System Operation Guideline |
| SOA | System Operation Agreement |
| SONI | System Operator for Northern Ireland |
| SOR | Secondary Operating Reserve |
| SPP | Southwest Power Pool |
| SWIS | South West Interconnected System |

| Acronym | Definition |
|---|---|
| TNG | TransnetBW (German TSO) |
| TOR | Tertiary Operating Reserve |
| TSO | Transmission System Operator |
| TTG | TenneT TSO GmbH |
| UCTE | Union for the Co-ordination of Transmission of Electricity |
| VF FCAS | Very Fast Frequency Control Ancillary Services |
| VOLL | Value of Lost Load |
| VRD | Variation of Residual Demand |
| WECC | Western Electricity Coordinating Council |
| WEM | Wholesale Electricity Market |
| WEMDE | WEM Dispatch Engine |

# Introduction

Maintaining the instantaneous balance between generation and load is a fundamental requirement of power system operation. Any deviation manifests as a frequency excursion which, if not corrected within the timescales defined by system dynamics, can lead to cascading failures and large-scale supply interruptions. Real-time balance is difficult to maintain because both demand and generation are subject to continuous uncertainty: load varies unpredictably, generating units can trip without warning and variable renewable output deviates from forecast. *Balancing reserves*, procured from generators, storage, and flexible demand, are the primary instrument through which transmission system operators (TSO) manage this risk.

Balancing reserves are held as pre-contracted headroom across a range of activation timescales. The classification into *primary*, *secondary*, and *tertiary* reserve, used throughout this thesis, is not the operational terminology of any specific TSO but a cross-system conceptual framework to describe the same hierarchical structure across different nomenclatures. *Primary reserve* provides automatic governor response within seconds, arresting the frequency deviation and stabilising it at a quasi-steady-state level. *Secondary reserve* is activated automatically by *Automatic Generation Control* (AGC) within minutes to restore frequency to its nominal value. *Tertiary reserve* is activated manually by the system operator over a timescale of several minutes to one hour, to relieve secondary reserve and manage sustained imbalances. In practice, different synchronous areas use different product names and activation boundaries; the primary/secondary/tertiary framework is used here because it captures the underlying logic consistently across all systems reviewed.

Reserve sizing is a central planning and operational decision. Insufficient reserve capacity leaves the system exposed to frequency excursions that active resources cannot contain; excess capacity withholds generation from the energy market and raises costs for the system operator. The sizing problem is therefore a risk-cost trade-off, and the methods used to quantify it determine directly the level of security and the procurement costs that result.

Reserve requirements depend on the statistical properties of the system being operated.

System scale, interconnection level, generation mix, and the extent of cross-border sharing mechanisms all affect the distribution of imbalances that reserves must cover. The rapid growth of variable renewable generation has substantially altered these properties, increasing forecast uncertainty and intra-interval variability while reducing synchronous inertia. In response, TSOs and researchers have progressively moved from deterministic sizing rules towards probabilistic and stochastic frameworks that model the underlying uncertainty sources explicitly. This transition has not been uniform: different synchronous areas have adopted different methodological approaches, producing a landscape of considerable diversity in reserve sizing practice.

This diversity raises a question that the literature has not yet addressed directly. Each methodology has been developed and validated on a specific power system, with its own generation mix, scale, and regulatory context. Differences in reported reserve volumes across studies are therefore difficult to interpret: they may reflect genuine methodological differences, or simply the characteristics of the systems to which the methods were applied. Isolating the methodological contribution from the system-specific one requires a controlled comparison, in which multiple methods are applied to the same system under identical conditions. To the best of the author's knowledge, no published study has done this systematically across a representative set of both TSO and academic methods. This thesis addresses that gap.

The work proceeds in two stages. The first surveys the methodological landscape. An initial chapter traces the historical evolution of reserve sizing practice, from the early deterministic rules of the UCTE era to the probabilistic and stochastic frameworks that have emerged in response to growing renewable penetration. In the following chapter the international review documents current TSO practice across five synchronous areas: Continental Europe, Ireland and Northern Ireland, the Nordic area, Australia, and North America. Chapter 3 then reviews methods from the academic literature, covering both probabilistic and stochastic approaches. The second stage applies eight of these methods within a Comparative Reserve Sizing Framework, using a common input dataset derived from a real power system. The framework, the reference system, and the implementation of each method are described in the fourth chapter; the results and discussion follow in the fifth.

# 1 | Historical Development and Methodological Evolution

This chapter traces the methodological evolution of reserve sizing from the deterministic rules that dominated twentieth-century practice to the probabilistic and stochastic frameworks that have emerged in response to growing renewable penetration. It provides the conceptual foundation for the comparative analysis developed in the subsequent chapters.

## 1.1. Deterministic Methods

For most of the twentieth century, reserve sizing relied on deterministic criteria: rule-based requirements derived from worst-case contingencies rather than from a statistical characterisation of system uncertainty. These *deterministic methods* were designed for systems dominated by a small number of large thermal and nuclear units supplying a slowly varying, broadly predictable load.

For primary reserve, the standard approach is the *N-1 rule*: the system must remain secure following the sudden loss of any single element. Applied to generation, this translates into the *largest single infeed criterion*: the primary reserve held must be at least equal to the output of the largest unit online. The risk being covered is discrete and well-defined, making it naturally suited to deterministic treatment. This criterion remains the basis for primary reserve sizing in most modern power systems, including the Continental European synchronous area.

For secondary reserve, deterministic practice relied on fixed percentages of forecast load or installed capacity. The intuition is straightforward: larger systems face larger absolute imbalances, and scaling the requirement with load size provides a simple proportional rule. The Union for the Co-ordination of Transmission of Electricity (UCTE) empirical formula [1] is a concrete example:

$$R = \sqrt{a \cdot L_{\max} + b^2} - b \tag{1.1}$$

where $R$ is the secondary reserve requirement, $L_{\max}$ is the maximum anticipated load of the LFC block, defined as the highest forecast peak load expected during the dimensioning period, and $a$ and $b$ are empirical coefficients calibrated to $a = 10$ MW and $b = 150$ MW for the CE synchronous area [1]. It captures the sub-linear scaling of secondary reserve with system size and was the standard sizing tool across European LFC blocks up until 2017.

Tertiary reserve, activated manually by the system operator to relieve secondary reserve following a disturbance, was similarly sized on deterministic grounds: the requirement was set equal to the secondary reserve volume, ensuring that the secondary reserve margin could be fully restored within the prescribed activation window [1].

The appeal of deterministic methods lies in their transparency and auditability. By construction, they are conservative: a system sized to survive the worst credible event will handle routine disturbances within the available margin. This conservatism was appropriate when system variability was low and well characterised. The limitation of the deterministic solution becomes apparent in secondary reserve sizing. Unlike the contingency risk covered by primary reserve, the imbalances that secondary reserve must cover arise from a continuous stochastic process: the aggregate of forecast errors and unpredictable fluctuations accumulating across the operating period. A fixed percentage of load captures none of this structure. It does not reflect actual system variability, does not respond to changes in the renewable mix, and provides no quantifiable link between the reserve level and the residual risk. As variable renewable penetration has grown, this limitation has become increasingly consequential.

## 1.2. Probabilistic and Stochastic Methods

Probabilistic reserve sizing replaces the worst-case contingency logic of deterministic methods with a statistical characterisation of the imbalances a system actually faces. Rather than requiring that the system survive a defined set of adverse events regardless of their frequency, probabilistic methods set the reserve requirement at the level needed to cover the imbalance distribution with a specified confidence. The reserve is calibrated to a target loss-of-load probability or a percentile of the imbalance distribution, making the residual risk explicit and quantifiable.

The most direct implementation fits a statistical distribution to historical imbalance records and sets the requirement at the target percentile. This captures the actual variability of the system and updates naturally as conditions change. It provides a transparent link between reserve level and risk, which percentage-of-load rules cannot.

## 1| Historical Development and Methodological Evolution

Stochastic methods construct the imbalance distribution analytically rather than from historical observations. They model the individual uncertainty sources explicitly: forecast error distributions for load and variable renewable, forced outage probabilities of generating units, variability of residual demand between intervals. These components are combined, typically through Monte Carlo simulation [2] or probabilistic convolution [3], to estimate the distribution of total system imbalance for a given operating condition. The forward-looking structure means the method can be applied to systems undergoing rapid change or to planning contexts where no operational history exists, by updating input parameters rather than waiting for new data.

Not all transmission system operators (TSO) have moved at the same pace. Some have developed probabilistic frameworks fully integrated into their operational and planning processes; others retain deterministic rules, supplemented at most by simple statistical adjustments. The result is a landscape of methodological diversity, where the choice of method has quantifiable consequences for reserve volumes, procurement costs and the level of security achieved.

This methodological evolution is driven by a structural transformation of the systems themselves. The growth of variable renewable generation, the retirement of large synchronous plants, and the deployment of battery storage and demand response are collectively altering the statistical properties of power system imbalances in ways that neither deterministic rules nor historically calibrated distributions can fully track. Forecast error distributions shift as the renewable mix changes; intra-interval variability increases as the residual demand ramp steepens; synchronous inertia declines as thermal units are displaced. Reserve sizing methods must evolve accordingly.

The direction of that evolution is clear: towards approaches that model uncertainty sources explicitly, adapt to changing system conditions, and quantify the residual risk associated with a given reserve level.

# 2 | International Practice Review

This chapter examines how transmission system operators across different synchronous areas approach the sizing of frequency regulation reserves. The analysis covers five systems: Continental Europe, Ireland and Northern Ireland, the Nordic synchronous area, Australia, and North America, highlighted in Figure 2.1. For each system, the chapter describes the governance framework within which reserve dimensioning takes place, the products that are procured, and the methodologies used to determine the required volumes, with particular attention to the distinction between deterministic, probabilistic, and stochastic approaches introduced in Chapter 1.

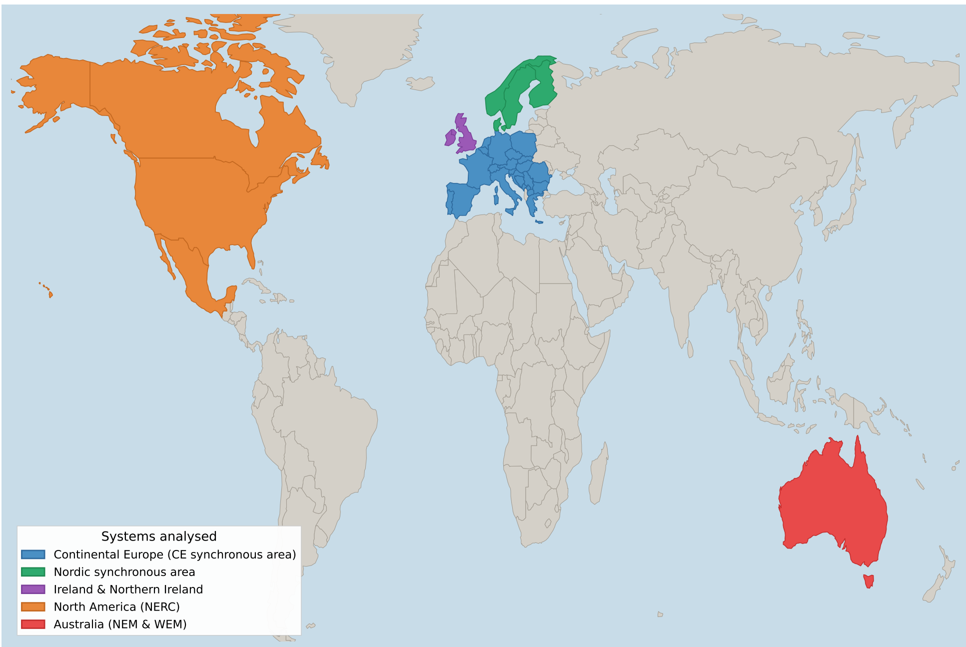


Figure 2.1: Map of power systems analysed in this thesis. Generated by the author

Two concepts recur throughout the chapter and are defined here for clarity. The Load Frequency Control block, or LFC block, is the organisational unit within which frequency restoration reserves are dimensioned and activated. In most European systems, an LFC block corresponds to a single TSO or a group of TSOs that jointly manage frequency balance within a defined area. The Area Control Error (ACE), is the real-time measure of the imbalance between scheduled and actual power flows within an LFC block, which serves as the control signal for automatic frequency restoration.

## 2.1. Continental Europe

European reserve dimensioning operates within a layered governance framework coordinated by the European Network of Transmission System Operators for Electricity (ENTSO-E). At the top level, Commission Regulation (EU) 2017/1485 (the System Operation Guideline, SO GL) [4] sets out mandatory minimum requirements for all TSOs within the EU's synchronous areas. Articles 153 to 161 establish the principles governing the dimensioning of Frequency Containment Reserves (FCR), Frequency Restoration Reserves (FRR), and Replacement Reserves (RR), while leaving TSOs and LFC blocks the flexibility to develop their own methodologies within these boundaries [5, 6]. Within this framework, the three-tier hierarchy introduced before is formalised through four reserve products. FCR corresponds to primary reserve: it activates automatically within seconds to arrest frequency deviations. Automatic Frequency Restoration Reserve (aFRR) and manual Frequency Restoration Reserve (mFRR) together constitute secondary and tertiary reserve respectively: aFRR corrects the frequency error automatically over minutes, while mFRR is activated manually by the TSO to relieve aFRR and restore normal operating conditions. RR provides an additional slower layer where implemented, used to replenish the mFRR band after significant activation events.

At the synchronous area level, the Synchronous Area Framework Agreement (SAFA) for Continental Europe [7] specifies binding methodologies for FCR dimensioning and for the assessment of FCR exhaustion risk. At the LFC block level, each TSO or group of TSOs must agree on a LFC Block Operational Agreement (LFCBOA, the document that formalises the reserve dimensioning rules applicable to that block), in line with Article 157(1) of the SO GL [4]. The European balancing market operates on a separation principle [8]: energy is traded through day-ahead and intraday power exchanges, while balancing reserves are procured by TSOs through dedicated capacity auctions on separate timescales, typically yearly, monthly, weekly, and daily. Generators and other flexible resources participate in these auctions as Balancing Service Providers (BSPs), offering their capacity to the TSO in exchange for availability payments. This procurement model means that reserve sizing and reserve procurement are two distinct steps: the TSO first determines how much reserve it needs and then contracts that volume through the market. This multi-level structure means that common principles coexist with considerable national diversity in methodology.

The Continental Europe (CE) synchronous area is the largest interconnected power system in the world, covering more than 25 countries. The four reserve products operate on distinct timescales [4]. FCR must be fully deployed within 30 seconds, reaching its maximum capacity at a quasi-steady-state deviation of ±200 mHz. aFRR has a full activation time of 5 minutes. mFRR is activated on a merit-order basis (selected in order of increasing cost) and must reach full activation within 12.5 minutes. RR, where implemented, has a full activation time of up to 30 minutes. A visual representation is shown in Figure 2.2.

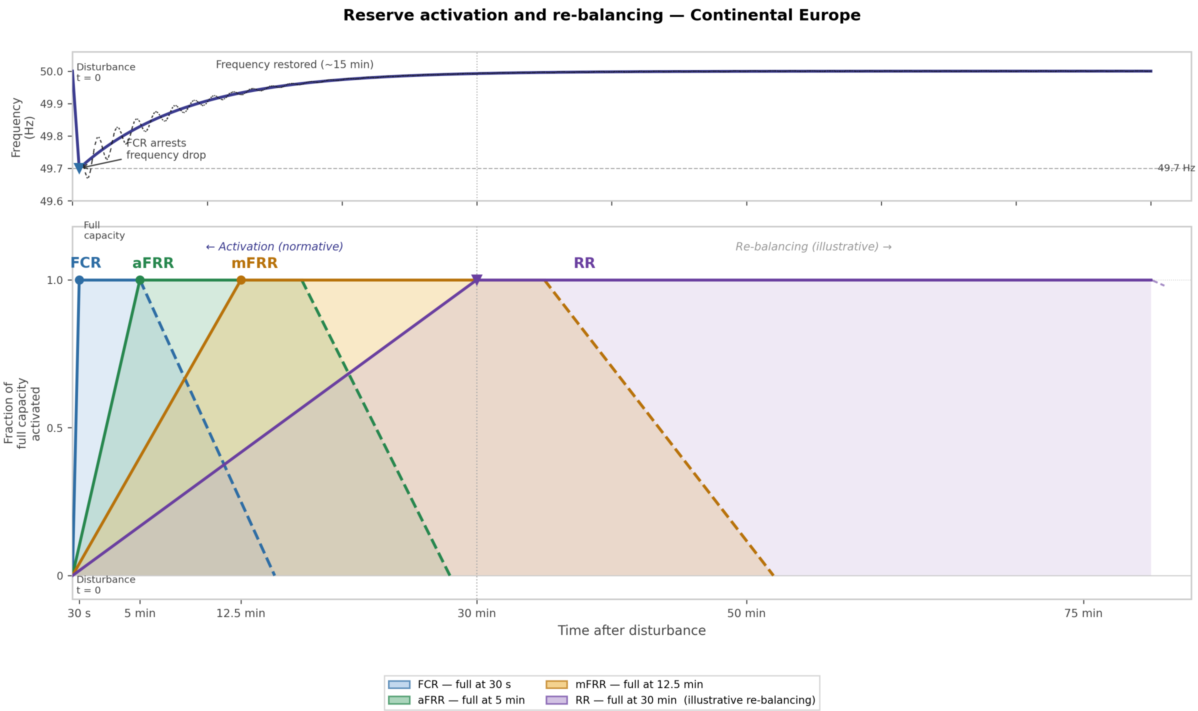


Figure 2.2: Reserve activation and re-balancing timeline for the Continental Europe synchronous area.

The upper panel shows the indicative frequency response following a generation loss; the lower panel shows the sequential activation and release of FCR, aFRR, mFRR, and RR. Solid lines indicate normative activation timeframes defined in Articles 154, 157, 158, and 160 of Commission Regulation (EU) 2017/1485 (SO GL) [4]; dashed lines indicate illustrative re-balancing profiles.

## FCR Dimensioning

The dimensioning of FCR in the CE area is governed by a probabilistic methodology approved by all National Regulatory Authorities on 15 January 2025 [9]. Before the new framework came into force, FCR sizing was based on a fixed deterministic rule: the total synchronous area obligation was set at 3,000 MW, symmetric in both the upward and downward direction. This value corresponds to an N-2 reference incident, defined as the simultaneous loss of the two largest generation units in the CE area, which are nuclear power plants [1, 7].

The new framework assesses the risk of FCR exhaustion, which is the risk that the total FCR capacity available is insufficient to arrest a frequency deviation caused by a large generation trip, meaning that frequency continues to fall beyond the quasi-steady-state threshold of ±200 mHz despite full FCR deployment. The assessment is done by modelling both the probability of large generation trips and the background imbalances already loading the FCR at any given moment. The methodology consists of three steps: (1) a Monte Carlo simulation derives the probability density function of FCR required due to generation tripping, run over at least $10^8$ minutes; (2) the background FCR already deployed due to continuous frequency deviations is modelled from historical data; and (3) the two distributions are convolved to obtain the total required FCR. The regulatory target is that the risk of FCR exhaustion does not exceed one event per 20 years.

The individual FCR obligation for each TSO is distributed using the K-factor, a parameter expressing how much active power the LFC block's generators collectively inject or withdraw for each Hz of frequency deviation. It is defined as:

$$K_i = \frac{\Delta P_i}{\Delta f} \tag{2.1}$$

where $\Delta P_i$ is the active power variation of LFC block $i$ and $\Delta f$ is the corresponding frequency deviation, expressed in MW/Hz. A higher K-factor means the block provides a larger share of the synchronous area's primary response per unit of deviation, and therefore carries a proportionally larger FCR obligation [7]. Table 2.1 reports the FCR obligations for the five CE LFC blocks analysed in this chapter, illustrating how the total 3,000 MW synchronous area requirement is distributed across TSOs of different sizes.

Table 2.1: FCR obligations for the five CE LFC blocks analysed in this chapter, 2023. Symmetric obligations. German block comprises TNG, TTG, AMP, 50HZT, EN, and CREOS. FCR values for other CE LFC blocks are available in individual national balancing reports. Sources: [10, 11] (BE); [12] (DE); [13] (NL); [14] (IT); [15] (FR).

| TSO | Country | FCR (MW) | Share of CE total (%) |
|---|---|---|---|
| German block | DE/DK-W/LU | 570 | 19.0 |
| RTE | FR | 514 | 17.1 |
| TERNA | IT | ~300 | ~10.0 |
| TenneT NL | NL | 111 | 3.7 |
| Elia | BE | 88 | 2.9 |
| **Total CE** | | **3,000** | **100** |

## FRR Dimensioning: General Framework

Unlike FCR, FRR dimensioning takes place at the LFC block level, meaning each TSO must individually determine its own FRR requirement. Article 157(2) of the SO GL [4] requires that FRR capacity cover the dimensioning incident (defined as the largest single credible loss of generation or load in the LFC block) and at least the 99th percentile of historical positive and negative LFC block imbalances [16].

Before the current statistical approach was adopted, the standard tool for sizing secondary control reserves across Europe was the UCTE empirical formula [1] introduced in Chapter 1 (Equation (1.1), repeated here for reference):

$$R = \sqrt{a \cdot L_{\max} + b^2} - b$$

Its fundamental limitation is that peak load is the only input: it is blind to variable renewable generation, forecast errors, and forced outage risk, all of which have grown substantially since the formula was calibrated on the generation mix of the early 2000s.

The statistical approach now recommended in the SAFA [17] addresses this directly. The ACE (Area Control Error, Equation (2.2)) signal is the real-time measure of the power imbalance within an LFC block:

$$ACE = \Delta P_{tie} - B \cdot \Delta f \tag{2.2}$$

where $\Delta P_{tie}$ is the deviation of net interchange from its scheduled value, $\Delta f$ is the frequency deviation from nominal, and $B$ is the frequency bias factor of the LFC block (expressed in MW/Hz), representing the sensitivity of the block's net power balance to frequency deviations. ACEol (Area Control Error open loop, Equation (2.3)) is then reconstructed by subtracting the measured reserve activations:

$$ACEol = ACE - \Delta P_{aFRR} - \Delta P_{mFRR} \tag{2.3}$$

where $\Delta P_{aFRR}$ and $\Delta P_{mFRR}$ are the power contributions from aFRR and mFRR activations respectively. The FRR requirement is set at the 99th percentile of the historical ACEol distribution, implicitly capturing all sources of imbalance without requiring these components to be modelled individually.

The following sections examine five CE LFC blocks: Elia (Belgium), the German block, TenneT NL (Netherlands), Terna (Italy), and RTE (France). Since FRR dimensioning takes place at the LFC block level, the methodology and resulting volumes differ across blocks; examining these five cases illustrates the range of approaches adopted within the common SO GL framework.

### 2.1.1. Belgium

Belgium's transmission system is operated by Elia Transmission Belgium SA/NV (Elia), which forms a single LFC block within the Continental Europe synchronous area. Elia operates under the supervision of CREG (Commission de Régulation de l'Électricité et du Gaz), the Belgian energy regulatory authority, and has developed one of the most methodologically advanced reserve dimensioning frameworks in Europe [18]. Table 2.2 reports the FCR and FRR dimensioning values for 2022–2023.

Table 2.2: FCR and FRR dimensioning requirements for Belgium (Elia), 2022–2023. FRR quantities refer to annual average. RES (%): wind and solar electricity generation as share of total electricity generation [MWh/MWh]. Source: [10, 11, 19, 20].

| | **Peak load (MW)** | **RES (%)** | **FCR (MW)** | **aFRR$^+$ (MW)** | **aFRR$^-$ (MW)** | **mFRR$^+$ (MW)** | **mFRR$^-$ (MW)** |
|---|---|---|---|---|---|---|---|
| 2022 | 13 094 | 21.6 | 93 | 131 | 131 | 910 | 700 |
| 2023 | 12 597 | 28.8 | 88 | 117 | 117 | 924 | 866 |

### FCR Dimensioning

Elia applies the CE-level methodology established by the SAFA. Elia's FCR obligation was 86 MW in 2022 and 88 MW in 2023, symmetric in both directions. FCR is procured entirely through the joint FCR Cooperation platform, a voluntary multi-TSO mechanism established in 2015.

### FRR Dimensioning

Elia's FRR dimensioning methodology is dynamic, probabilistic, and applied on a day-ahead basis with quarter-hourly resolution. The methodology was first approved by CREG in December 2019 (decision (B)2025) [11] and last revised in February 2024 (decision (B)2748) [20].

The total FRR capacity requirement for a given quarter-hour is the maximum of three independently computed values. The first is a dynamic probabilistic convolution of prediction risk and forced outage risk, whose 99th percentile defines the minimum total FRR requirement. The second is a deterministic criterion corresponding to the dimensioning incident. The third is a static floor based on the 99th percentile of historical LFC block imbalances, computed directly from the observed ACEol time series without decomposing the individual uncertainty sources. This criterion acts as a backstop ensuring that the dynamic probabilistic calculation does not produce a requirement below what historical experience would suggest.

The aFRR dimensioning uses oracle-based mFRR, a simulation methodology that assumes perfect-foresight mFRR dispatch to isolate the residual aFRR requirement. The logic is as follows: to determine how much aFRR is genuinely needed, one must first remove from the imbalance signal the component that would be covered by mFRR activation. Since mFRR dispatch is not known in advance, the oracle approach simulates an idealised scenario in which mFRR responds perfectly and instantaneously, representing a theoretical upper bound on what mFRR can achieve. The oracle assumption abstracts from activation timescales by working at 5-minute resolution, aligned with the full activation time of aFRR. The conservative assumption of perfect mFRR dispatch is justified by the use of a 99th percentile reliability threshold, ensuring that the underestimation of aFRR needs implicit in the oracle is compensated by the stringency of the statistical criterion [21]. The residual imbalance that remains after this perfect mFRR dispatch is, by construction, the portion that only aFRR can cover, and its statistical distribution defines the minimum aFRR requirement. The method recalculates the requirement for each quarter-hour using features correlated with expected imbalance risk: wind infeed, solar generation, system load, and day type. The fully dynamic oracle-based methodology was approved in 2023 [21] and entered into operation in October 2024 [20]. The mFRR capacity is determined residually as the difference between total FRR and aFRR for each quarter-hour.

### 2.1.2. Germany

Germany operates the largest LFC block in Continental Europe, encompassing four TSOs: TransnetBW (TNG), TenneT TSO GmbH (TTG), Amprion (AMP), and 50Hertz Transmission (50HZT), as well as Energinet (EN) for the synchronously connected part of western Denmark (DKW area) and CREOS in Luxembourg.

The German balancing framework is jointly managed through the Grid Control Cooperation (GCC, a joint operational framework that allows the four German TSOs to manage frequency balance as a single virtual LFC area). The result is a single reserve capacity requirement for the whole of Germany, procured jointly through regelleistung.net (the shared internet platform through which all German balancing capacity is tendered and contracted). The primary regulatory authority is the Bundesnetzagentur (BNetzA). Table 2.3 reports the FCR and FRR dimensioning values for the German LFC block for years 2022–2023.

Table 2.3: FCR and FRR dimensioning requirements for Germany (DE area, DKW excluded), 2022–2023.
Reserve values are annual averages. RES (%): wind and solar electricity generation as share of total electricity generation [MWh/MWh]. Source: [12].

| | **Peak load (MW)** | **RES (%)** | **FCR (MW)** | **$\mathbf{aFRR^+}$ (MW)** | **$\mathbf{aFRR^-}$ (MW)** | **$\mathbf{mFRR^+}$ (MW)** | **$\mathbf{mFRR^-}$ (MW)** |
|---|---|---|---|---|---|---|---|
| 2022 | 78 681 | 37.0 | 555 | 1 995 | 1 901 | 921 | 432 |
| 2023 | 73 587 | 44.3 | 570 | 1 922 | 1 842 | 681 | 372 |

#### FCR Dimensioning

Germany's share of the CE total FCR requirement is recalculated annually using the K-factor mechanism described in Section 2.1. Germany tendered 555 MW in 2022, 570 MW in 2023, and 564 MW in 2024.

### FRR Dimensioning

In December 2019, the German TSOs replaced their static probabilistic approach with a dynamic dimensioning process [22, 23] that determines the reserve capacity requirement separately for each rolling 4-hour product time slice, updated daily. Germany was the first major CE LFC block to make this transition. The starting point is a historical imbalance dataset covering up to five years, with data points weighted by their relevance to the specific 4-hour block being dimensioned using seasonal characteristics: time of day, date and month, day of week, and type of day. The FRR capacity requirement is set at the 99th percentile of positive and negative imbalances.

Between 2022 and 2023, all four products show a declining trend, with the positive direction falling more sharply (−11%) than the negative (−5%). The main driver was a structural break in mid-2022: when the anomalous imbalances of June 2019 dropped out of the five-year reference window, dimensioned volumes fell immediately, illustrating how sensitive the dynamic methodology is to the composition of its historical dataset.

### Observations

The German dynamic dimensioning methodology is characterised by its temporal granularity and transparency requirements. Looking ahead, the planned incorporation of meteorological variables, particularly wind and solar forecast errors, into the dimensioning logic represents a pending development of methodological interest.

## 2.1.3. Netherlands

The Netherlands is operated by TenneT TSO B.V. (TenneT NL), which forms a single LFC block within the Continental Europe synchronous area. The balancing market is organised on a self-dispatching basis, in which Balance Responsible Parties (BRPs, market participants financially responsible for keeping their generation and consumption portfolios in balance) are financially incentivised to keep their portfolios in balance. Table 2.4 reports the FCR and FRR dimensioning values for TenneT NL for 2023.

Table 2.4: FCR and FRR dimensioning requirements for the Netherlands (TenneT NL), 2023.
FRR quantities refer to annual average. RES (%): wind and solar electricity generation as share of total electricity generation [MWh/MWh]. Source: [13]; [4].

| | Peak load (MW) | RES (%) | FCR (MW) | $aFRR^+$ (MW) | $aFRR^-$ (MW) | $mFRR^+$ (MW) | $mFRR^-$ (MW) |
|---|---|---|---|---|---|---|---|
| 2023 | 20 060 | 41.7 | 111 | 380 | 400 | 880 | 880 |

### FCR Dimensioning

TenneT NL's FCR obligation for 2023 was approximately 111 MW, corresponding to a frequency bias factor of roughly 3.7% of the CE total.

### FRR Dimensioning

TenneT NL applies a three-track dimensioning approach combining deterministic, stochastic, and probabilistic criteria. The minimum FRR requirement in each direction is the maximum across these three thresholds. The remaining FRR volume was allocated between aFRR and mFRR by economic optimisation among pre-qualified BSPs (Balancing Service Providers, entities that offer balancing capacity to the TSO). For 2023, contracted volumes were approximately 380 MW upward aFRR, 400 MW downward aFRR, and 880 MW for both upward and downward mFRR.

### Observations

From September 2025, TenneT NL replaced the static semi-annual framework with a daily day-ahead dimensioning process (DyDi) [24] covering all FRR products, representing a recent evolution towards higher temporal granularity among the CE blocks reviewed in this chapter.

## 2.1.4. Italy

Italy's transmission system is operated by Terna S.p.A. (Terna). The Italian regulatory framework is overseen by ARERA (Autorità di Regolazione per Energia Reti e Ambiente). The Italian balancing framework is built on a central dispatching model, a system in which the TSO has direct control over the unit commitment and dispatch of all qualifying generation and demand facilities rather than relying on market-based self-dispatch.

A structural feature of the Italian system is the presence of multiple electrically separate zones connected by High-Voltage Direct Current (HVDC) links [25, 26]. Three zonal aggregations are defined: "Continente", "Sicilia", and "Sardegna". Reserves are dimensioned independently for each aggregation and for each individual bidding zone. Table 2.5 reports the FCR and FRR dimensioning values for Terna in 2022–2023.

Table 2.5: FCR and FRR dimensioning requirements for Italy (Terna), 2022–2023. Values represent indicative ranges across operating periods and zonal aggregations. RES (%): wind and solar electricity generation as share of total electricity generation [MWh/MWh]. Source: [14]; [27].

| | **Peak load (MW)** | **RES (%)** | **FCR (MW)** | **aFRR$^+$ (MW)** | **aFRR$^-$ (MW)** | **FRR$^+$ (MW)** | **FRR$^-$ (MW)** |
|---|---|---|---|---|---|---|---|
| 2022–23 | 52 630 | 17–20 | 280–320 | 325–850 | 325–850 | 950–1 240 | 425–760 |

### FCR Dimensioning

FCR obligations for the Terna LFC block are determined by the CE-wide SAFA framework. Based on Italy's share of CE net generation, the indicative value is in the range of 280–320 MW.

### FRR Dimensioning

The aFRR requirement is computed for each hourly period by taking the maximum of a minimum baseline derived from load forecasts and the output of a statistical forecasting tool using load, wind, and solar generation forecasts [28].The average values for a weekday are reported in Figure 2.3. The mFRR requirement follows a deterministic approach anchored to the dimensioning incident and the corresponding upward FRR profile, which is the sum of aFRR and mFRR, is shown in Figure 2.4.

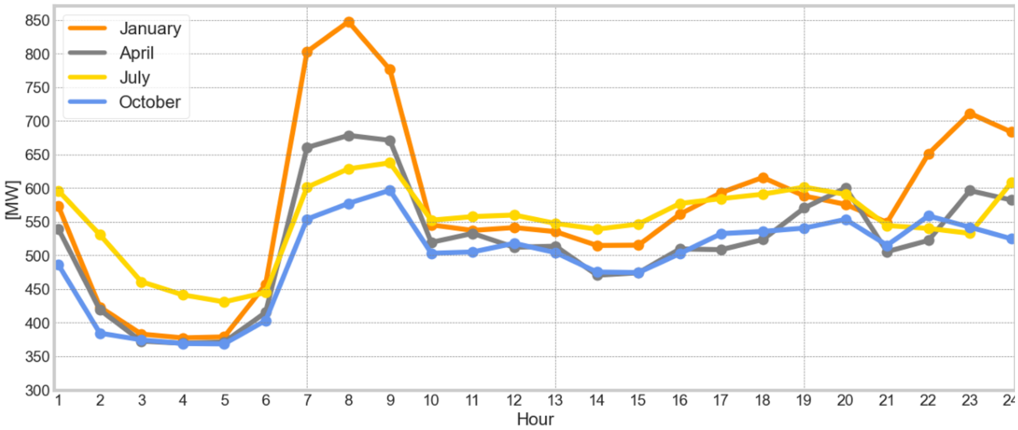


Figure 2.3: Average hourly aFRR requirement for Italy (Terna), by season, weekdays, December 2021–December 2023.
Source: Report Balancing Terna 2022–2023 [14].

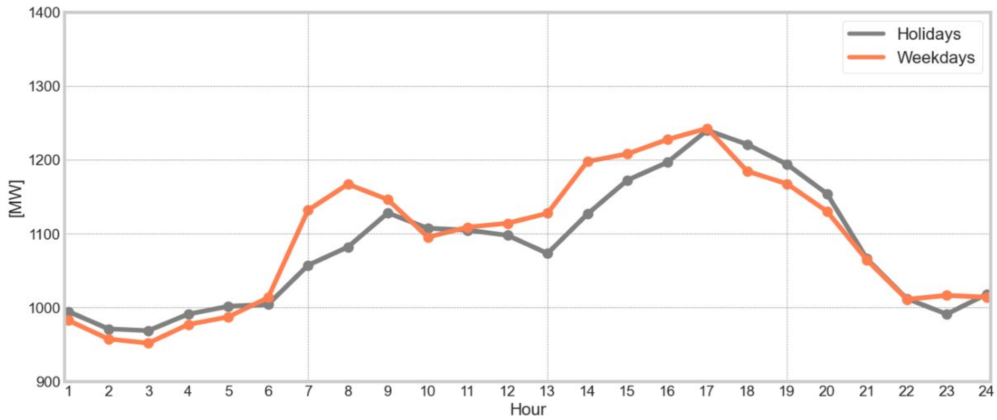


Figure 2.4: Average hourly upward FRR requirement for Italy (Terna), weekdays vs. holidays, December 2021–December 2023.
Source: Report Balancing Terna 2022–2023 [14].

### Observations

A distinctive institutional feature of the Italian framework is the explicit waiver of FRR sharing agreements in the LFCBOA (Article 3.15) [27]: Italy does not reduce its FRR requirement through cross-border sharing. This provision is expected to be revised in a future LFCBOA update.

### 2.1.5. France

France's transmission system is operated by Réseau de Transport d'Électricité (RTE). The French regulatory framework for balancing is overseen by the Commission de Régulation de l'Énergie (CRE). Table 2.6 reports the FCR and FRR dimensioning values for RTE for 2022–2023.

Table 2.6: FCR and FRR dimensioning requirements for France (RTE), 2022–2023. FRR quantities refer to annual average contracted volumes. $mFRR^{+}$ combines annual tender (750 MW) and daily tender (750 MW). Downward mFRR progressively introduced after RT17; no consolidated MW figure for 2023. RES (%): wind and solar electricity generation as share of total electricity generation [MWh/MWh]. Source: [29]; [30].

| | **Peak load (MW)** | **RES (%)** | **FCR (MW)** | **$aFRR^{+}$ (MW)** | **$aFRR^{-}$ (MW)** | **$mFRR^{+}$ (MW)** | **$mFRR^{-}$ (MW)** |
|---|---|---|---|---|---|---|---|
| 2022 | 82 521 | 12.6 | 489 | 720 | 720 | 1 500 | — |
| 2023 | 81 747 | 14.6 | 514 | 698 | 698 | 1 500 | — |

#### FCR Dimensioning

RTE's FCR obligation was 489 MW in 2022 and 514 MW in 2023. FCR is procured through the joint FCR Cooperation platform.

#### FRR Dimensioning

The RTE LFCBOA [15, 29] defines two sets of dimensioning rules separated by a regulatory transition milestone called "RT19". Under the current pre-RT19 regime, the total FRR requirement is set deterministically at the dimensioning incident in both directions: 1,500 MW upward (loss of the largest nuclear unit). The aFRR requirement is set subject to a statutory floor of 500 MW in both directions, the highest explicit floor among the CE LFC blocks reviewed in this chapter.

Under the post-RT19 regime, the total FRR requirement will transition to the maximum of the dimensioning incident and the 1st or 99th percentile of the real-time system imbalance, computed at 1-minute resolution, net of both domestic balancing mechanism activations and mFRR balancing energy exchanged through the *Manually Activated Reserves Initiative* (MARI). No implementation date for RT19 has been published at the time of writing.

### Observations

The RTE LFCBOA provides explicit documentation of the planned transition from a purely deterministic FRR framework to a hybrid statistical approach, including the full specification of the post-RT19 regime. The minimum aFRR floor of 500 MW is the highest explicit statutory floor observed among the CE LFC blocks reviewed in this chapter.

## 2.2. Ireland and Northern Ireland

Ireland and Northern Ireland constitute a distinct synchronous area (the IE/NI synchronous area), separate from Continental Europe. The two TSOs responsible for this area are EirGrid (Republic of Ireland) and SONI Ltd. (Northern Ireland). The governance framework is the LFC Block Operational Agreement for Ireland and Northern Ireland (LFCBOA), with the current version (2.1) approved in December 2024 [31].

The IE/NI synchronous area has several characteristics that set it apart from CE. It is a relatively small, islanded system without any AC interconnection to a continental grid; its only interconnections are three HVDC links: EWIC, Moyle, and Greenlink, connecting it to Great Britain. The system operates under central dispatch (a model in which the TSOs directly control the output of all generation above a 4 MW threshold). The share of variable renewable energy, particularly wind, is among the highest in Europe. Notably, the IE/NI system does not currently operate an aFRR process, meaning all FRR is manual, so activated through dispatch instructions rather than a closed-loop AGC signal (mFRR).

The IE/NI framework defines five sequential reserve products: Primary Operating Reserve (POR), Secondary Operating Reserve (SOR), Tertiary Operating Reserve 1 and 2 (TOR1, TOR2), and Replacement Reserve Raise and Lower (RRS/RRD). Each product targets a distinct phase of the frequency recovery process, from the initial arrest of the deviation through to full re-balancing. The defined activation timescales for each product are reported in Figure 2.5 [31].

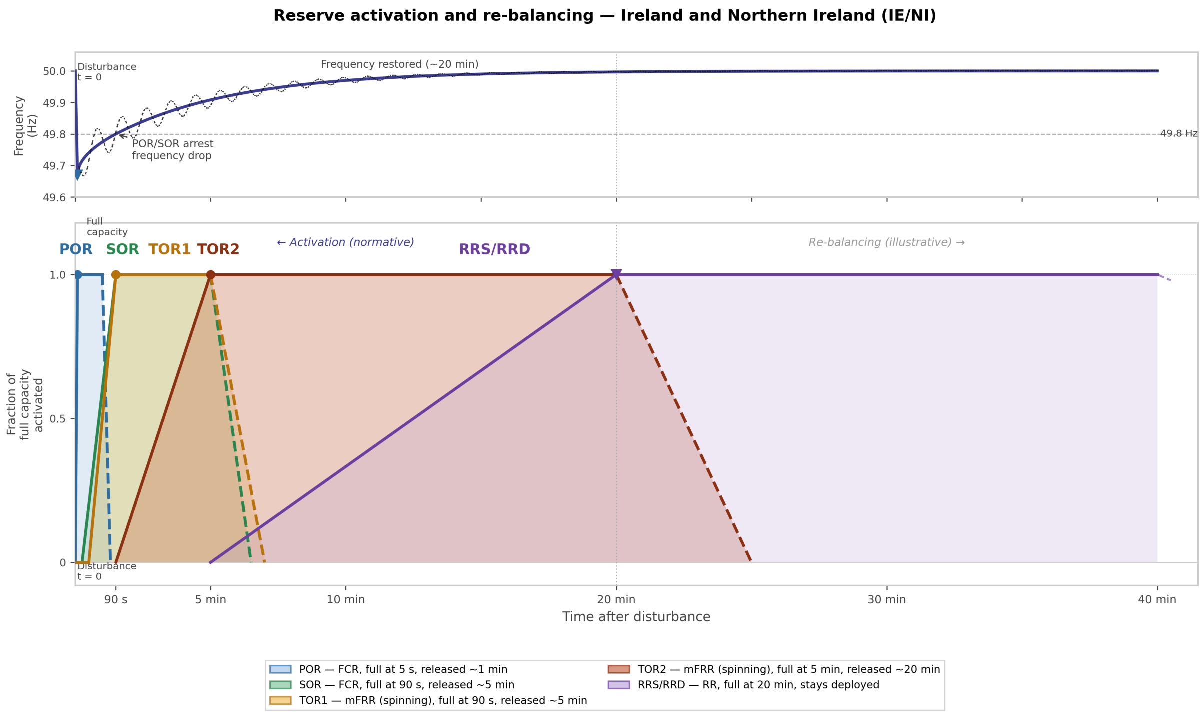


Figure 2.5: Reserve activation and re-balancing timeline for the Ireland and Northern Ireland synchronous area.
The upper panel shows the indicative frequency response following a generation loss; the lower panel shows the sequential activation and release of POR, SOR, TOR1, TOR2, and RRS/RRD. Solid lines indicate normative activation timeframes defined in the LFC Block Operational Agreement for Ireland and Northern Ireland (LFCBOA, version 2.1, December 2024) [31]; dashed lines indicate illustrative re-balancing profiles.

## FCR Dimensioning

The IE/NI synchronous area applies its own FCR framework, defined in the Synchronous Area Operational Agreement (SAOA) [32]. FCR maps to the concepts of Primary Operating Reserve (POR) and Secondary Operating Reserve (SOR) as defined in the EirGrid and SONI Grid Codes. The required volume is set at a minimum of 75% of the largest single infeed or outfeed, and may be increased beyond this threshold where real-time transient security analysis indicates that a larger volume is needed to prevent the frequency from falling outside the permissible range following a loss event [33].

The dimensioning process relies on a dynamic stability assessment tool that runs continuously in real time, computing the expected frequency excursion following the most severe credible loss of infeed or outfeed from live system data. If the tool indicates that frequency quality parameters would be violated, the TSOs may either increase the FCR requirement or reduce the effective size of the reference incident used for scheduling purposes. The inputs to this assessment include the magnitude of the reference incident, the frequency response of load, the required level of system inertia derived from stability studies calibrated against historical events, and the predicted frequency trajectory following the loss [32]. To further constrain frequency dynamics, the system is operated with a minimum all-island inertia floor of 23,000 MWs and a Rate of Change of Frequency (RoCoF) limit of 1 Hz/s, the latter having been raised from the previous standard of 0.5 Hz/s following a multi-year programme concluded in 2022 [34].

### FRR Dimensioning

The FRR dimensioning approach for IE/NI is fundamentally deterministic, based entirely on the dimensioning incident. EirGrid and SONI jointly set the FRR reserve capacity at 100% of the dimensioning incident in both positive and negative directions [35]. Reserve requirements are initially scheduled on a day-ahead basis for each half-hour interval and are updated intra-day as more accurate demand, renewable generation, and interconnector schedule information becomes available. The resulting all-island and jurisdictional requirements are published in the *Operational Constraints Update*, maintained by EirGrid and SONI on the Single Electricity Market Operator (SEMO) website.

Geographical constraints apply to reserve holding: EirGrid may hold up to 155 MW during daytime (07:00–24:00) and 150 MW during night-time (24:00–07:00), while SONI may hold up to 50 MW in both periods. The slight asymmetry between daytime and night-time values reflects the capacity limits imposed by the North-South interconnector between the Irish and Northern Irish transmission systems.

In parallel with the established FRR framework, EirGrid and SONI are progressing a structural reform through the Future Arrangements for System Services (FASS) programme [36, 37], aiming to move reserve requirement calculation closer to real time.

### Observations

The IE/NI framework is the only one reviewed in this chapter that operates without aFRR: unlike the CE blocks, frequency restoration relies entirely on manual FRR activated through dispatch instructions. The FCR dimensioning process incorporates a dynamic stability assessment tool that adjusts the POR/SOR requirement continuously in real time, introducing an element of adaptivity absent from a purely static deterministic approach. The operational constraints on system inertia and RoCoF, namely a minimum inertia floor of 23,000 MWs and a RoCoF limit of 1 Hz/s, function as binding parameters that directly influence FCR sizing, reflecting the system's exposure to rapid frequency dynamics as a small, islanded network with high renewable penetration.

## 2.3. Nordic Synchronous Area

The Nordic synchronous area comprises the transmission systems of Norway, Sweden (including the Åland subsystem), Finland, and eastern Denmark (bidding zone DK2). The four TSOs, Statnett SF (Norway), Svenska kraftnät (Sweden), Fingrid Oyj (Finland), and Energinet (Denmark, DK2), jointly operate the Nordic LFC block. Svenska kraftnät holds the role of Synchronous Area Monitor (SAM), while Statnett acts as LFC Block Monitor.

The Nordic reserve framework shares a similar layered structure to the CE architecture, but differs in two key aspects: rather than a single FCR product, the system deploys three distinct primary reserve products (FCR-N for normal operating conditions, FCR-D for disturbances, and FFR for low-inertia conditions), and the FRR dimensioning methodology embeds the Available Transmission Capacity (ATC, the remaining transfer capacity on an interconnector after accounting for already scheduled flows) as a binding constraint at every stage of the sizing calculation. All products have defined activation timescales, illustrated in Figure 2.6, while in Table 2.7 are reported the dimensioning values for 2025.

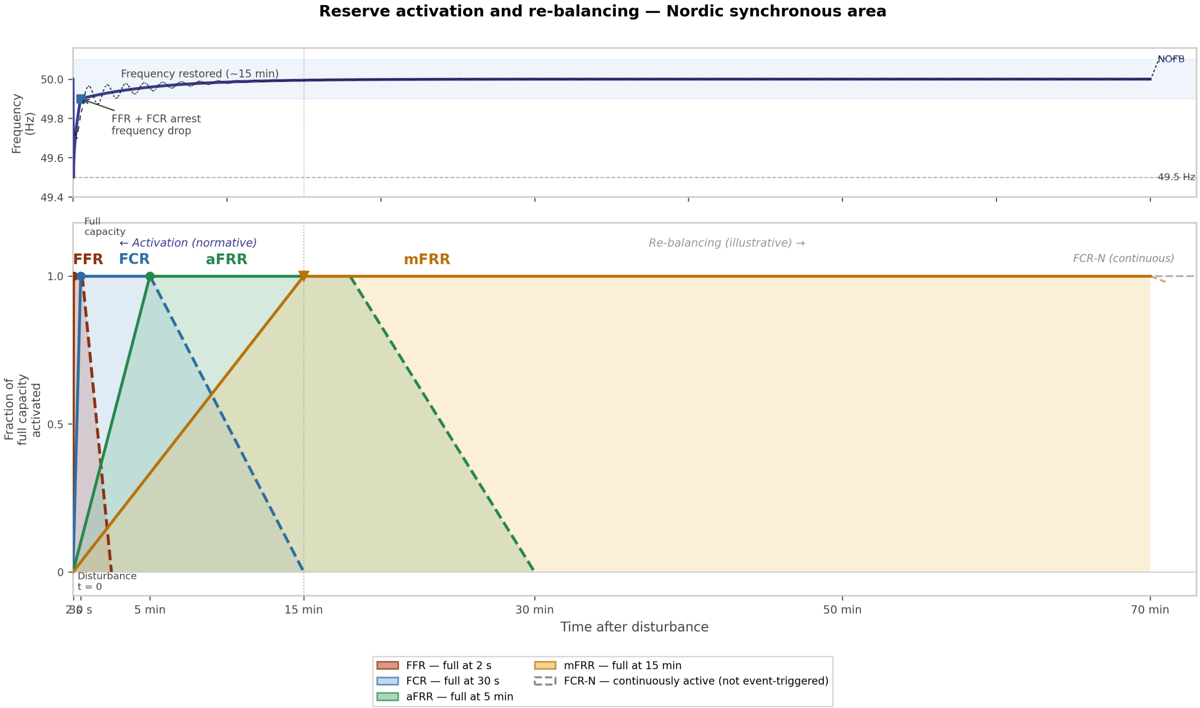


Figure 2.6: Reserve activation and re-balancing timeline for the Nordic synchronous area. The upper panel shows the indicative frequency response including the Normal Operating Frequency Band (NOFB); the lower panel shows FFR, FCR-D, aFRR, and mFRR activation, with FCR-N operating continuously. Source: Nordic Synchronous Area Operational Agreement (SOA) [38]; Statnett Balancing Report 2026 [39].

Table 2.7: FCR and FRR dimensioning requirements for the Nordic synchronous area, 2025.
Combined Nordic LFC block (Statnett, Svenska kraftnät, Fingrid, Energinet DK2). FRR quantities refer to annual average contracted volumes. Peak load and RES share estimated from [40–42]. $\sim =$ approximate. RES (%): wind and solar electricity generation as share of total electricity generation [MWh/MWh]. Source: [39]; [43].

| Year | Peak (MW) | RES (%) | FFR (MW) | FCR-D$^{+}$ (MW) | FCR-D$^{-}$ (MW) | FCR-N (MW) | aFRR$^{+}$ (MW) | aFRR$^{-}$ (MW) | mFRR$^{+}$ (MW) | mFRR$^{-}$ (MW) |
|---|---|---|---|---|---|---|---|---|---|---|
| 2025 | ~59 000 | ~75 | 300 | 1 450 | 1 400 | 600 | 200–500 | 200–500 | ~1 400 | ~1 400 |

## FCR Dimensioning

The Nordic system deploys two distinct FCR products, each targeting a different frequency regime.

FCR-N (Frequency Containment Reserve for Normal operation) is activated continuously and proportionally within the standard frequency range of 49.90–50.10 Hz. The required Nordic volume is set at 600 MW [43].

FCR-D (Frequency Containment Reserve for Disturbance) is designed to contain large frequency deviations resulting from disturbances. It is an asymmetric product dimensioned against the reference incident, defined as the full loss of power on one of the two major HVDC interconnectors to Continental Europe. As of 2025, the total Nordic FCR-D upward requirement is 1,450 MW and the downward requirement is 1,400 MW [43].

A third reserve product specific to the Nordic synchronous area is the Fast Frequency Reserve (FFR), which has no equivalent in the Continental Europe framework. FFR was introduced to address the risk that, during periods of low system inertia, a large generation loss can cause the frequency to fall so rapidly that neither FCR-D nor aFRR can arrest the decline before it reaches the automatic under-frequency load shedding threshold of approximately 49.0 Hz. FFR must reach its full activation level within 2 seconds. As of 2025, the total Nordic FFR volume is approximately 300 MW [38]. A structural safeguard in the System Operation Agreement (SOA) requires each TSO to hold at least two-thirds of its FCR obligation within its own control area, the so-called 2/3 rule.

### FRR Dimensioning

The methodology distinguishes two categories of reserve requirements dimensioned separately and then combined: FRR for reference incidents and FRR for normal imbalances. For normal imbalances, a probabilistic approach requires that total FRR capacity be sufficient to cover LFC block imbalances at least 99% of the time. The defining structural feature is the two-step imbalance netting process [44], which exploits the statistical offset between simultaneous imbalances of opposite sign in different LFC areas, constrained by available inter-area ATC.

### Observations

The Nordic FCR architecture is split by frequency regime: FCR-N is dimensioned probabilistically against load variability, while FCR-D is dimensioned deterministically against the reference incident. This dual structure has no direct equivalent among the CE blocks reviewed here. The FRR dimensioning embeds ATC as a binding constraint at every stage of the sizing process, making congestion an explicit input rather than a post-hoc check. The most significant operational development of the period under review is the shift of mFRR to the primary balancing instrument. The mFRR Energy Activation Market went live on 4 March 2025 [38], and the impact was immediate: the number of minutes the

Nordic system frequency remained outside the standard band fell from 10,330 in 2024 to 5,094 in 2025 [39], a reduction of more than 50%.

## 2.4. Australian Electricity Markets

Australia operates two distinct electricity markets, both managed by the Australian Energy Market Operator (AEMO). The National Electricity Market (NEM) covers Queensland, New South Wales, Victoria, South Australia, the Australian Capital Territory, and Tasmania, regulated under the National Electricity Rules (NER). The Wholesale Electricity Market (WEM) covers the South West Interconnected System (SWIS) of Western Australia. The geographical extent of the two markets is shown in Figure 2.7.

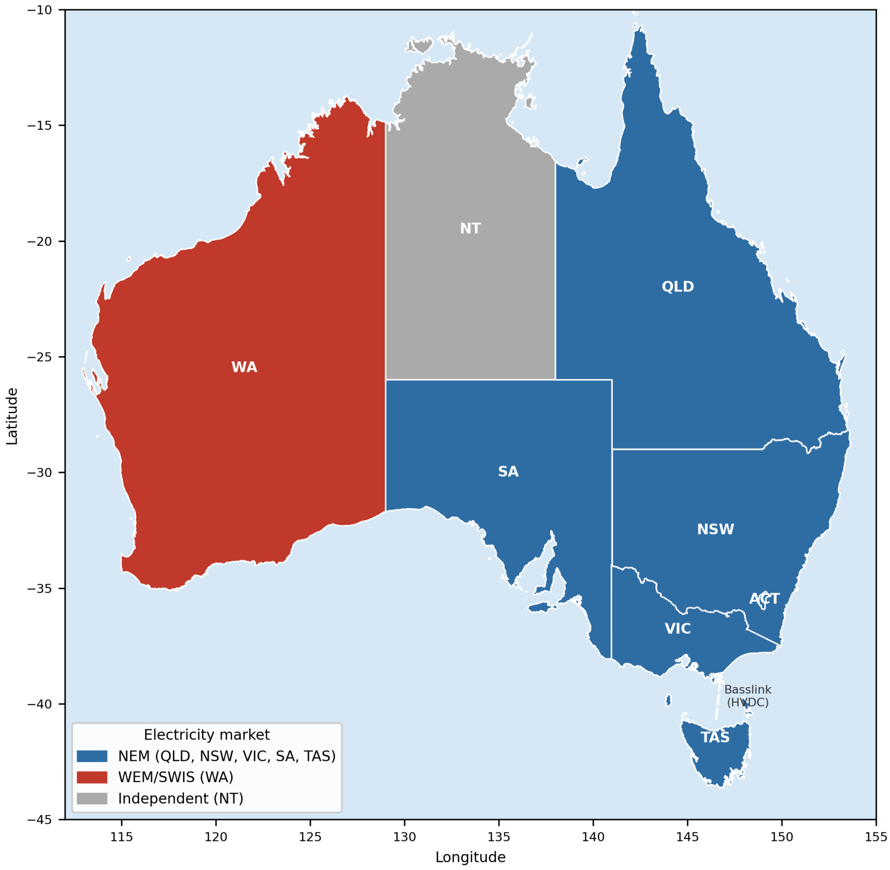


Figure 2.7: Geographical extent of the NEM and WEM electricity markets in Australia. The NEM covers Queensland (QLD), New South Wales (NSW), Victoria (VIC), South Australia (SA), and Tasmania (TAS), interconnected via the Basslink HVDC link. The WEM covers Western Australia (WA) via the South West Interconnected System (SWIS). The Northern Territory (NT) operates independently. Map generated by the author.

Unlike the European systems reviewed in the preceding sections, Australia has no equivalent to the SO GL. The Australian equivalent of frequency reserves is the Frequency Control Ancillary Services (FCAS) framework in the NEM, and the Essential System Services (ESS) framework in the WEM, both of which are procured through co-optimised spot markets, where energy dispatch and reserve procurement are cleared simultaneously in a single optimisation so that the cost of holding reserve is directly traded off against the cost of energy. Primary frequency response (PFR) is a mandatory technical obligation and is not a market product.

### 2.4.1. National Electricity Market

AEMO operates the NEM as a gross pool with centralised dispatch at five-minute intervals [45]. The dispatch engine, known as NEMDE (NEM Dispatch Engine, the centralised optimisation engine that clears energy and ancillary service markets simultaneously) [46] co-optimises energy and all ten FCAS markets simultaneously in each dispatch interval. The NEM uses a single synchronous grid for the mainland (QLD, NSW, VIC, SA) with Tasmania connected via the Basslink HVDC interconnector (500 MW capacity). Table 2.8 reports the FCAS indicative enablement volumes for the NEM for years 2023–2026.

Table 2.8: FCAS indicative enablement volumes for the NEM (Australia), 2023–2026. Contingency volumes anchored to largest credible contingency (∼800 MW mainland). Very Fast Frequency Control Ancillary Services (VF FCAS) markets introduced October 2023. FCAS volumes are co-optimised dynamically by NEMDE every 5 minutes. Emergency reserve (RERT) excluded as last-resort mechanism. Peak load = NEM maximum operational demand (summer peak, Q4). RES = wind + grid-scale solar + rooftop PV share of annual generation; derived from [47]. [48–50]; [51].

| **Peak load (MW)** | **RES (%)** | **Reg. (R/L)** | **VeryFast Cont. R1/L1** | **Fast Cont. R6/L6** | **Slow Cont. R60/L60** | **Delayed Cont. R5/L5** |
|---|---|---|---|---|---|---|
| ∼30 180 (2023); ∼33 716 (2024) | ∼31% (2023); ∼34% (2024) | ∼210–220 | R: ∼400–500 L: ∼300–400 (2026) | ∼500 | ∼500 | ∼400 |

#### Regulation FCAS

Regulation FCAS is the NEM's closest equivalent to automatic frequency restoration reserves in the European framework. It comprises two symmetric markets, Regulating

Raise (RREG) and Regulating Lower (LREG), and is designed to maintain continuous control of system frequency and time error within normal operating conditions. The Regulation FCAS requirement is determined dynamically by NEMDE in each dispatch interval, based on observed system frequency and accumulated time error.

## Contingency FCAS

Contingency FCAS is designed to manage frequency deviation following a credible contingency event. Rather than a single FCR product, the NEM uses four sequential timeframes: Very Fast (R1/L1, 1 second; introduced on 9 October 2023 [52]), Fast (R6/L6, 6 seconds), Slow (R60/L60, 60 seconds), and Delayed (R5/L5, 5 minutes). The sizing logic is deterministic and based on the largest credible contingency, reduced by an estimate of passive load relief of approximately 0.5% of instantaneous system load [53] (∼114–120 MW for a mainland load of 22,800–23,700 MW in 2023–2024). A visual representation of the activation timescale is reported in Figure 2.8.

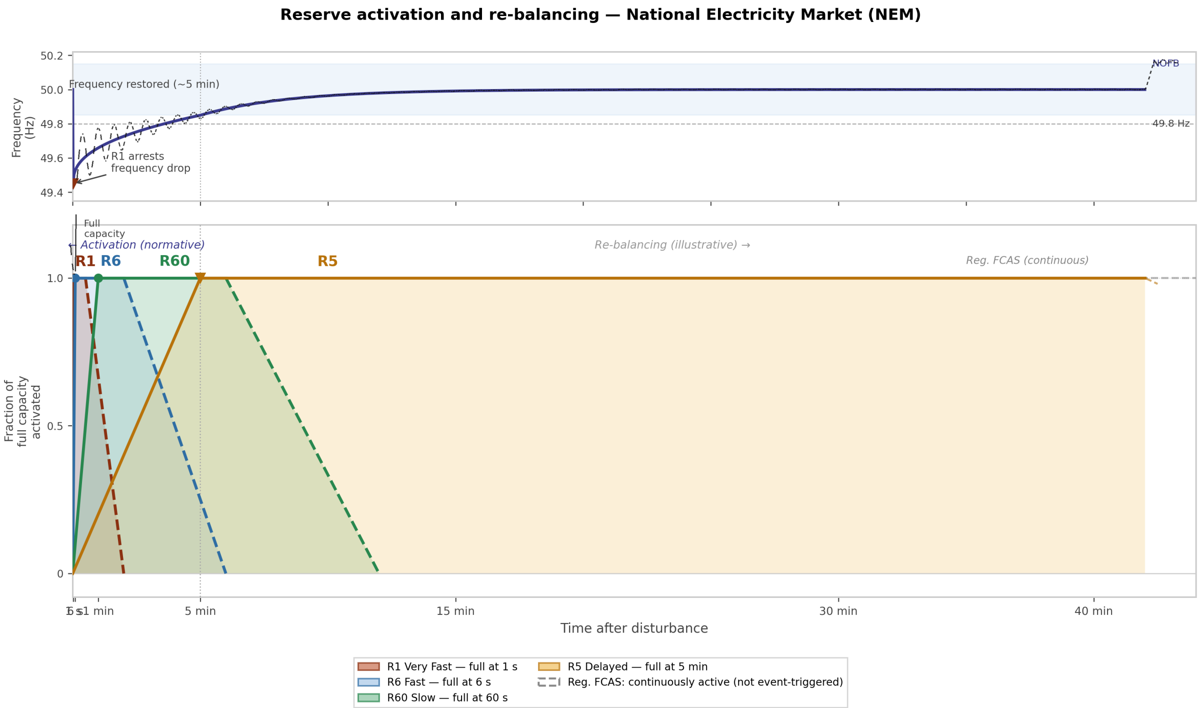


Figure 2.8: Reserve activation and re-balancing timeline for the National Electricity Market (NEM), Australia.
The four sequential contingency FCAS timeframes (R1, R6, R60, R5) are shown alongside continuous Regulation FCAS. Source: AEMO Market Ancillary Services Specification (MASS) [52]; AEMO Guide to Ancillary Services [53].

### Reserve Adequacy and Emergency Reserve

Beyond the FCAS framework, the NEM manages capacity adequacy through the Lack of Reserve (LOR) declaration system [54] and the Reliability and Emergency Reserve Trader (RERT) [55, 56]. The RERT is AEMO's instrument of last resort when an LOR2 or LOR3 condition is forecast and normal market mechanisms are insufficient to restore adequate reserves.

### Observations

The co-optimisation architecture is the defining structural feature of the NEM: energy and all ten FCAS markets are cleared simultaneously by NEMDE every five minutes, meaning the cost of holding reserve is always traded off against the cost of energy in real time. The sequential contingency response across four timeframes (R1, R6, R60, R5) means each layer provides a safety net for the one before, with the sizing of each anchored to the same largest credible contingency reduced by passive load relief. Tasmania is treated as a separate frequency area when islanded from the mainland [57, 58], a design choice with direct implications for contingency sizing in that zone.

## 2.4.2. Wholesale Electricity Market

The WEM serves the South West Interconnected System of Western Australia (SWIS), electrically isolated from the NEM. The reserve products in the WEM are collectively called Frequency Co-optimised Essential System Services (ESS) and are procured through the Wholesale Electricity Market Dispatch Engine (WEMDE).

### Essential System Services

The WEM defines three categories of frequency-related ESS: Regulation Raise and Lower services (analogous to Regulation FCAS in the NEM), Contingency Reserve Raise and Lower services [59], sized using a Dynamic Frequency Control Model (DFCM) that pre-computes secure operating zones offline and uses interpolation in real time, and RoCoF Control Service [59], a product specific to the WEM with no direct equivalent in the NEM, addressing the risk that the Rate of Change of Frequency following a contingency event exceeds safe limits for connected plant even before contingency reserve can respond.

### Observations

The WEM framework differs from the NEM's in one specific respect: the explicit integration of inertia into the contingency reserve sizing through the DFCM and the dedicated

RoCoF Control Service. This reflects the relative isolation of the SWIS: as a smaller, islanded system with no HVDC connection to external networks, the WEM is more exposed to inertia shortfalls.

## 2.5. North American Electricity System

The North American bulk power system is divided into four synchronous interconnections as shown in Figure 2.9: the Eastern Interconnection, the Western Interconnection, the Texas Interconnection (known as ERCOT), and the Québec Interconnection. These four systems operate at a nominal frequency of 60 Hz.

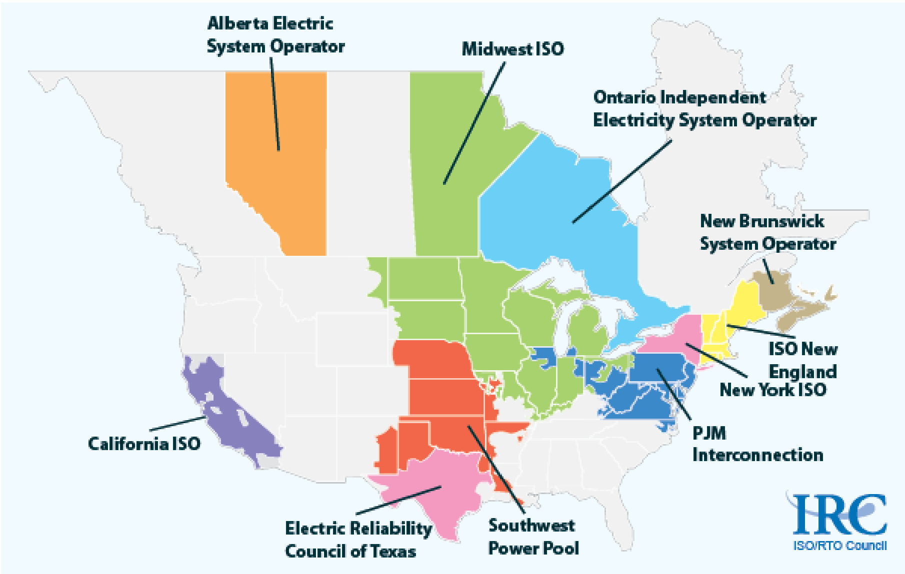


Figure 2.9: Map of Regional Transmission Organizations and Independent System Operators in North America.
Source: ISO/RTO Council (IRC).

Unlike the European system, where the SO GL provides a unified regulatory framework, North America has no equivalent supranational instrument. Instead, reliability standards are developed and enforced by the North American Electric Reliability Corporation (NERC), which operates as the Electric Reliability Organization (ERO) certified by the Federal Energy Regulatory Commission (FERC). The North American reserve framework is best understood at two levels: the NERC Reliability Standards BAL-001 [60], BAL-002 [61], and BAL-003 [62], which define minimum performance requirements for all Balancing Authorities (BAs, the entities responsible for maintaining real-time balance between generation and load within a defined area) and the RTO/ISO-level frameworks that build upon them.

### 2.5.1. Regulatory Framework

#### BAL Framework

BAL-001 (Real Power Balancing Control Performance) requires each Balancing Authority (BA) to control its ACE within defined limits using Automatic Generation Control (AGC).

BAL-002 [61] (Disturbance Control Standard, Contingency Reserve) requires each BA or Reserve Sharing Group (RSG, a pool of BAs that jointly meet their contingency reserve obligations) to hold contingency reserve sufficient to recover from a Balancing Contingency Event within the Disturbance Recovery Period (DRP) of 15 minutes [63].

BAL-003 [62] (Frequency Response and Frequency Bias Setting) requires each BA to contribute a minimum amount of frequency response to the interconnection's collective response to sudden generation losses. The Interconnection Frequency Response Obligation (IFRO) is set using a performance-based methodology calibrated to demonstrated historical performance [62, 64].

#### Primary Frequency Response

Primary frequency response (PFR) in North America is a mandatory technical obligation, not a separately compensated market product in most jurisdictions. FERC Order 842 [65], issued on 15 February 2018, requires all new synchronous and non-synchronous generators seeking interconnection to install, maintain, and operate equipment capable of providing PFR. Governor droop is typically set between 4% and 5% across all interconnections [66]. A critical operational concern is the distinction between sustained and non-sustained PFR: non-sustained PFR occurs when plant-level controllers override governor action before secondary frequency control has restored frequency to nominal, potentially causing frequency to decline a second time during the stabilising period.

### 2.5.2. ERCOT: Texas Interconnection

The Electric Reliability Council of Texas (ERCOT) operates as both the Regional Transmission Organization (RTO) and the sole Balancing Authority (BA) for the Texas Interconnection. ERCOT procures ancillary services through a co-optimised market mechanism embedded in the Security-Constrained Economic Dispatch (SCED) engine [67], which runs every five minutes and simultaneously clears the real-time energy market and the ancillary service markets. ERCOT currently procures five ancillary service products:

Regulation Up, Regulation Down, RRS, ECRS, and Non-Spin, each with defined activation timescales illustrated in Figure 2.10. Table 2.9 reports the ancillary service quantities and system statistics for ERCOT for 2023–2024.

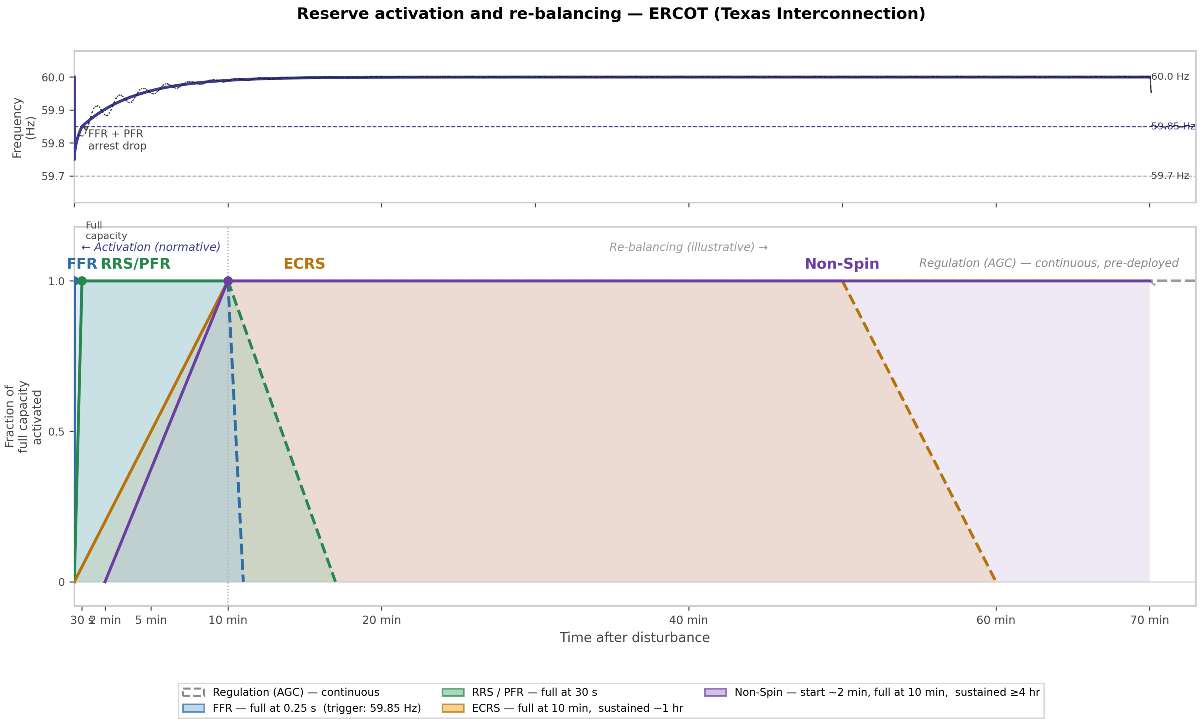


Figure 2.10: Reserve activation and re-balancing for ERCOT (Texas Interconnection). The upper panel shows the indicative frequency response at 60 Hz; the lower panel shows FFR, RRS/PFR, Regulation (AGC), ECRS, and Non-Spin deployment sequences. Source: ERCOT Ancillary Services Study White Paper [67]; ERCOT Market Information System Report 13036 [68].

Table 2.9: ERCOT ancillary service quantities and system statistics, 2023–2024. Values represent the range across all 24 hourly intervals and all published monthly periods within the year. RES (%): wind and solar electricity generation as share of total electricity generation [MWh/MWh]. Source: [68]; [69]; [70]; [71]; [72].

| Year | Peak Load (MW) | RES (%) | Reg Up (MW) | Reg Down (MW) | RRS (MW) | ECRS (MW) | Non-Spin (MW) |
|---|---|---|---|---|---|---|---|
| 2023 | 85 508 | 33.7 | 67–921 | 152–880 | 2 300–3 335 | 1 098–2 875 | 1 688–5 633 |
| 2024 | 85 559 | 35.7 | 55–1 110 | 182–1 020 | 2 300–3 178 | 889–3 007 | 1 430–4 482 |

### Regulation Service

Regulation Up and Regulation Down are the analogues of aFRR in the CE framework. The Regulation quantity is sized to cover the 95th percentile of deployed regulation or net load variability [73].

### Responsive Reserve Service

Responsive Reserve Service (RRS) is ERCOT's primary contingency response product, required to deliver sustained PFR. The minimum RRS requirement has been 2,800 MW during peak hours and 2,300 MW during off-peak hours since 2022 [74]. Fast Frequency Response (FFR), embedded within the RRS product, requires full activation within approximately 250 milliseconds and was introduced in 2020 [67, 75] in response to declining system inertia.

### Contingency Reserve Service

ERCOT Contingency Reserve Service (ECRS) was introduced in June 2023 [75] as the first new ancillary service product in the ERCOT market in more than 20 years, occupying a middle tier between RRS and Non-Spin.

### Non-Spinning Reserve Service

Non-Spinning Reserve Service (Non-Spin) covers the remaining capacity needed to respond to contingency events within 10 minutes, provided by offline resources.

## 2.5.3. Eastern and Western Interconnection

The Eastern and Western Interconnections each contain multiple BAs and RTOs with distinct reserve frameworks, all subject to the NERC BAL standards.

### Eastern Interconnection

The major RTOs operating within the Eastern Interconnection are PJM Interconnection, MISO (Midcontinent Independent System Operator), SPP (Southwest Power Pool), ISO-NE (Independent System Operator New England), and NYISO (New York Independent System Operator). Contingency reserve sizing follows the N-1 approach mandated by BAL-002 [61] but with RTO-specific multipliers. Reserve sharing in the Eastern Interconnection is extensive, with most BAs within PJM, MISO, and SPP participating in Reserve Sharing Groups.

### Western Interconnection

The Western Interconnection is operated by CAISO (California ISO) and approximately 35 other BAs, coordinated through the Western Electricity Coordinating Council (WECC) [76]. CAISO applies a more detailed sizing approach: its minimum contingency reserve is the greater of the single largest contingency and the sum of 3% of hourly integrated load plus 3% of hourly integrated generation [77], with an additional potential upward adjustment of up to 25% of solar capacity to account for intra-hour solar forecast uncertainty.

## 2.5.4. Observations

Four structural features of the North American reserve framework stand out from a comparative perspective.

The most fundamental difference from the European frameworks is the performance-based nature of the primary frequency response obligation: under BAL-003 [62], the IFRO is calibrated to demonstrated historical performance rather than derived from a forward-looking risk model, in contrast to the CE probabilistic FCR methodology [9].

The absence of a universal co-optimisation requirement is the second distinguishing feature: only ERCOT and CAISO fully co-optimise energy and ancillary services in their real-time market. Elsewhere, reserve procurement and energy dispatch remain separate processes, with reserve requirements set independently of real-time market conditions.

The treatment of PFR as a mandatory technical obligation rather than a market product creates a free-rider problem: generators that invest in governor capability bear a cost that benefits the entire interconnection, with no mechanism to recover it. The issue remains unresolved at FERC.

Finally, ERCOT's introduction of ECRS in 2023 and the earlier introduction of FFR in 2020 represent the most methodologically significant reserve product innovations in North America in recent years. Both were driven by the same structural shift: declining synchronous inertia and increasing RoCoF risk as inverter-based resources displace synchronous generators. The parallel product innovations in the Nordic and Australian systems confirm that this challenge is common to all systems undergoing rapid decarbonisation, regardless of market structure.

## 2.6. Comparative Overview

Table 2.10 summarises the key characteristics of the seven reserve frameworks examined in this chapter across nine comparative dimensions. Several patterns emerge from the cross-system analysis [78]. The most fundamental divide is between systems that size reserves through a separation of sizing and procurement, like the European approach, and those that co-optimise energy and reserves in real time, as in Australia and ERCOT. A second axis of differentiation concerns the treatment of primary frequency response: in Continental Europe and the Nordic area it is a procured market product with explicit volumetric requirements, while in North America it remains largely a mandatory technical obligation without direct compensation, a distinction with significant implications for investment incentives as generation portfolios shift towards inverter-based resources. A third pattern is the uneven adoption of inertia-sensitive reserve products: the Nordic FFR, the WEM RoCoF Control Service, and ERCOT's Fast Frequency Response all address the same underlying challenge, declining synchronous inertia, but through architectures shaped by each system's specific regulatory and market context. Finally, the degree of temporal granularity in reserve sizing ranges from real-time co-optimisation in Australia and ERCOT to annual or semi-annual processes in parts of Europe and North America, with the most advanced European TSOs converging towards dynamic day-ahead dimensioning. These differences in architecture, granularity, and risk philosophy are precisely what makes a controlled comparison on a single system dataset meaningful: the same underlying uncertainty, sized by different methods, produces different results, and Chapter 4 quantifies that gap.

Table 2.10: Comparative overview of reserve frameworks across the systems analysed.

| Criterion | CE | IE/NI | Nordic | NEM | WEM | ERCOT | East./West. |
|---|---|---|---|---|---|---|---|
| **Market structure** | Self-dispatch; separate auctions | Central dispatch | Self-dispatch; separate auctions | Gross pool; co-optimised | Gross pool; co-optimised | Gross pool; co-optimised | Self-dispatch (varies) |
| **Primary** | FCR | POR/SOR | FCR-N/ FCR-D/FFR | Contingency FCAS (not compensated | Contingency R/L (not compensated) | PFR (not compensated); RRS (market procured) | PFR (not compensated) |
| **Secondary** | aFRR | None | aFRR | Regulation FCAS | Regulation ESS | Reg Up/Down | Regulation |
| **Tertiary** | mFRR + RR | TOR1 /TOR2/ RRS | mFRR | Contingency FCAS (R60 + R5) | Contingency ESS | ECRS + Non-Spin | Non-spinning |
| **Sizing: Primary** | Probabilistic (Monte Carlo; $\leq$1/20 yrs) | Deterministic (75% of largest infeed; real-time adj.) | Deterministic (LCC minus load relief) | Dynamic (DFCM; inertia-dep.) | Deterministic | Performance-based (IFRO) | varies by RTO |
| **Sizing: Secondary** | Dynamic probabilistic (99th pct ACEol; varies by TSO) | — | Probabilistic (99th pct; ATC-netted) | Co-optimised real-time | Co-optimised real-time | Statistical (95th pct net load) | varies by RTO |
| **Sizing: Tertiary** | Deterministic (N-1; ENTSO-E policy) | Deterministic (100% of incident) | Deterministic (100% of incident) | Co-optimised real-time | Dynamic (DFCM; inertia-dep.) | Deterministic (min. 3,000 MW Non-Spin) | varies by RTO |
| **Sizing: inputs** | Historical ACE; wind, solar and load forecast errors | Largest infeed/outfeed; load frequency response; system inertia; RoCoF limit | Reference incident (FCR-D); historical imbalance data; available ATC (aFRR) | Largest credible contingency; passive load relief estimate | Largest contingency; system inertia; RoCoF limit (DFCM) | Historical net load variability; system inertia; largest contingency | Largest contingency (N-1); historical performance data (IFRO) |
| **Inertia product** | No (FFR under discussion) | No | Yes: FFR ($\leq$2 s) | Yes: VF FCAS R1 (1 s; 2023) | Yes: RoCoF Control Service | Yes: FFR ($\leq$250 ms; 2020) | No |
| **Reserve sharing** | Yes (FCR Coop.; IGCC; MARI) | No | Yes (intra-Nordic; ATC-constrained) | No | No | No | Yes (RSGs) |

Figure 2.11 places the reserve requirements of the seven systems examined in this chapter in a common reference frame, expressing each requirement as a fraction of the system's peak load and plotting it against the share of renewable generation. The normalisation by peak load removes the effect of system size, allowing a meaningful cross-system comparison of reserve intensity, while the renewable penetration axis tests whether a higher share of variable generation is associated with higher reserve requirements across real operational systems.

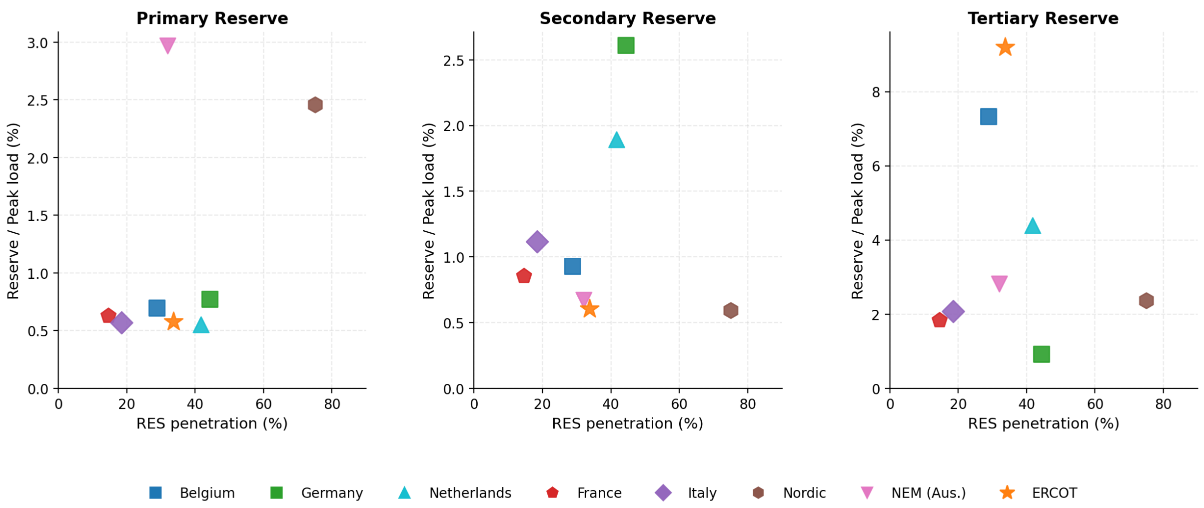


Figure 2.11: Reserve requirements as a fraction of peak load against RES penetration for the seven systems examined in this chapter. Primary reserve (FCR), secondary reserve (aFRR) and tertiary reserve (mFRR) are shown separately.
For NEM: primary= FCAS (R1 + R6)secondary= Regulation , tertiary= FCAS (R60 + R5). For ERCOT: primary= PFR, secondary= Regulation Up, tertiary= RRS + ECRS + Non-Spin.

For the primary reserve, one might expect a positive relationship with system load, since larger systems face larger absolute imbalances and some sizing frameworks scale requirements proportionally. In practice, however, no such trend is visible across the systems examined. The reason lies in the diversity of sizing philosophies: within Continental Europe, the total FCR requirement is anchored to a fixed reference incident, and each TSO's individual obligation is then allocated in proportion to the active power that the LFC block's generators collectively inject or withdraw for each Hz of frequency deviation, a measure of the block's natural frequency response contribution that does not scale directly with peak load. Outside Continental Europe, systems such as ERCOT and the Nordic area anchor the primary reserve to the largest credible contingency, which is similarly fixed and does not track peak load. The result is that primary reserve intensity varies widely across systems for structural reasons unrelated to load level.

For the secondary and tertiary reserve, one might expect a positive relationship with RES penetration, since higher renewable shares introduce greater forecast uncertainty that reserve must absorb. The figure shows that this relationship is not evident in the cross-country data either. The reason is that secondary and tertiary reserve sizing methodologies differ substantially across systems in their treatment of renewable variability: some methods target a statistical percentile of the observed imbalance signal, others apply deterministic rules anchored to the dimensioning incident, and others use hybrid approaches. These methodological differences, together with the diversity of system scale and market structure, dominate the renewable penetration signal, making it impossible to identify a consistent trend from aggregate cross-country data alone.

The absence of clear relationships in both dimensions motivates the controlled comparative analysis developed in Chapter 4: by applying multiple methodologies to the same system under identical conditions, the methodological contribution to reserve volumes can be isolated from the system-specific one.

# 3 | Academic Methods for Reserve Sizing

The preceding chapter has documented how TSO methodologies for reserve sizing are shaped by institutional constraints, regulatory frameworks, and the operational history of each system. Academic research has approached the same problem from a different angle: treating reserve sizing as a quantitative optimisation problem and developing methods that make the underlying uncertainty sources explicit. These methods span a wide spectrum, from purely data-driven approaches that derive reserve requirements from historical imbalance records, to model-driven frameworks that construct the relevant distributions analytically from technology-level parameters.

## 3.1. Classification of Academic Methods

Academic reserve sizing methods can be characterised along three dimensions: the *type of uncertainty* they address, whether the sizing decision is *static or dynamic*, and the *data requirements* of the approach [79, 80].

Methods differ first in which sources of uncertainty they consider: *normal variability*, that is, the continuous, small-scale fluctuations in generation and load between scheduling intervals, *forecast error*, *contingency events*, or some combination of the three. This distinction matters because each source requires different data and modelling assumptions, and it produces reserves with different activation timescales.

A second distinction concerns whether the sizing decision is *static* or *dynamic*. A static method produces a single reserve requirement, typically fixed for a season or a year, calibrated on aggregate statistics. A dynamic method produces a different requirement for each scheduling interval, computed using the forecast information available at that specific moment. Static approaches are computationally simpler and administratively easier to implement, but tend to over-procure reserve in low-uncertainty conditions and under-procure it when uncertainty is high [2]. Dynamic approaches address this trade-off directly, at the cost of greater data and modelling requirements.

A third dimension, less commonly highlighted but particularly relevant for the purposes of this thesis, concerns the *data requirements* of each method. Some approaches are purely data-driven: they require a long and representative record of historical imbalances or forecast errors to estimate the statistical distributions from which reserve requirements are derived. Others are model-driven: they construct those distributions analytically from the physical and statistical properties of individual uncertainty sources, such as the forecast error variance of a specific wind technology or the forced outage rate of a generation unit. Data-driven methods are more accurate when there is great availability of historical data and the system is stable but lose validity when the system is evolving rapidly or when no operational history exists. Model-driven methods can be parameterised from engineering databases and technical specifications, making them applicable to planning studies for future systems or to contexts where no balancing data is available [81].

The methods reviewed in this chapter address the sizing of secondary and tertiary reserves. Primary reserve (FCR) sizing is governed by deterministic criteria and has not been the subject of probabilistic or stochastic methods, with the exception of Giglio et al. [81], which covers all four ENTSO-E reserve products.

Table 3.1 summarises the methods reviewed in this chapter along these dimensions.

Table 3.1: Classification of academic reserve sizing methods reviewed in Chapter 3. 'Mixed' denotes methods that combine analytical modelling of some uncertainty sources with statistical fitting to historical data for others. RES: whether the method explicitly incorporates variable renewable generation uncertainty.

| Method | Uncertainty scope | Temporal scope | Data requirement | RES |
|---|---|---|---|---|
| Zima et al. (2008) [82] | Forecast error + outages | Static | Data-driven | × |
| Ortega-Vazquez & Kirschen (2009) [3] | Forecast error + outages | Static | Model-driven | ✓ |
| Holttinen et al. (2012) [2] | Variability + forecast error | Static | Mixed | ✓ |
| Jost et al. (2015) [83] | Forecast error | Dynamic | Data-driven | ✓ |
| Khodadadi et al. (2023) [84] | Forecast error + sharing | Dynamic | Mixed | ✓ |
| Bovera et al. (2021) [85] | Forecast error + outages | Dynamic | Data-driven | ✓ |
| Giglio et al. (2025) [81] | Variability + forecast error + outages | Static / planning | Model-driven | ✓ |

## 3.2. Static Probabilistic Methods

The first wave of academic work on reserve sizing, emerging in the late 2000s and early 2010s, shared a common motivation: deterministic rules like the UCTE formula were no longer adequate as wind penetration grew, and a more rigorous treatment of uncertainty was needed. The methods reviewed in this section represent that shift, replacing fixed engineering heuristics with a statistical characterisation of the uncertainty sources that reserves are meant to cover. The result is still a single reserve requirement, fixed for a season or a year, but one derived from data rather than convention [2, 80].

### 3.2.1. Zima, Koch and Andersson (2008)

Zima, Koch and Andersson [82] propose a probabilistic framework for dimensioning secondary and tertiary control reserves. Developed at ETH Zurich and grounded in the UCTE operational context, the framework classifies the sources of imbalance between scheduled and actual generation and load into three independent contributions: forced outages of generating units, load forecast error, and spontaneous load variations. Each is described by a probability distribution: outages by a discrete distribution derived from unit-specific failure rates, load forecast error and spontaneous variations by zero-mean Gaussian distributions whose standard deviations scale with system size.

The reserve requirement for each category is determined by combining these distributions. For secondary reserves, which must respond within fifteen minutes, only spontaneous load variations and outage probabilities scaled to that timeframe are included; load forecast error, which materialises over longer horizons, is excluded. For tertiary reserves, which cover a one-hour window, all three contributions enter the combined distribution. In both cases, the joint distribution is constructed by convolving the individual distributions, an operation that is analytically tractable when the continuous components are Gaussian, since the convolution of independent normal distributions is itself normal with variance equal to the sum of the individual variances. The outage distribution, being discrete, is handled separately and then combined with the continuous component. The reserve requirement is then identified as the quantile of the resulting distribution corresponding to an accepted deficit probability $P_D$: the smallest reserve level $X_{CR}$ such that the probability of the imbalance exceeding that level is no greater than $P_D$.

The framework has two properties that are directly relevant to the comparative application in Chapter 4. It treats positive and negative reserve requirements symmetrically, including generator outages in both directions rather than only in the positive (upward) reserve calculation, a choice the authors justify on the grounds that outages affect the balance in both directions through their interaction with dispatch. All input parameters, including failure rates and standard deviations of load deviations, can be estimated from engineering databases and historical load statistics without requiring a record of past imbalances or forecast errors, making the method applicable to planning contexts where no operational balancing data is available.

The framework does not, however, incorporate forecast errors from variable renewable generation, a source of uncertainty that was marginal at the time of writing but has since become a primary driver of reserve requirements in most European systems. This omission limits the method's direct applicability to systems with significant wind or solar penetration, and motivates the extensions proposed in the methods that follow.

### 3.2.2. Holttinen et al. (2012)

The approach of Zima et al. is one instance of a broader family of probabilistic methods that were being developed and applied across multiple systems during this period. A systematic comparison of these approaches is provided by Holttinen et al. [2], a multi-author study conducted under the IEA Wind Task 25 programme, valuable here as a cross-system reference that contextualises the individual contributions reviewed in this chapter.

The paper organises existing methods into three categories. *Deterministic methods* linearly or geometrically sum the maximum possible contributions from load uncertainty, wind uncertainty, and the largest contingency, without accounting for the probability of simultaneous occurrence; the authors note that arithmetic summation overestimates the reserve requirement and that geometric summation, while an improvement, still yields conservative results. *Statistical methods with Gaussian non-correlated inputs* assume that load and generation errors follow independent normal distributions, so that the variance of the net error is the sum of the individual variances; the additional reserve required due to wind integration is then derived from the increase in the combined standard deviation, scaled by a factor $n$ chosen to cover a target fraction of occurrences. The paper notes that wind variability and forecast errors are not always normally distributed and that higher values of $n$ may be needed to cover tail events not captured by the Gaussian approximation. *Convolution methods with non-Gaussian non-correlated inputs* relax the Gaussian assumption by computing the full probability density distribution of the net error through recursive convolution of the individual distributions for load, wind, and generator outages; the reserve requirement is then derived by applying a reliability criterion such as a target loss-of-load probability.

All three categories are presented in their static form as the baseline. The paper also notes that dynamic allocation, recomputing the requirement as a function of current system state, reduces the need to carry large reserves in all hours and can be applied on top of any of the three approaches, a point developed further in Section 3.3.

### 3.2.3. Ortega-Vazquez and Kirschen (2009)

While the methods surveyed by Holttinen et al. set the reserve requirement by applying a reliability criterion to a combined error distribution, Ortega-Vazquez and Kirschen [3] take a different starting point: rather than asking what level of reserve covers a given fraction of imbalances, they ask what level minimises the total cost of operating the system. The reserve requirement is the quantity that minimises the sum of the operating cost and the expected cost of interruptions, which is the product of the expected energy not served (EENS) and the value of lost load (VOLL). This formulation makes the reserve requirement sensitive to economic conditions as well as to technical uncertainty: a system where customers place a high value on continuity of supply will procure more reserve than one where interruption costs are low, even if the underlying uncertainty is identical.

The probabilistic inputs to the framework are load forecast error and wind power forecast error, both modelled as Gaussian random variables with zero mean and standard deviations that scale with the actual load and with the installed wind capacity respectively. Since the two errors are assumed statistically independent, the standard deviation of the net demand forecast error is their quadratic sum. Generator outages are incorporated explicitly through capacity outage probability tables, treating each unit as a two-state device with a known forced outage rate.

The relationship between wind penetration and reserve requirements is non-linear and non-monotonic: depending on the level of demand and the shape of the marginal cost curve of committed generators, a higher wind forecast can either increase or decrease the optimal reserve requirement. This motivates the case-by-case, condition-specific approach that later dynamic methods would develop further.

## 3.3. Dynamic Probabilistic Methods

The methods reviewed in this section share the same probabilistic foundation as those in Section 3.2, but depart from them in one essential respect: rather than producing a single reserve requirement fixed for a planning period, they recompute the requirement at each scheduling step using the most recent forecast information available at the time of procurement. The term *dynamic* therefore refers to the temporal resolution of the sizing decision, not to the nature of the uncertainty modelled. This distinction matters because the forecast error variance of variable renewables is strongly time-structured, varying with time of day, season, weather regime, and forecast horizon, and a static requirement calibrated to the worst expected conditions will systematically over-procure reserve during low-uncertainty periods and may under-procure it during high-uncertainty ones [80].

### 3.3.1. Jost et al. (2015)

A practically-oriented dynamic sizing framework for aFRR and mFRR is proposed by Jost et al. [83] at the Fraunhofer Institute for Wind Energy and Energy System Technology. The core methodological contribution is the use of quantile regression to model the relationship between observable forecast variables, including wind power forecast, solar forecast, load forecast, and time-of-day indicators, and the quantiles of the resulting net load forecast error distribution. Rather than assuming a fixed distributional form, quantile regression allows the shape and spread of the error distribution to vary with the conditioning variables, capturing the fact that forecast uncertainty is not constant but depends on the current system conditions. The reserve requirement for each scheduling interval is then the difference between the target quantile and the point forecast, producing an interval-specific quantity that reflects the actual uncertainty of that interval rather than the average uncertainty over the season.

The paper applies the methodology to the German balancing area and demonstrates that dynamic sizing can reduce total aFRR procurement by a significant margin compared to the static approach then in use, without any deterioration in reliability. This result was subsequently influential in the German regulatory debate that led to the 2019 Bundesnetzagentur decisions on dynamic dimensioning [22, 23]. The Jost et al. contribution is one of the few cases in this literature where the link between academic model and regulatory change is directly documented: the same quantile regression framework, applied to the same German dataset, appears both in the paper and in the methodological documentation filed with BNetzA. This precedent is relevant here because it demonstrates that academic reserve sizing methods can be adopted in operational practice when the regulatory context is favourable.

### 3.3.2. Khodadadi et al. (2023)

A more recent contribution by Khodadadi et al. [84] from KTH Royal Institute of Technology addresses dynamic reserve sizing in the context of multi-area reserve capacity markets, using the Nordic system as a case study. The methodological framework is based on chance-constrained optimisation: the reserve requirement for each area is formulated as the solution to an optimisation problem that minimises total procurement cost subject to a probabilistic constraint on the adequacy of the combined reserve portfolio. The chance constraint requires that the probability of the total imbalance exceeding available reserve capacity be no greater than a specified threshold, analogous to the reliability target used in the static probabilistic methods of Section 3.2.

The innovation lies in how this constraint is handled in a multi-area setting: rather than sizing each area independently and then aggregating, the model optimises the allocation of reserve obligations across areas jointly, taking into account the statistical dependence between area imbalances and the transmission capacity available for cross-border activation. The paper compares independent static sizing, independent dynamic sizing, and joint dynamic sizing with the chance constraint, finding that the last approach achieves the largest reduction in total reserve procurement, up to 15% relative to static independent sizing, with the benefit concentrated in periods where the imbalances of neighbouring areas are negatively correlated. The key methodological insight is that dynamic sizing and reserve sharing are complementary mechanisms: the first captures temporal variation in uncertainty, the second exploits spatial diversification, and their combined effect is larger than either in isolation. This result has direct implications for the European integration process described in Chapter 2, where the simultaneous development of dynamic sizing frameworks [22, 24] and cross-border sharing platforms [5] is precisely the trajectory being pursued.

## 3.4. Data-Driven and Machine Learning Methods: Bovera et al. (2021)

The methods reviewed in this section derive reserve requirements directly from patterns learned from historical system data, without imposing a fixed distributional form on the underlying uncertainty. The term *data-driven* covers a spectrum ranging from statistical learning methods that fit flexible non-parametric models to forecast error data, to machine learning approaches that use neural networks or ensemble methods to capture complex, non-linear relationships between system conditions and reserve needs. Although these methods produce dynamic requirements, adapting to the specific conditions of each scheduling interval, they differ from the approaches in Section 3.3 in one fundamental respect: rather than fitting a parametric model to the error distribution, they derive reserve requirements directly from the data, without any prior assumption on its shape. This data dependence is both their strength and their principal limitation: in systems with long and representative operational records, data-driven methods can outperform the Gaussian-based approaches reviewed in Section 3.2 by capturing structure in the error distribution that a fixed distributional assumption would miss, but in systems undergoing rapid transformation or in planning studies for future generation mixes, models trained on past data will produce biased estimates.

A data-driven framework for evaluating secondary and tertiary reserve needs under high renewable penetration is proposed by Bovera et al. [85] at Politecnico di Milano. The paper addresses the Italian system, which, as described in Chapter 2, operates a zonal structure with reserves dimensioned independently for each aggregation, and uses a sizing methodology that combines a statistical forecasting tool with a minimum baseline derived from load forecasts [28].

The method takes as input the historical time series of net load forecast errors, computed as the difference between the day-ahead forecast of residual demand and its realised value, and derives from them both the required reserve volumes and their optimal temporal disaggregation across scheduling intervals. Rather than fitting a single distribution to the aggregate error record, the method segments the data by relevant conditioning variables, including season, time of day, and renewable forecast level, and estimates a separate error distribution for each segment. The reserve requirement for each interval is then the target quantile of the corresponding conditional distribution.

The paper evaluates the method against the static sizing approach then in use by Terna and finds that conditional sizing reduces total reserve procurement by approximately 12% while maintaining the same reliability level, with the largest reductions occurring during overnight hours when solar uncertainty is absent and wind forecast errors are relatively small. The result provides empirical support for the dynamic sizing argument in a real system with well-documented operational data.

## 3.5. Integrated Stochastic Methods: Giglio et al. (2025)

The methods reviewed in the preceding sections each address a subset of the reserve sizing problem: static probabilistic methods model forecast errors but fix the requirement over a season or a year; dynamic methods adapt to changing conditions but remain data-dependent; data-driven approaches learn from historical records but lose validity when the system evolves. The framework proposed by Giglio et al. [81] addresses these limitations simultaneously, combining a stochastic model that covers all major uncertainty sources with a parametric structure that allows the reserve requirements to be embedded directly into a long-term energy system planning optimisation.

The paper identifies a specific gap in the existing literature: no prior methodology simultaneously covers all four reserve products of the ENTSO-E framework (FCR, aFRR, mFRR, and RR), incorporates tripping events alongside forecast errors and residual demand variability, and is structured to be integrated into a long-term capacity expansion model. The framework is validated on the South African power system for the 2050 planning horizon, a context chosen for its distance from the European systems for which most prior methods were designed, demonstrating the generalisability of the approach beyond the ENTSO-E area.

The core of the framework is a Monte Carlo simulation that models the total system imbalance as the sum of three independent contributions. The first is the forced outage of generating units and storage converters, modelled through technology-specific failure rates that determine the probability and duration of tripping events. The second is the forecast error of load and variable renewable generation, represented as a zero-mean Gaussian distribution whose standard deviation scales with the installed capacity of each technology and its characteristic forecast accuracy. The third is the variation of residual demand within each market interval, modelled as a sawtooth wave that captures the intra-interval ramp that must be covered by reserve even in the absence of forecast errors. This last component is absent from all the methods reviewed in the preceding sections.

Reserve requirements for each product are extracted as percentiles of the simulated imbalance distribution: the 99th percentile of total imbalance for FCR, the 95th for aFRR, the 99th for mFRR, and the 99.7th for RR, of the total imbalance minus the 15-min average of the total imbalance, with each product covering the imbalance not addressed by the faster products below it. Because all input parameters, including failure rates, forecast error standard deviations, and the residual demand variation, can be estimated from technical databases and publicly available generation data rather than from operational balancing records, the method is applicable to systems with no balancing history and to planning scenarios with generation mixes that differ substantially from current conditions.

To enable integration with a Mixed Integer Linear Programming (MILP) capacity expansion model, the non-linear reserve requirements are first approximated by a parametric function and then linearized iteratively using a Taylor expansion, with the planning optimisation and the reserve estimation alternating until convergence. The validation against Eskom data confirms that this approach reproduces actual reserve levels with acceptable accuracy, and the planning results demonstrate that endogenous reserve requirements substantially affect the optimal technology mix, with storage capacity increasing significantly when reserves are treated as a first-order planning constraint rather than a post-hoc correction.

# 4 | Comparative Application of Reserve Sizing Methodologies

## 4.1. Motivation and Scope

The preceding three chapters have approached reserve sizing from complementary perspectives: Chapter 1 established the theoretical foundations of the problem; Chapter 2 documented how TSOs across five synchronous areas translate those foundations into operational practice; and Chapter 3 reviewed the academic methods that model the underlying uncertainty sources analytically. Each of these methods was developed and validated on a specific power system, with its own generation mix, regulatory context, and input dataset. Differences in reported reserve volumes across studies are therefore difficult to interpret: they may reflect genuine methodological disagreement, or simply the characteristics of the systems to which the methods were applied. To the best of the author's knowledge, no published study has systematically applied multiple reserve sizing methodologies to the same power system using a common input dataset. The present chapter addresses this gap by developing a unified comparative framework, referred to hereafter as the *Comparative Reserve Sizing Framework*, and applying it to eight reserve sizing methodologies under identical input conditions.

The eight methodologies span the full spectrum from deterministic to integrated stochastic approaches: four are drawn from TSO practice introduced in Chapter 2 (France RTE, Nordic, ERCOT, and UCTE), three from the academic literature reviewed in Chapter 3 (Zima et al. 2008, $n$-sigma, and Giglio et al. 2025), and one proprietary method developed at CESI SpA (CESI). The computational framework, the implementation of each method and the reference system are described in the sections that follow.

The objective is not to identify a universally superior method. The relative merits of different approaches depend on the context in which they are used. The objective is instead to examine whether different methodological philosophies, from fully deterministic to integrated stochastic, lead to meaningfully different reserve requirements when the underlying system conditions are held constant.

## 4.2. Comparative Reserve Sizing Framework

The *Comparative Reserve Sizing Framework* is designed to be system-agnostic: the same structure can be applied to any power system for which the required input data are available. Figure 4.1, shown at the end of this section, illustrates the overall structure of the comparative analysis.

All methodologies share the same system inputs (System Inputs block in Figure 4.1): the generation fleet parameters and the time series of load, solar, and wind production, ensuring that any differences in reserve requirements reflect methodological choices rather than differences in the underlying system data.

The procedure structures the comparative application around a set of representative operating scenarios, each paired with a dedicated Monte Carlo imbalance simulation. This two-stage structure is inspired by the approach of Giglio et al. [81], which the *Comparative Reserve Sizing Framework* extends in two respects: the scenarios are derived from real operational data rather than constructed synthetically, and the framework is applied to eight methodologies simultaneously under identical conditions, constituting an original comparative contribution not present in any prior work.

In the original Giglio formulation, designed for planning contexts where no historical dispatch data are available, the scenario set is constructed to cover all combinations of online generation and load that the system may take, without reference to observed operational records. The present application is instead grounded in real operational data, which makes a data-driven scenario construction more appropriate. Rather than processing each quarter-hourly interval independently, which would require one Monte Carlo simulation per interval and result in a prohibitive computational cost, the operating year is summarized into a compact set of representative scenarios. This reduction is justified by the observation that reserve requirements vary smoothly with system state: intervals with similar load levels, renewable output, and committed generation capacity yield similar imbalance distributions and thus similar reserve requirements. The 35,040 quarter-hour intervals of the year, each characterised by the generation output of individual technical units and the corresponding system load, are clustered into a representative set of operating conditions using $k$-means clustering applied to the joint distribution of load, renewable generation, and online generation capacity (Operating Scenarios block in Figure 4.1). The number of clusters is determined by inspecting the within-cluster sum of squares (WCSS) as a function of $k$ and selecting the value at which the marginal reduction in WCSS becomes negligible (elbow criterion). Each cluster centroid defines one scenario, characterised by the load level, the capacity factors of offshore wind, onshore wind, and solar, and the number of units online for each dispatchable technology, representing a typical system configuration within that operating regime. The Monte Carlo simulation is run once per scenario, reducing the computational burden while preserving the statistical representativeness of the full operating range.

For each scenario, a Monte Carlo imbalance signal is generated. The total system imbalance $R_{\bar{t}}^{\text{imb}}$ is represented as the sum of three independent contributions (Equation (4.1)):

$$R_{\bar{t}}^{\text{imb}}(\mathbf{x}) = R_{\bar{t}}^{\text{trip}}(\mathbf{x}) + R_{\bar{t}}^{\Delta f}(\mathbf{x}) + R_{\bar{t}}^{\text{VRD}}(\mathbf{x}) \tag{4.1}$$

where $\bar{t}$ denotes the simulation time step within the Monte Carlo domain $\Omega_{MC}$, and $\mathbf{x}$ is the system state vector, defined by the nominal power of each component $P_a$, the renewable capacity factors $CF_r$, the load $L_l$, and the variation of residual demand $VRD$. Each time step $\bar{t}$ belongs to a Monte Carlo domain $\Omega_{MC}$ equivalent to 192 years of 1-minute operation, consistent with ENTSO-E guidelines [7]. This domain is not intended to represent a continuous temporal sequence of system operation, but rather to provide a sufficiently large statistical sample for reliable estimation of rare events within a fixed operating scenario. In the real system, operating conditions shift continuously from one scenario to another; the Monte Carlo simulation captures the stochastic behaviour of the system within each snapshot, independently of this temporal evolution.

The *tripping contribution* $R_{\bar{t}}^{\text{trip}}$ models the sudden loss of a generating unit or storage converter. For each asset $a$, a trip event occurs when a uniformly distributed random variable $Z$ exceeds the trip probability $\mu_a^{\text{trip}}$, derived from the annual failure rate $\lambda_a$ (Equation (4.2)):

$$\mu_a^{\text{trip}} = 1 - e^{-\lambda_a} \tag{4.2}$$

Once triggered, the impact of the trip persists for a duration $t_{\text{OFF}} = 30$ min, consistent with ENTSO-E guidelines [7]. The resulting imbalance signal is (Equation (4.3)):

$$R_{\bar{t}}^{\text{trip}}(\mathbf{x}) = \sum_{a \in \Omega_G \cup \Omega_S} u_{a,\bar{t}} \cdot P_a + \sum_{r \in \Omega_R} u_{r,\bar{t}} \cdot P_r \cdot CF_r \tag{4.3}$$

where $\Omega_G$, $\Omega_S$, and $\Omega_R$ denote the sets of conventional generating units, storage units, and renewable technologies respectively; $u_{a,\bar{t}} \in \{0, 1\}$ is a binary indicator equal to 1 if asset $a$ trips at time step $\bar{t}$, and 0 otherwise.

The *forecasting uncertainty contribution* $R_{\bar{t}}^{\Delta f}$ captures the discrepancy between predicted and actual power for loads and variable renewable sources. Uncertainty distributions are modelled as Gaussian, with total standard deviation computed as a quadrature sum of linear contributions [2, 3] (Equation (4.4)):

$$\sigma_{\Delta f}(\mathbf{x}) = \sqrt{(\sigma_l \cdot L_l)^2 + \sum_{r \in \Omega_R} (\sigma_r \cdot P_r \cdot CF_r)^2} \tag{4.4}$$

where $\sigma_l$ and $\sigma_r$ are the normalised forecast error standard deviations of load and renewable technology $r$ respectively, $L_l$ is the load level in the current scenario, and $P_r \cdot CF_r$ is the generated power of technology $r$ in the current scenario. The forecasting uncertainty imbalance is sampled as (Equation (4.5)):

$$R_{\bar{t}}^{\Delta f}(\mathbf{x}) \sim \mathcal{N}[0,\, \sigma_{\Delta f}], \quad \forall\, \bar{t} \in \Omega_{MC} \tag{4.5}$$

The *VRD contribution* $R_{\bar{t}}^{\text{VRD}}$ accounts for the ramp of residual demand within each 15-minute market interval that is not captured by the interval-average dispatch signal. It is modelled as a sawtooth wave with semi-amplitude $A^{\text{VRD}}$ (Equation (4.6)):

$$R_{\bar{t}}^{\text{VRD}}(\mathbf{x}) = A^{\text{VRD}} \cdot 2 \cdot \left( \frac{\bar{t}}{t_{\text{VRD}}} - \left\lfloor \frac{\bar{t}}{t_{\text{VRD}}} + \frac{1}{2} \right\rfloor \right), \quad A^{\text{VRD}} = \frac{VRD}{t_{\text{VRD}} \cdot 2} \tag{4.6}$$

where $t_{\text{VRD}} = 15$ min is the market interval duration.

Four of the eight methodologies (Giglio, France, Nordic, and ERCOT) derive their reserve requirements from a Monte Carlo imbalance signal generated independently for each of the scenarios (Imbalance Model block in Figure 4.1), applying different statistical criteria to the same signal as described in Section 4.3. Two further methods (UCTE and $n$-sigma) do not use the Monte Carlo signal: their sizing equations depend directly on the load level and renewable capacity factors of each scenario, and are applied analytically to each one of the scenario-set (Scenario-based block in Figure 4.1). The remaining two methods (Zima and CESI) bypass the operating scenarios entirely: Zima derives a single system-level result from the generation fleet parameters, and CESI operates on four representative seasonal profiles (Input-based block in Figure 4.1).

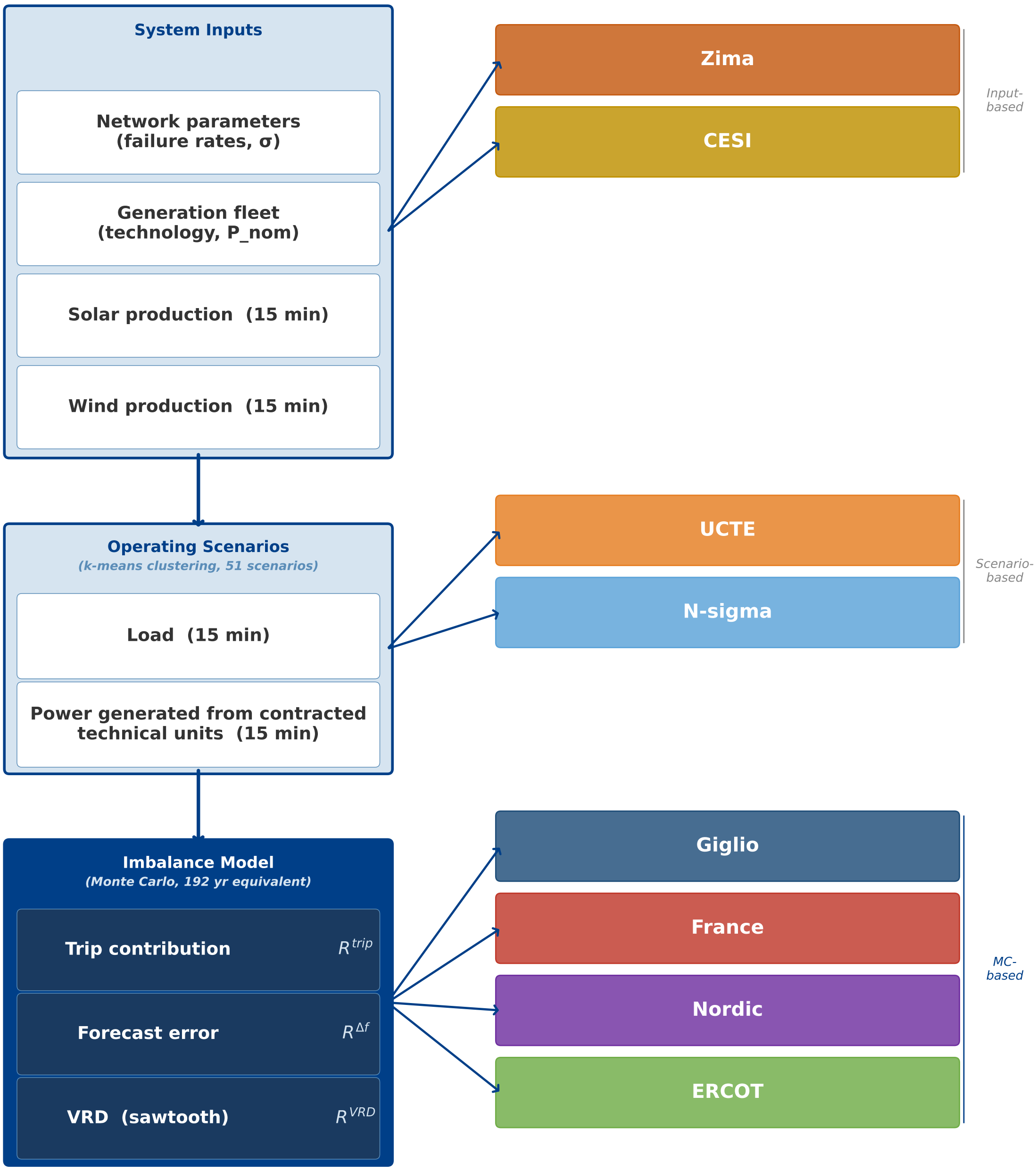


Figure 4.1: Computational framework of the comparative analysis.

## 4.3. Methodology Implementations

The Monte Carlo simulation described in Section 4.2 generates, for each operating scenario, a synthetic time series of 192 years of 1-minute system imbalance. This common signal is then processed differently by each methodology: the four Monte Carlo methods (Giglio et al.(2025), France, Nordic, and ERCOT) extract reserve requirements by applying different statistical criteria to its percentile structure, while UCTE and $n$-sigma apply analytical expressions directly to the scenario parameters, and Zima and CESI operate on their own dedicated inputs independently of the Monte Carlo signal.

### 4.3.1. Monte-Carlo Based Methods

#### Giglio et al. (2025)

The Giglio et al. method, whose stochastic imbalance model is described in Section 4.2, sizes the four reserve products by extracting percentiles from the Monte Carlo imbalance distribution. FCR is sized on the full imbalance signal $R_{\bar{t}}^{\text{imb}}$, which includes the tripping contribution and therefore captures contingency events. The slower reserve categories (aFRR, mFRR, RR) are instead sized on the residual imbalance $R_{\bar{t}}^{\Delta\text{imb}}$, obtained by subtracting the 15-minute running mean from $R_{\bar{t}}^{\text{imb}}$. This distinction reflects the different activation timescales of FCR, which must respond to contingency events in real time, and aFRR/mFRR, which address slower variability over longer horizons.

The four reserve requirements are defined as [81] (Equations (4.7)–(4.10)):

$$R^{\text{FCR}}(\mathbf{x}) = PC_{99}\big(R_{\bar{t}}^{\text{imb}}\big) \tag{4.7}$$

$$R^{\text{aFRR}}(\mathbf{x}) = PC_{95}\big(R_{\bar{t}}^{\Delta\text{imb}}\big) \tag{4.8}$$

$$R^{\text{mFRR}}(\mathbf{x}) = PC_{99}\big(R_{\bar{t}}^{\Delta\text{imb}}\big) - R^{\text{aFRR}}(\mathbf{x}) \tag{4.9}$$

$$R^{\text{RR}}(\mathbf{x}) = PC_{99.7}\big(R_{\bar{t}}^{\Delta\text{imb}}\big) - R^{\text{mFRR}}(\mathbf{x}) \tag{4.10}$$

where $PC_p$ denotes the $p$-th percentile of the distribution. The percentile level for FCR (99%) and aFRR (95%) is consistent with the ENTSO-E recommendation in the SAFA [7]; those for mFRR (99%) and RR (99.7%) are adopted by Giglio et al. [81], corresponding to increasing levels of statistical confidence in covering the imbalance.

#### France (RTE)

The French methodology for reserve dimensioning is defined in the RTE Load-Frequency Control Block Operational Agreement [29], specifically in Annex 1, which describes the rules in force until date $\text{RT}_{19}$. The methodology combines a deterministic contingency criterion for FCR with a statistical moving-average approach for aFRR.

FCR is sized deterministically as the largest generating unit online, here called Dimensioning Incident (DI) (Equation (4.11)):

$$R_{\text{FR}}^{\text{FCR}} = DI \tag{4.11}$$

aFRR is sized using a statistical method based on the deviation of the 1-minute average of the open-loop control deviation $\Delta E_{bo}$ from its 30-minute moving average (Equation (4.12)):

$$\Delta E_{30} = \text{MA}_{1\,\text{min}}(\Delta E_{bo}) - \text{MA}_{30\,\text{min}}(\Delta E_{bo}) \tag{4.12}$$

In the original RTE methodology, the upward aFRR requirement is set at the absolute value of the 1st percentile of $\Delta E_{30}$, and the downward requirement at the 99th percentile, producing an asymmetric sizing. In this implementation, $\Delta E_{bo}$ is approximated by the total system imbalance $R_{\bar{t}}^{\text{imb}}$, which does not distinguish between upward and downward contributions. A symmetric sizing at the 95th percentile of $|\Delta E_{30}|$ is therefore adopted (Equation (4.13)):

$$R_{\text{FR}}^{\text{aFRR}} = PC_{95}\left(\left|R_{\bar{t}}^{\text{imb}} - \text{MA}_{30}\left(R_{\bar{t}}^{\text{imb}}\right)\right|\right) \tag{4.13}$$

This approximation is consistent with the intent of the RTE methodology, which targets coverage of the fast variability component of the imbalance signal not captured by the 30-minute average.

mFRR is sized following the original RTE formulation in Annex 1 of the LFCBOA, as the difference between the positive dimensioning incident and the aFRR requirement already sized (Equation (4.14)):

$$R_{\text{FR}}^{\text{mFRR}} = DI - R_{\text{FR}}^{\text{aFRR}} \tag{4.14}$$

This reflects the RTE principle that mFRR is contracted to cover the residual portion of the dimensioning incident not already addressed by the automatic reserve, ensuring that the total FRR capacity is at all times sufficient to respond to the positive dimensioning incident.

### Nordic

The Nordic methodology for FRR dimensioning is defined in the explanatory document for the amended Nordic LFC block methodology [44]. It shares the same deterministic contingency criterion for FCR as the French methodology, but adopts a different signal for aFRR sizing based on the band between two moving averages of the imbalance at different timescales.

FCR is sized as the maximum between the stochastic component, computed following the same percentile criterion as the Giglio et al. model (Section 4.3.1), and the deterministic dimensioning incident (Equation (4.15)):

$$R_{\mathrm{NO}}^{\mathrm{FCR}} = \max\Big(PC_{99}\big(R_{\bar{t}}^{\mathrm{imb}}\big)\,,\ DI\Big) \tag{4.15}$$

aFRR is sized based on the so-called short-term imbalance, defined in the Nordic methodology as the difference between two rolling averages of the imbalance signal at timescales matching the full activation times of aFRR (5 min) and mFRR (15 min) respectively (Equation (4.16)):

$$\Delta E_{\mathrm{ST}} = \mathrm{MA}_5\big(R_{\bar{t}}^{\mathrm{imb}}\big) - \mathrm{MA}_{15}\big(R_{\bar{t}}^{\mathrm{imb}}\big) \tag{4.16}$$

This isolates the variability component that falls between the two FRR activation timescales: too fast to be captured by the 15-minute average, but smoothed out by the 5-minute average. The aFRR requirement is then set at (Equation (4.17)):

$$R_{\mathrm{NO}}^{\mathrm{aFRR}} = PC_{95}(|\Delta E_{\mathrm{ST}}|) \tag{4.17}$$

mFRR is derived as the residual between a total FRR requirement, sized at the 99th percentile of the absolute imbalance signal (Equation (4.18)), and the aFRR already sized (Equation (4.19)):

$$R_{\mathrm{NO}}^{\mathrm{FRR}} = PC_{99}\big(\big|R_{\bar{t}}^{\mathrm{imb}}\big|\big) \tag{4.18}$$

$$R_{\mathrm{NO}}^{\mathrm{mFRR}} = R_{\mathrm{NO}}^{\mathrm{FRR}} - R_{\mathrm{NO}}^{\mathrm{aFRR}} \tag{4.19}$$

The main difference from the French method is the aFRR signal: whereas RTE uses the deviation from a 30-minute average, the Nordic approach uses the band between the 5-minute and 15-minute averages, targeting specifically the variability band between the two FRR activation timescales.

### ERCOT

The ERCOT methodology for ancillary service sizing is defined in the Methodologies for Determining Minimum Ancillary Service Requirements document [73], with the ECRS product introduced through NPRR863 in June 2023 [75]. The ERCOT framework differs structurally from the European methods on two counts: it uses asymmetric products for upward and downward regulation, and it defines six distinct reserve products covering different activation timescales and contingency levels.

The implementation presented here is a proxy adaptation of the ERCOT methodology. The ERCOT methodology in its original form is grounded in the specific characteristics of the ERCOT system, including its islanded topology, its ACE-based regulation signal, and product-specific ramping obligations that have no direct equivalent in the *Comparative Reserve Sizing Framework* Monte Carlo output. The adaptations made in this implementation are described explicitly for each product below.

Primary Frequency Response (PFR) is sized deterministically as the dimensioning incident, consistent with the ERCOT approach of sizing the primary contingency reserve on the largest credible single contingency (Equation (4.20)):

$$R_{\mathrm{ER}}^{\mathrm{PFR}} = DI \tag{4.20}$$

Regulation Up and Regulation Down are sized on the positive and negative minute-to-minute variations of the imbalance signal respectively. In the original ERCOT methodology, these products are determined from the historical ACE signal and the net load variability of the ERCOT control area, with separate adjustment tables for wind and solar forecast error growth. Here they are approximated using the signed first differences of the Monte Carlo imbalance time series, capturing the fast variability component without system-specific ACE data (Equations (4.21)–(4.22)):

$$R_{\mathrm{ER}}^{\mathrm{RegUp}} = PC_{95}\big(\max\big(\Delta R_{\bar{t}}^{\mathrm{imb}}, 0\big)\big) \tag{4.21}$$

$$R_{\mathrm{ER}}^{\mathrm{RegDown}} = PC_{95}\big(\max\big(-\Delta R_{\bar{t}}^{\mathrm{imb}}, 0\big)\big) \tag{4.22}$$

where $\Delta R_{\bar{t}}^{\mathrm{imb}} = R_{\bar{t}+1}^{\mathrm{imb}} - R_{\bar{t}}^{\mathrm{imb}}$ denotes the 1-minute change in the imbalance signal.

Responsive Reserve Service (RRS) is sized as the residual between the larger of the dimensioning incident and the 99th percentile of the absolute imbalance signal, and the

Regulation Up already sized. This reflects the ERCOT requirement that RRS, combined with Regulation Up, must be sufficient to arrest frequency decline following the largest credible contingency (Equation (4.23)):

$$R_{\text{ER}}^{\text{RRS}} = \max\bigl(DI,\ PC_{99}\bigl(\bigl|R_{\bar{t}}^{\text{imb}}\bigr|\bigr)\bigr) - R_{\text{ER}}^{\text{RegUp}} \tag{4.23}$$

ERCOT Contingency Reserve Service (ECRS) was introduced in 2023 to provide a faster-activating contingency reserve bridging the gap between RRS and Non-Spin [75]. In the official ERCOT methodology, ECRS is computed as the sum of two components: a frequency recovery component derived from historical inertia conditions and large unit trip scenarios, and an intra-hour net load forecast uncertainty component based on the 90th percentile of historical intra-hour net load uncertainty. The frequency recovery component cannot be reproduced without system-specific inertia data. The implementation here therefore captures only the intra-hour uncertainty component, approximated as the 90th percentile of the deviation of the imbalance signal from its 10-minute moving average (Equation (4.24)):

$$R_{\text{ER}}^{\text{ECRS}} = PC_{90}\bigl(\bigl|R_{\bar{t}}^{\text{imb}} - \text{MA}_{10}\bigl(R_{\bar{t}}^{\text{imb}}\bigr)\bigr|\bigr) \tag{4.24}$$

Non-Spinning Reserve (Non-Spin) is sized as the residual at the 99.7th percentile of the absolute imbalance distribution, net of RRS and ECRS already sized, with a floor at zero (Equation (4.25)):

$$R_{\text{ER}}^{\text{NonSpin}} = \max\bigl(PC_{99.7}\bigl(\bigl|R_{\bar{t}}^{\text{imb}}\bigr|\bigr) - R_{\text{ER}}^{\text{RRS}} - R_{\text{ER}}^{\text{ECRS}},\ 0\bigr) \tag{4.25}$$

The floor at zero is applied because the residual can become negative when $DI$ is large relative to system size. Whether Non-Spin collapses to zero depends on the relationship between the dimensioning incident and the total system load.

## 4.3.2. Operating Scenario Based Methods

### UCTE

The UCTE methodology for reserve dimensioning is defined in Policy 1 of the UCTE Operation Handbook [1]. Among the methods that require no Monte Carlo simulation, it is the most parsimonious: all three reserve products are sized deterministically using only the dimensioning incident and the system load level.

FCR is sized as the dimensioning incident (Equation (4.26)):

$$R_{\mathrm{UC}}^{\mathrm{FCR}} = DI \tag{4.26}$$

aFRR is sized using the empirical square-root formula defined in the UCTE Operation Handbook, which relates the secondary reserve requirement to the maximum load of the control area (Equation (4.27)):

$$R_{\mathrm{UC}}^{\mathrm{aFRR}} = \sqrt{a \cdot L_{\max} + b^2} - b \tag{4.27}$$

where $L_{\max}$ is the maximum load of the control area in MW, and $a = 10$ MW and $b = 150$ MW are the empirical coefficients specified in the UCTE handbook. In this implementation, $L_{\max}$ is taken as the load value of each operating scenario, so the aFRR requirement varies across scenarios as a function of load level.

mFRR is sized as the residual between the dimensioning incident and the aFRR already sized, with a floor at zero (Equation (4.28)):

$$R_{\mathrm{UC}}^{\mathrm{mFRR}} = \max\bigl(DI - R_{\mathrm{UC}}^{\mathrm{aFRR}},\ 0\bigr) \tag{4.28}$$

Since $DI$ is fixed and $R_{\mathrm{UC}}^{\mathrm{aFRR}}$ is determined by the load-dependent UCTE formula, the floor condition $R_{\mathrm{UC}}^{\mathrm{mFRR}} \geq 0$ may or may not be binding depending on the system. This reflects the original design intent of the UCTE formula, which was calibrated for large interconnected systems where the secondary reserve is a small fraction of the contingency reserve.

### *n*-sigma Method

The $n$-sigma method is a parametric approach for reserve sizing based on the combined standard deviation of forecast errors across all uncertainty sources. The formulation adopted here follows Holttinen et al. [2], who describe it as the standard statistical approach then in use for systems with significant wind penetration (Section 3.2.2). The reliability factor $n_{\mathrm{RR}} = 3.5$ is taken from Ortega-Vazquez and Kirschen [3], who adopt this value to account for the heavier tails of wind forecast error distributions relative to a Gaussian approximation. Unlike the four Monte Carlo methods, the $n$-sigma method does not require a simulation infrastructure: reserve requirements are derived analytically from the system parameters and are computed for each of the operating scenarios, since the forecast error standard deviation of variable renewable sources depends on their mean produced power, which varies across scenarios.

The per-technology standard deviations in MW are computed following Ortega-Vazquez eq. (2) and Holttinen eq. (1) (Equation (4.29)):

$$\sigma_i = \sigma_i^{\%} \cdot P_{\text{mean},i} \tag{4.29}$$

where $\sigma_i^{\%}$ is the forecast error coefficient from `network_BE` and $P_{\text{mean},i}$ is the mean produced power of technology $i$ in the current scenario. For load, $P_{\text{mean,load}} = P_{\text{nom,Load}} = 13300$ MW, consistent with the calibration basis of $\sigma_L$. For variable renewables (Equation (4.30)):

$$P_{\text{mean},r} = n_{\text{mod},r} \cdot P_{\text{nom},r} \cdot \frac{CF_r}{100} \tag{4.30}$$

where $CF_r$ is the capacity factor of technology $r$ in the current scenario, taken from the `CombToStudy_BE_50` file.

Since the uncertainty sources are assumed statistically independent, the combined net demand standard deviation is (Holttinen eq. 1, Equation (4.31)):

$$\sigma_{\text{net}} = \sqrt{\sigma_{\text{load}}^2 + \sigma_{\text{wind,off}}^2 + \sigma_{\text{wind,on}}^2 + \sigma_{\text{solar}}^2} \tag{4.31}$$

Reserve requirements are derived by applying reliability factors $n$ to $\sigma_{\text{net}}$, with each product covering an incremental band of the combined distribution (Holttinen eq. 2, Equations (4.32)–(4.34)):

$$R_{\text{NS}}^{\text{aFRR}} = n_{\text{aFRR}} \cdot \sigma_{\text{net}} \tag{4.32}$$

$$R_{\text{NS}}^{\text{mFRR}} = (n_{\text{mFRR}} - n_{\text{aFRR}}) \cdot \sigma_{\text{net}} \tag{4.33}$$

$$R_{\text{NS}}^{\text{RR}} = (n_{\text{RR}} - n_{\text{mFRR}}) \cdot \sigma_{\text{net}} \tag{4.34}$$

The reliability factors are consistent with the percentile levels used throughout this comparative analysis: $n_{\text{aFRR}} = \Phi^{-1}(0.95) = 1.645$, $n_{\text{mFRR}} = \Phi^{-1}(0.99) = 2.326$, and $n_{\text{RR}} = 3.5$ following Ortega-Vazquez eq. (15) [3].

FCR is not defined in this framework and is not computed.

The wind-induced incremental reserve, introduced by Holttinen et al. [2] as a measure of the additional reserve attributable to variable renewable integration, is computed as (Equation (4.35)):

$$\Delta R_{\mathrm{NS}}^{\mathrm{wind}} = n_{\mathrm{RR}} \cdot (\sigma_{\mathrm{net}} - \sigma_{\mathrm{load}}) \tag{4.35}$$

This quantity serves as an indicator of the sensitivity of the $n$-sigma sizing to renewable penetration across scenarios.

### 4.3.3. System Input Based Methods

#### Zima, Koch and Andersson (2008)

The method of Zima, Koch and Andersson [82], described in Section 3.2.1, produces a single system-level reserve requirement derived from the statistical properties of the load and the failure rates of the generation fleet, without reference to the Monte Carlo imbalance signal. The reserve is sized for the full system rather than for individual operating scenarios, consistent with the original formulation where the input is the system size $P_{\mathrm{system}}$ rather than a specific dispatch state.

In this implementation, $P_{\mathrm{system}}$ is set equal to the maximum load capacity of the reference system, $P_{\mathrm{system}} = P_{\mathrm{nom,Load}} = 13300$ MW, taken from the `network_BE` file. The total load standard deviation is (Equation (4.36)):

$$\sigma_{\mathrm{load}} = \sigma_L \cdot P_{\mathrm{system}} \tag{4.36}$$

where $\sigma_L = 1.64\%$ is the load forecast error coefficient from `network_BE`, calibrated on the reference year load data. Since the `network_BE` file provides a single standard deviation for load combining both spontaneous load variations and load forecast error, while Zima treats these as separate inputs, the total is split equally between the two components (Equation (4.37)):

$$\sigma_{\mathrm{lsv}} = 0.5 \cdot \sigma_{\mathrm{load}}, \qquad \sigma_{\mathrm{lfe}} = 0.5 \cdot \sigma_{\mathrm{load}} \tag{4.37}$$

This 50/50 split is a conservative approximation; a sensitivity analysis of the results to this choice is left for future work.

aFRR, corresponding to secondary reserve covering spontaneous load variations over a 15-minute horizon, is sized at the 95th percentile of the distribution obtained by convolving the Gaussian load variability component with the discrete outage distribution over 15 minutes (Equation (4.38)):

$$R_{\mathrm{ZI}}^{\mathrm{aFRR}} = PC_{95}\big(\mathcal{N}[0,\, \sigma_{\mathrm{lsv}}] * f_{\mathrm{out}}^{15}\big) \tag{4.38}$$

where $f_{\mathrm{out}}^{15}$ is the discrete probability distribution of total outage power over a 15-minute timeframe, constructed by convolving independent Binomial distributions across generator types (Equation (4.39)):

$$p_{\mathrm{tf},a} = 1 - \left(1 - \mu_a^{\mathrm{trip}}\right)^{t_{\mathrm{tf}}} \tag{4.39}$$

with $t_{\mathrm{tf}} = 15$ min for secondary and $t_{\mathrm{tf}} = 60$ min for tertiary reserves, and the number of outaged units per type following Binomial$(n_{\mathrm{mod}}, p_{\mathrm{tf},a})$.

mFRR covers the tertiary horizon (60 min) and incorporates both spontaneous load variations and load forecast error. The combined tertiary standard deviation is (Equation (4.40)):

$$\sigma_{\mathrm{ter}} = \sqrt{\sigma_{\mathrm{lsv}}^2 + \sigma_{\mathrm{lfe}}^2} \tag{4.40}$$

mFRR is the incremental reserve between the 99th and 95th percentile levels of the tertiary combined distribution (Equation (4.41)):

$$R_{\mathrm{ZI}}^{\mathrm{mFRR}} = PC_{99}\big(\mathcal{N}[0,\, \sigma_{\mathrm{ter}}] * f_{\mathrm{out}}^{60}\big) - R_{\mathrm{ZI}}^{\mathrm{aFRR}} \tag{4.41}$$

RR is the further incremental at the 99.7th percentile (Equation (4.42)):

$$R_{\mathrm{ZI}}^{\mathrm{RR}} = PC_{99.7}\big(\mathcal{N}[0,\, \sigma_{\mathrm{ter}}] * f_{\mathrm{out}}^{60}\big) - R_{\mathrm{ZI}}^{\mathrm{aFRR}} - R_{\mathrm{ZI}}^{\mathrm{mFRR}} \tag{4.42}$$

FCR is not defined in the Zima framework and is not computed here.

Two structural limitations of this implementation are noted. First, the method does not incorporate forecast errors from variable renewable generation: only the load contributes to the Gaussian component, consistent with the 2008 paper but not representative of a system with significant wind and solar penetration. Second, the single system-level nature of the calculation means that the result does not vary with the renewable capacity factor or the commitment state of the system, unlike all other methods in this comparison. Both limitations are relevant to interpreting the results in Chapter 5.

#### CESI

The last methodology included in this comparative analysis was developed internally at CESI SpA and is not publicly available. For this reason, the underlying equations and parametrisation cannot be reproduced here, and is therefore included on the basis of its numerical results only.

From a structural standpoint, the CESI methodology differs from the other methods described above in two ways. First, it produces asymmetric reserve requirements, sizing the upward and downward reserves independently rather than applying a single symmetric estimate. Second, it operates on four seasonal operating profiles: hot day, hot night, cold day, and cold night, each representing a distinct combination of load level and generation mix. For each profile, the methodology produces an hourly time series of upward and downward reserve requirements, from which a representative sizing value is derived statistically. The resulting reserve volumes are incorporated into the comparative analysis in Chapter 5.

## 4.4. Reference System and Input Data

### 4.4.1. The reference system

The case study is built around data from the Belgian power system for the year 2024, published by Elia, the Belgian TSO, through its open data portal. Belgium was selected primarily for the breadth and quality of its publicly available operational data: Elia publishes quarter-hourly time series for total load, generation by fuel type and connection level, and separate renewable output series for solar, onshore wind, and offshore wind, all under a consistent methodology. The year 2024 was chosen as the reference period on account of its completeness and recency.

The results of this chapter *do not represent or approximate the actual reserve requirements of the Belgian system*, and are not comparable with published Belgian procurement figures. Belgium is a deeply interconnected system that participates in cross-border reserve sharing arrangements, including the IGCC imbalance netting mechanism and the PICASSO and MARI platforms for aFRR and mFRR exchange. These mechanisms substantially reduce the reserve volumes that Elia holds domestically. Throughout the analysis, the reference system is treated as electrically isolated: this is a deliberate methodological choice to hold system conditions constant across all methods, not a description of how Belgium actually operates.

Two scalar parameters are derived from the reference system and applied uniformly across all methodologies. The dimensioning incident is set to $DI = 1013$ MW, corresponding to the NU_1 nuclear unit, the largest generating unit online in the reference system. The variation of residual demand is set to $VRD = 580$ MW, derived as the 99.7th percentile of the absolute quarter-hourly changes in residual demand over the 2024 Elia dataset.

## 4.4.2. Input files and parameters

The model takes two input files and a set of scalar parameters derived from the 2024 Elia dataset.

### Generation park: `network_BE`

The first input file defines the generation park of the reference system. Each row corresponds to a technology cluster, characterised by the available nominal power per unit ($P_{\text{nom}}$, MW), the annual failure rate ($\lambda_a$, trips/yr), the forecast error standard deviation ($\sigma_r$), and the number of units assumed online ($n_{\text{mod}}$). All parameters are reported in Table 4.1.

Table 4.1: Generation park of the reference system.
$P_{\text{nom}}$: available nominal power per unit; $\lambda_a$: annual failure rate; $\sigma$: forecast error standard deviation; $n_{\text{mod}}$: maximum units online. Sources for $\lambda_a$: [86] (CCGT, OCGT, NU, CHP, PSP, TJ, WASTE); [87] (HYDRO); [88] (WIND_offshore); [81] (SOLAR, WIND_onshore, BESS).

| Component | Type | $P_{\text{nom}}$ (MW) | $\lambda_a$ (trips/yr) | $\sigma$ (%) | $n_{\text{mod}}$ |
|---|---|---|---|---|---|
| BESS | Store | 37.6 | 0.80 | – | 2 |
| CCGT | Generator | 325.0 | 9.40 | – | 14 |
| CHP_1 | Generator | 139.1 | 2.90 | – | 2 |
| CHP_2 | Generator | 46.1 | 2.90 | – | 13 |
| CHP_3 | Generator | 15.3 | 2.90 | – | 6 |
| NU_1 | Generator | 1013.0 | 1.30 | – | 3 |
| NU_2 | Generator | 445.0 | 1.30 | – | 2 |
| OCGT | Generator | 56.2 | 9.20 | – | 6 |
| HYDRO | Generator | 7.2 | 1.46 | – | 12 |
| PSP_1 | Store | 36.0 | 6.70 | – | 4 |
| PSP_2 | Store | 194.0 | 6.70 | – | 6 |
| SOLAR | Generator | 99.0 | 0.40 | 4.15 | 1 |
| TJ | Generator | 19.6 | 3.20 | – | 9 |
| WASTE | Generator | 22.2 | 2.90 | – | 11 |
| WIND_offshore | Generator | 226.0 | 2.19 | 8.09 | 10 |
| WIND_onshore | Generator | 28.0 | 0.80 | 6.18 | 11 |
| LOAD | Load | 13300 | – | 2.43 | 1 |

### Operating scenarios: `CombToStudy_BE_50`

The second input file defines the operating scenarios that form the common basis for six of the eight methodologies. As said before, the number of scenarios is determined by applying the elbow criterion to the within-cluster sum of squares (WCSS) as a function of $k$; for the Belgian 2024 dataset this yields $k = 51$ representative operating conditions. For the four Monte Carlo methods (Giglio, France, Nordic, ERCOT), each scenario drives a separate simulation run; for UCTE and $n$-sigma, the same scenarios provide the load and renewable capacity factor values used in the analytical sizing expressions.

Each scenario specifies the number of units online for the dispatchable technologies whose commitment varies across the year, the capacity factors of offshore wind, onshore wind, and solar, the total system load and the weight in hours per year ($w_t$). The 51 scenarios span the full range of operating conditions observed in 2024, from low-load high-solar summer conditions to the peak-load winter evening recorded on 10 December 2024 (S51). All scenarios are briefly presented in Table 4.2.

Table 4.2: Summary of the 51 operating scenarios.
A complete description of each scenario is provided in Appendix A.

| ID | Wt (%) | Load (MW) | Dom. feature | Season |
|---|---|---|---|---|
| S01 | 0.9 | 3193 | Low Nuclear | All |
| S02 | 1.5 | 3280 | High Solar | Sum |
| S03 | 1.6 | 3658 | High Solar | Sum |
| S04 | 6.1 | 4068 | Low Nuclear | All |
| S05 | 3.2 | 4227 | Low Nuclear | Spr/Fall |
| S06 | 2.0 | 4388 | High Solar | Sum |
| S07 | 2.8 | 4485 | Low Nuclear | All |
| S08 | 0.9 | 4548 | High Solar | Sum |
| S09 | 3.5 | 4713 | Low Nuclear | All |
| S10 | 1.0 | 4797 | Low Nuclear | All |
| S11 | 0.8 | 4842 | Low Nuclear | All |
| S12 | 1.4 | 4864 | Low Nuclear | All |
| S13 | 3.3 | 4901 | High Solar | Sum |
| S14 | 3.5 | 4949 | Off-peak / Night | Spr/Fall |
| S15 | 2.0 | 4976 | Low Nuclear | All |
| S16 | 1.3 | 4996 | Low Nuclear | All |
| S17 | 7.6 | 5026 | Off-peak / Night | All |
| S18 | 2.6 | 5391 | Off-peak / Night | All |
| S19 | 1.1 | 5485 | Low Nuclear | All |
| S20 | 3.0 | 5526 | Mid-load Baseload | All |
| S21 | 1.5 | 5584 | High Solar | Sum |
| S22 | 2.6 | 5618 | Low Nuclear | All |
| S23 | 1.9 | 5665 | Mid-load Baseload | All |
| S24 | 0.6 | 5754 | Low Nuclear | All |
| S25 | 3.6 | 5766 | High Wind Offshore | Win/Fall |
| S26 | 1.6 | 5854 | High Wind Offshore | Sum |

| ID | Wt (%) | Load (MW) | Dom. feature | Season |
|---|---|---|---|---|
| S27 | 1.5 | 5856 | Low Nuclear | Win/Fall |
| S28 | 1.0 | 5885 | Wind-dominated | All |
| S29 | 1.1 | 5891 | High Wind Offshore | Win/Fall |
| S30 | 2.8 | 5987 | Mid-load Baseload | All |
| S31 | 1.6 | 6056 | Mid-load Baseload | All |
| S32 | 1.4 | 6157 | High Wind Offshore | Win/Fall |
| S33 | 1.7 | 6458 | Mid-load Baseload | Win/Fall |
| S34 | 2.5 | 6518 | High Wind Offshore | Win/Fall |
| S35 | 0.9 | 6591 | High Solar | Sum |
| S36 | 2.5 | 6691 | High Wind Offshore | Win/Fall |
| S37 | 3.1 | 6710 | Mid-load Baseload | All |
| S38 | 2.1 | 6959 | Low Nuclear | All |
| S39 | 0.8 | 7023 | Mid-load Baseload | Win/Fall |
| S40 | 2.6 | 7061 | High Wind Offshore | Win/Fall |
| S41 | 1.6 | 7090 | Low Nuclear | All |
| S42 | 1.0 | 7155 | High Wind Offshore | Win/Fall |
| S43 | 1.3 | 7156 | High Wind Offshore | Win/Fall |
| S44 | 1.1 | 7373 | Mid-load Baseload | All |
| S45 | 1.1 | 7381 | Low Nuclear | Win/Fall |
| S46 | 1.5 | 7456 | Low Nuclear | All |
| S47 | 0.9 | 7642 | Low Nuclear | All |
| S48 | 2.3 | 8221 | High Gas Demand | All |
| S49 | 0.8 | 8776 | High Wind Offshore | Win/Fall |
| S50 | 0.8 | 9054 | High Gas Demand | All |
| S51 | 0.07 | 10500 | Peak Load (Dec 10) | Win |
| tot | 99.97 | | | |

# 5 | Results and Comparative Analysis

This chapter presents the reserve sizing results obtained by applying the methodologies described in Chapter 4. Section 5.1 reports an overview of the results of all the methods and reserve categories together with a chart representing how much impact each contribution (tripping, forecasting uncertainty, VRD) has on the total imbalance for the methods based on the Monte Carlo imbalance. In the following Sections 5.1.1–5.1.4, tables with the minimum, weighted mean and maximum values of reserve across all scenarios are reported for each method and reserve product, where the weights correspond to the number of hours per year assigned to each scenario ($w_t$). For Zima, which produces a single static estimate, the three statistics are identical. For the N-sigma method, the three values refer to the range across all the scenarios. For CESI, which operates on four seasonal profiles and produces asymmetric upward and downward estimates, the minimum and maximum are taken across the four profiles and both directions are reported separately. The dependence of reserve requirements on system load and renewable penetration is then examined in Sections 5.2 and 5.3.

## 5.1. Overview

Figure 5.1 provides an overview of the results across all methods and all four reserve categories. Each panel shows the weighted mean and scenario range for each method, allowing a first comparison across the full set of methodologies before the detailed analysis in the following sections.

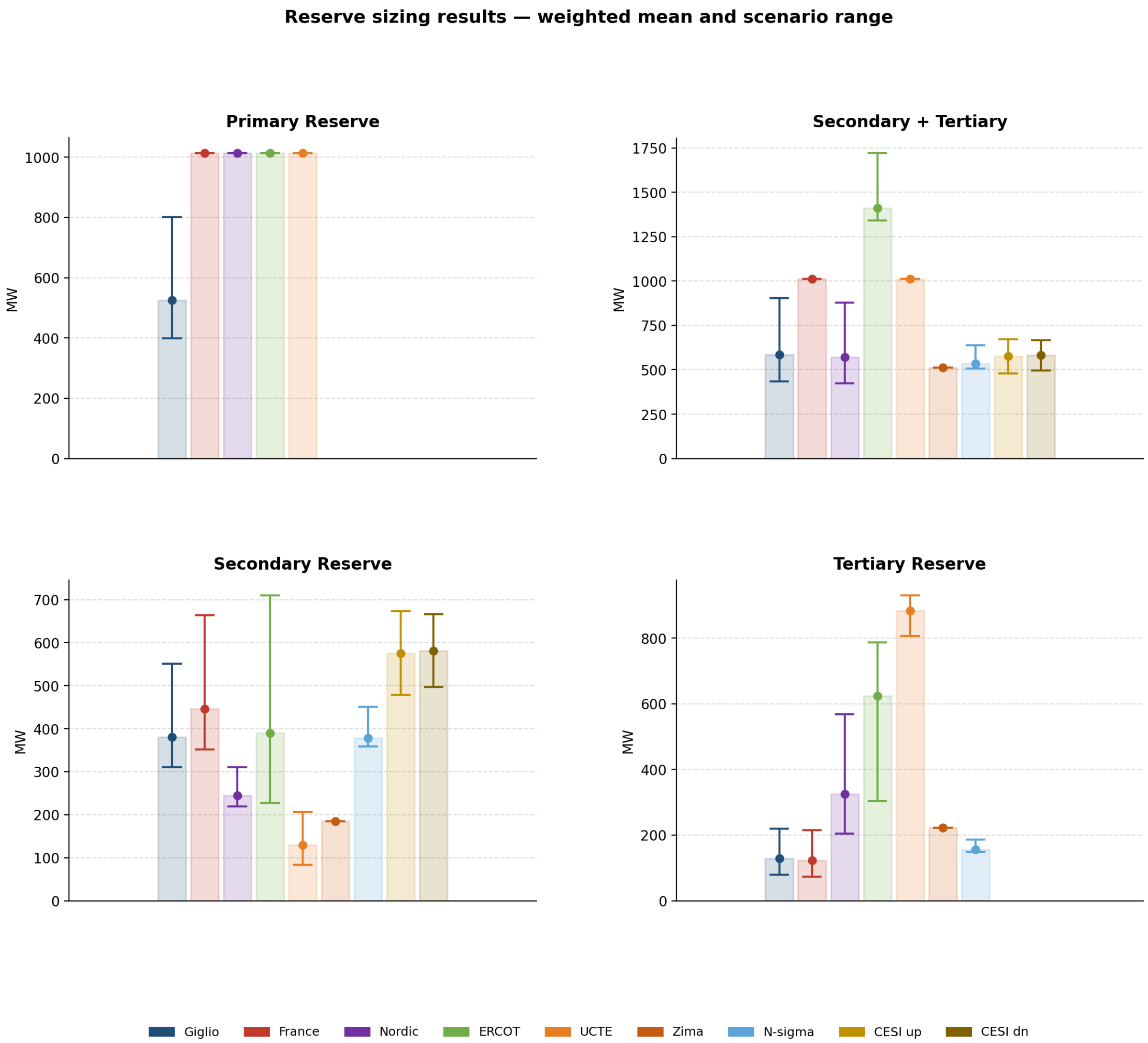


Figure 5.1: Overview of reserve sizing results. Each panel shows the weighted mean (filled circle) and scenario range (T-bar) for each method and reserve category. Primary reserve not available for Zima, N-sigma and CESI.

As explained in Chapter 4, the Giglio, France, Nordic and ERCOT methodologies base their reserve sizing on a Monte Carlo imbalance signal, which combines three distinct error contributions: the tripping contribution from generating unit outages, the forecasting uncertainty from renewable and load forecast errors, and the VRD contribution from the variation of residual demand. Figure 5.2 shows the relative magnitude of each contribution across the 51 operating scenarios, together with the $PC_{99}$ of the total imbalance signal that determines the Giglio FCR.

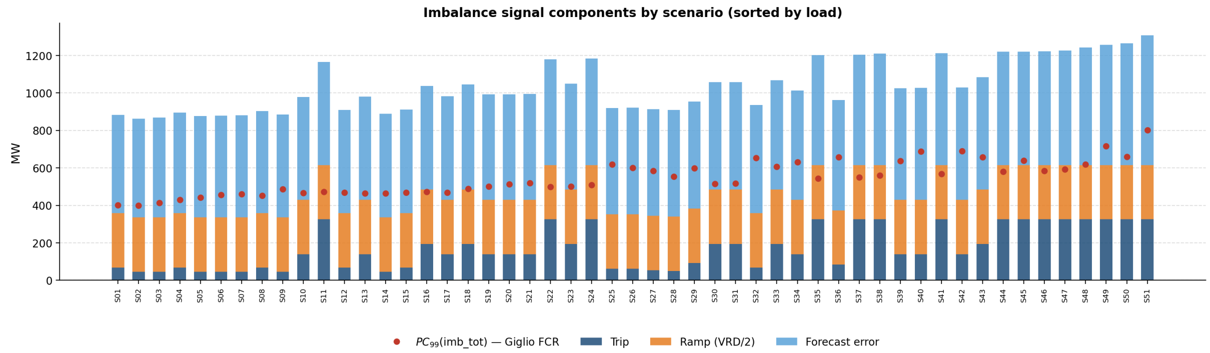


Figure 5.2: Decomposition of the Monte Carlo imbalance signal into its three components across the 51 operating scenarios, sorted by system load. Stacked bars show the tripping (dark blue), ramp (orange) and forecast error (light blue) contributions. Red markers show the $PC_{99}$ of the total imbalance signal (Giglio FCR).

The figure shows that the forecast error component (light blue) is the dominant contribution to the total imbalance in all scenarios, reflecting the combined effect of renewable and load forecast uncertainty across the 51 operating conditions. The ramp component (orange), derived from the variation of residual demand ($VRD = 580$ MW), is constant across all scenarios by construction, as it depends only on the fixed VRD parameter and not on the specific generation mix. The tripping contribution (dark blue) is instead scenario-dependent: it is determined by the number and size of units online in each scenario, and therefore increases with system load. This explains the strong positive relationship between load and Giglio FCR observed in Section 5.2: as load grows, more large units are online, increasing the tripping contribution and pushing the 99th percentile of the total imbalance upward.

The red markers show the $PC_{99}$ of the total imbalance signal, which represents the Giglio FCR as implemented in this study. The markers are systematically lower than the sum of the three analytical components, reflecting the fact that the three sources of imbalance do not simply add up in time: they partially compensate each other across the minute-by-minute simulation, so the actual percentile of the combined signal is lower than what a linear superposition would suggest.

### 5.1.1. Primary Reserve

Table 5.1: Primary reserve sizing results. Min, weighted mean and max across the 51 operating scenarios, expressed in MW.
Nordic FCR-N covers normal frequency deviations; Nordic FCR-D covers the dimensioning incident. Zima, N-sigma and CESI do not produce a primary reserve estimate.

| Method | Product | Min (MW) | Mean (MW) | Max (MW) |
|---|---|---|---|---|
| Giglio | FCR | 398.1 | 525.7 | 801.8 |
| France | FCR | 1013.0 | 1013.0 | 1013.0 |
| Nordic | FCR-N | 398.1 | 525.7 | 801.8 |
| Nordic | FCR-D | 1013.0 | 1013.0 | 1013.0 |
| ERCOT | PFR | 1013.0 | 1013.0 | 1013.0 |
| UCTE | FCR | 1013.0 | 1013.0 | 1013.0 |
| Zima | N/A | – | – | – |
| N-sigma | N/A | – | – | – |
| CESI | N/A | – | – | – |

The primary reserve results illustrate the fundamental distinction between methods that size FCR for normal system operation and those that size it for contingency events. Four methods (France, ERCOT and UCTE, plus the Nordic FCR-D), set the primary reserve equal to the dimensioning incident ($DI = 1013$ MW), treating it as the binding constraint regardless of operating conditions. The Giglio FCR and the Nordic FCR-N take a different approach, sizing the primary reserve probabilistically at the 99th percentile of the Monte Carlo imbalance distribution. The resulting values range from 398.1 MW to 801.8 MW across the 51 scenarios, with a weighted mean of 525.7 MW, substantially below the deterministic threshold.

This difference reflects two distinct design philosophies. The deterministic approach guarantees that the system can absorb the loss of the largest unit under any operating condition, at the cost of potentially over-sizing the reserve relative to the actual statistical risk. The probabilistic approach sizes the reserve to cover the combined effect of all imbalance sources at a given confidence level, which includes the tripping contribution but does not force coverage of the full dimensioning incident in every scenario.

### 5.1.2. Secondary and Tertiary Reserve

Table 5.2: Secondary and Tertiary reserve across the 51 operating scenarios.
For Giglio, the total includes RR. For ERCOT, the total is Reg Up + RRS + ECRS + Non-Spin. For CESI, values refer to the final sizing result across the four seasonal profiles. All values in MW.

| Method | Product | Min (MW) | Mean (MW) | Max (MW) |
|---|---|---|---|---|
| Giglio | FRR + RR | 435.2 | 585.7 | 903.9 |
| France | FRR | 1013.0 | 1013.0 | 1013.0 |
| Nordic | FRR | 424.2 | 569.8 | 878.9 |
| ERCOT | AS total | 1342.4 | 1410.3 | 1720.6 |
| UCTE | FRR | 1013.0 | 1013.0 | 1013.0 |
| Zima | FRR + RR | 511.8 | 511.8 | 511.8 |
| N-sigma | FRR | 507.9 | 534.7 | 636.8 |
| CESI | Upward | 478.1 | 575.4 | 672.8 |
| CESI | Downward | 496.8 | 581.4 | 665.9 |

The Secondary plus Tertiary results reveal three broad groupings. Giglio and Nordic produce the lowest estimates, with weighted means of 585.7 MW and 569.8 MW respectively, and show a substantial degree of scenario variability. The slight difference between the two methods arises from their structure: while both size the total FRR at the 99th percentile of the imbalance distribution, Giglio includes the Replacement Reserve (weighted mean 75.7 MW) as an additional layer above mFRR, whereas Nordic does not, resulting in a marginally higher total for Giglio. France and UCTE are fixed at 1013 MW by construction, as their mFRR formula forces FRR to equal $DI$ regardless of the aFRR value. ERCOT produces the highest total at approximately 1410 MW, reflecting the cumulative effect of its six ancillary service products: unlike the European frameworks, which size a single FRR total and decompose it into aFRR and mFRR, the ERCOT methodology stacks six independently sized products (PFR, Regulation Up, Regulation Down, RRS, ECRS and Non-Spin), each targeting a different timescale or contingency type, so their sum exceeds the FRR total of any single-product framework.

The Zima and N-sigma academic methods occupy an intermediate position, producing FRR estimates in the range of 508 to 637 MW, substantially above Giglio and Nordic but well below the deterministic methods. The CESI results (478 to 673 MW upward, 497 to 666 MW downward) fall in a similar range, though the asymmetric structure and seasonal differentiation of the CESI methodology make a direct comparison with the other methods difficult.

### 5.1.3. Secondary Reserve

Table 5.3: Secondary reserve sizing results across the 51 operating scenarios. For CESI, values refer to the final sizing result across the four seasonal profiles. All values in MW.

| Method | Product | Min (MW) | Mean (MW) | Max (MW) |
|---|---|---|---|---|
| Giglio | aFRR | 310.7 | 381.0 | 551.2 |
| France | aFRR | 351.5 | 446.7 | 663.6 |
| Nordic | aFRR | 219.7 | 245.1 | 310.4 |
| ERCOT | Reg Up | 226.9 | 389.7 | 709.6 |
| ERCOT | Reg Down | 474.1 | 513.5 | 745.1 |
| UCTE | aFRR | 83.3 | 130.0 | 207.1 |
| Zima | aFRR | 184.7 | 184.7 | 184.7 |
| N-sigma | aFRR | 359.2 | 378.2 | 450.4 |
| CESI | Upward | 478.1 | 575.4 | 672.8 |
| CESI | Downward | 496.8 | 581.4 | 665.9 |

Giglio, France and Nordic show the most moderate aFRR estimates, with weighted means of 381.0, 446.7 and 245.1 MW respectively, though their scenario ranges differ markedly. Giglio aFRR spans from 310.7 to 551.2 MW, reflecting the strong dependence of the tripping contribution on the online generation mix across scenarios. France is systematically higher than Giglio, as the $MA_{30}$ signal retains a contribution from the tripping component. Nordic is the lowest of the three, isolating only the variability band between the 5-minute and 15-minute activation timescales, with a range of 219.7 to 310.4 MW.

The UCTE aFRR shows the widest scenario range (83.3 to 207.1 MW) as the only method that sizes the secondary reserve as a direct function of load. The ERCOT framework stands apart through its asymmetric structure: Regulation Up (226.9 to 709.6 MW) spans a wide range driven by the minute-to-minute upward variability of the imbalance signal, while Regulation Down (474.1 to 745.1 MW) is systematically higher, reflecting the directional imbalance characteristics of the ERCOT system that are not captured by the symmetric Giglio imbalance model.

The Zima aFRR (184.7 MW) falls below the Giglio-France-Nordic range, consistent with its static probabilistic foundation. The N-sigma method (359.2 to 450.4 MW) and CESI (478 to 673 MW) produce substantially higher estimates.

### 5.1.4. Tertiary Reserve

Table 5.4: Tertiary reserve sizing results across the 51 operating scenarios.
mFRR results are reported first, followed by RR and equivalent products. All values in MW.

| Method | Product | Min (MW) | Mean (MW) | Max (MW) |
|---|---|---|---|---|
| Giglio | mFRR | 79.9 | 129.0 | 219.6 |
| France | mFRR | 349.4 | 566.3 | 661.5 |
| Nordic | mFRR | 204.4 | 324.6 | 568.3 |
| ERCOT | RRS | 303.4 | 623.3 | 786.1 |
| ERCOT | ECRS | 329.4 | 397.2 | 560.0 |
| ERCOT | Non-Spin | 0.0 | 0.1 | 147.5 |
| UCTE | mFRR | 805.9 | 883.0 | 929.7 |
| Zima | mFRR | 223.1 | 223.1 | 223.1 |
| N-sigma | mFRR | 148.7 | 156.5 | 186.4 |
| Giglio | RR | 44.5 | 75.7 | 133.1 |
| Zima | RR | 104.0 | 104.0 | 104.0 |
| N-sigma | RR | 256.4 | 269.9 | 321.4 |

The tertiary reserve results show the largest spread of the comparison. The Giglio mFRR (weighted mean 129.0 MW) and RR (75.7 MW) are the lowest among the stochastic methods, as the framework allocates a substantial share of the slow-variability imbalance to aFRR through the percentile decomposition, leaving a smaller residual for the tertiary products.

The France mFRR (349.4 to 661.5 MW) shows a wide scenario range, computed as $DI -$

$R_{\mathrm{FR}}^{\mathrm{aFRR}}$. Since the France aFRR varies considerably across scenarios (351.5 to 663.6 MW), the mFRR residual is correspondingly variable. The Nordic mFRR (204.4 to 568.3 MW) is of comparable magnitude, reflecting the larger FRR target used by Nordic relative to Giglio.

The ERCOT tertiary products show a different structure from all other methods. RRS (303.4 to 786.1 MW) is the dominant component with a wide range driven by the scenario-dependent imbalance distribution. ECRS (329.4 to 560.0 MW) also shows substantial variability, reflecting its dependence on system inertia conditions and intra-hour uncertainty across scenarios. Non-Spin is zero in all scenarios except the highest-load conditions, where it reaches up to 147.5 MW as the residual at the 99.7th percentile exceeds the combined RRS and ECRS coverage. The UCTE mFRR (805.9 to 929.7 MW) shows the widest scenario range of all methods, driven by the load-dependent aFRR formula: at low load, a smaller aFRR leaves a larger mFRR residual.

The Zima and N-sigma tertiary estimates occupy a middle ground. The Zima mFRR (223.1 MW) and RR (104.0 MW) are moderate values consistent with its probabilistic foundation. The N-sigma mFRR (148.7 to 186.4 MW) and RR (256.4 to 321.4 MW) are broadly consistent with Zima, suggesting reasonable agreement between the two probabilistic academic approaches on the tertiary reserve component.

## 5.2. Dependence on System Load

The 51 operating scenarios cover a load range from approximately 3200 MW to 10500 MW, providing a natural basis for examining how each method responds to changing demand conditions. The relationship between load and reserve is not uniform across methods: some produce requirements that are essentially constant regardless of load level, while others show a clear positive correlation. Understanding this dependence is relevant for planning purposes, as it determines whether a method can capture the higher reserve needs that typically accompany peak demand conditions.

### 5.2.1. Primary Reserve

Figure 5.3 shows the FCR requirement as a function of system load for all methods. Four of the five methods return the fixed value of $DI = 1013$ MW regardless of operating conditions. Only the Giglio FCR responds to load, increasing from approximately 398 MW at the lowest load scenarios to approximately 802 MW at the highest. The trend line confirms a strong positive relationship: a load increase of roughly 7000 MW (from the lightest to the heaviest scenario) is associated with an FCR increase of approximately 400 MW.

The insensitivity of the deterministic methods is by design: FCR is anchored to the dimensioning incident, which does not depend on how much load is currently on the system. The Giglio FCR increases strongly with load because higher load scenarios in the reference system coincide with higher online generation capacity and therefore a larger aggregate tripping contribution to the imbalance distribution, pushing the 99th percentile upward. The relationship is substantial, suggesting that load level is the primary driver of FCR variability in the Giglio framework.

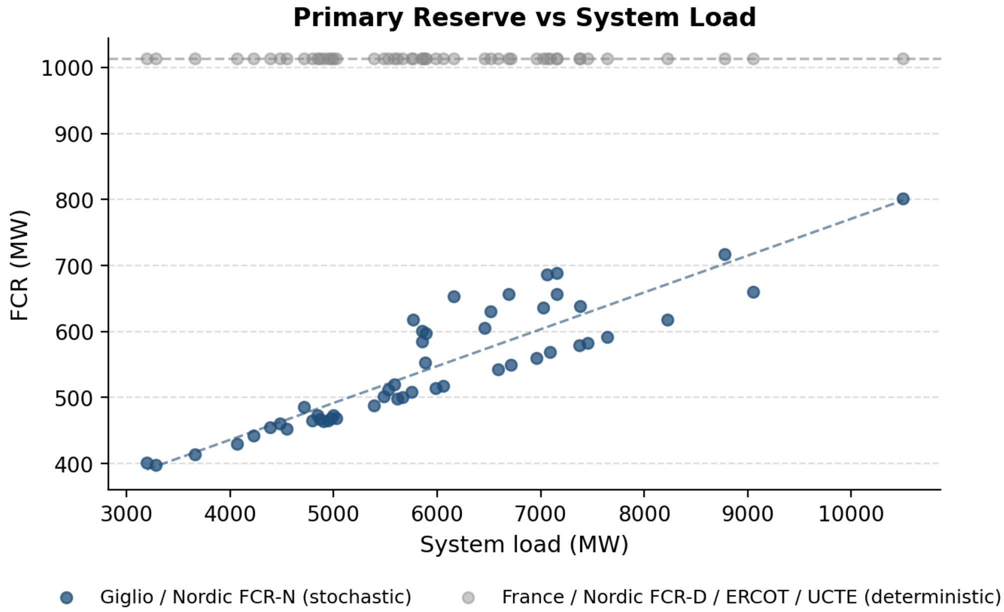


Figure 5.3: Primary reserve as a function of system load.
Dashed lines indicate linear trend fits. The grey horizontal line represents the deterministic value adopted by France, Nordic FCR-D, ERCOT and UCTE.

### 5.2.2. Secondary Reserve

Figure 5.4 shows the secondary reserve as a function of load. AS expected, the UCTE method stands out as the one with the strongest and structurally determined positive dependence on load: since aFRR is computed as $\sqrt{aL + b^2} - b$, it grows monotonically with $L_{\max}$, and the trend line traces this relationship closely across the full load range. The four Monte Carlo methods (Giglio, France, Nordic, and ERCOT) all show a positive trend with load, though through different mechanisms and with different magnitudes, as discussed below.

The Giglio, France and Nordic aFRR estimates span a wide range across scenarios, driven by the strong dependence of the imbalance signal on the online generation mix. While the three methods differ in their sizing signals (the $MA_{30}$ deviation for France, the $MA_5$–$MA_{15}$ band for Nordic, and the percentile-based decomposition for Giglio), all show a positive trend with load, reflecting the growth of the tripping contribution at higher generation levels. The ERCOT Regulation Up also increases with load as the minute-to-minute variability of the imbalance signal grows.

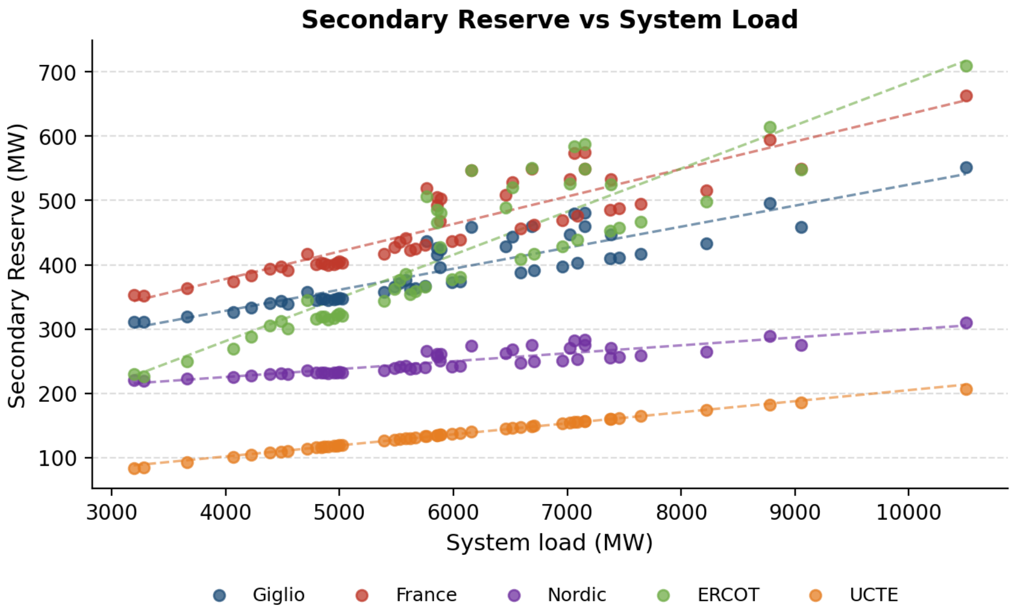


Figure 5.4: Secondary reserve as a function of system load.
Dashed lines indicate linear trend fits. For ERCOT, the value shown is Regulation Up.

### 5.2.3. Secondary + Tertiary Reserve

Figure 5.5 shows the secondary + tertiary reserve (aFRR + mFRR, plus RR where applicable) as a function of load. The results reflect the structural distinction identified in Section5.1.2: France, UCTE and ERCOT are fixed at 1013 MW and approximately 1410 MW, irrespective of load, while Giglio and Nordic show a modest positive trend.

The Giglio and Nordic FRR increase substantially with load, driven by both the aFRR and mFRR components growing with the online generation mix. The effect is considerable, with FRR increasing by roughly 466 MW for Giglio and 452 MW for Nordic across the full load range. The France and UCTE FRR flatness is structural: since their mFRR equals $DI$ − aFRR and $DI$ is fixed, any increase in aFRR with load (as in UCTE) is exactly offset by a decrease in mFRR, leaving the total unchanged.

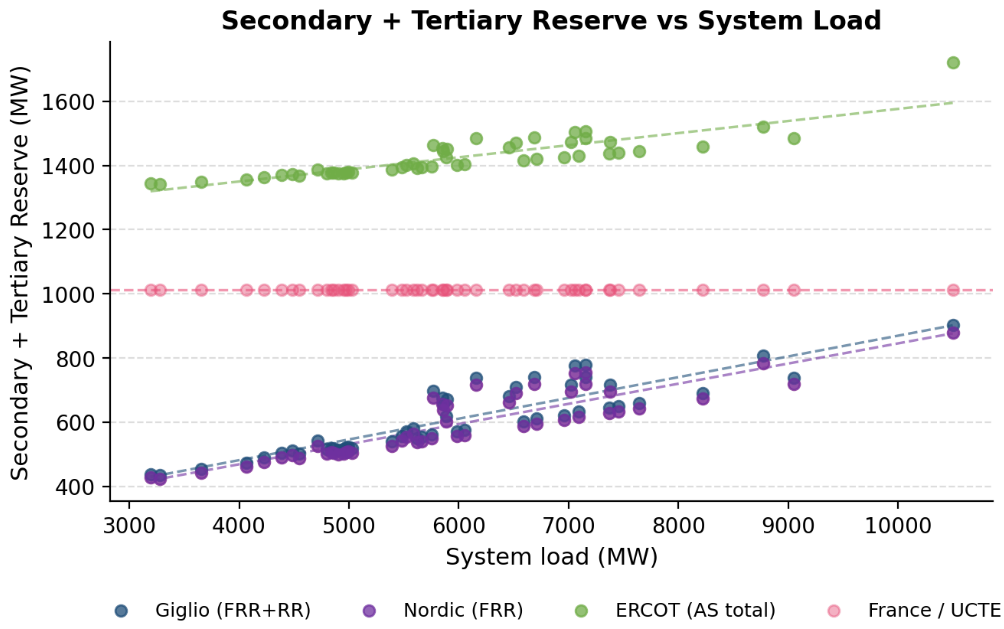


Figure 5.5: Seconary + Tertiary Reserve as a function of system load.
aFRR + mFRR + RR where applicable. For ERCOT, the total shown is Reg Up + RRS + ECRS + Non-Spin.

## 5.3. Dependence on Renewable Penetration

The 51 operating scenarios span a renewable share ranging from approximately 2% to 36% of system load, reflecting the seasonal and diurnal variability of the reference year generation mix. Examining how reserve requirements vary with renewable penetration allows assessing which methods are sensitive to the structural shift towards variable generation that characterises the energy transition.

### 5.3.1. Primary Reserve

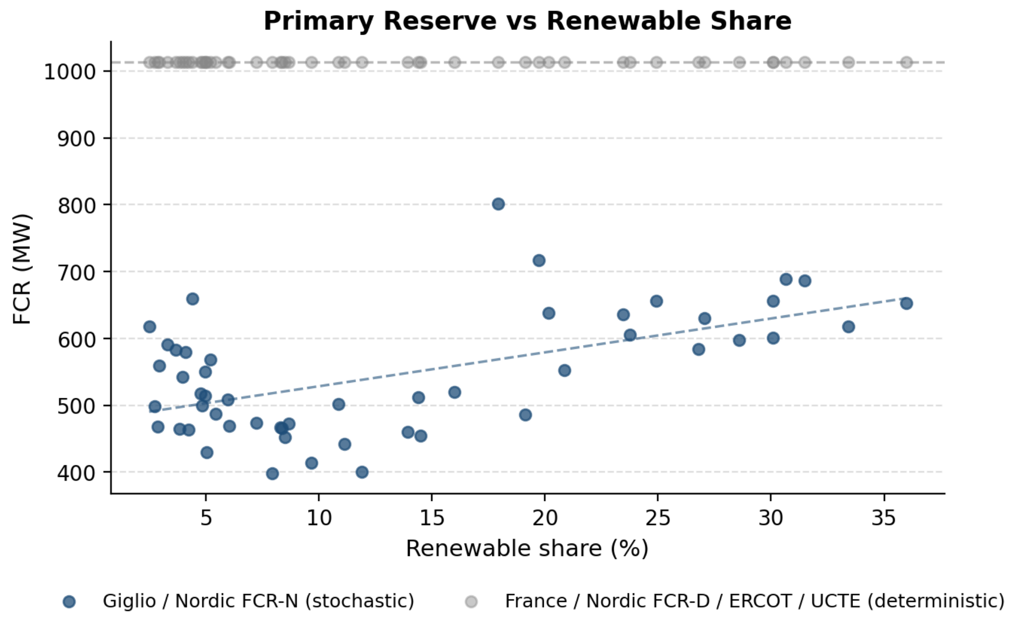


Figure 5.6: Primary reserve as a function of renewable share.
Dashed lines indicate linear trend fits.

As with load, the deterministic methods are insensitive to renewable penetration by construction. The Giglio FCR, shown in Figure 5.6, displays a weak negative trend with renewable share. In the reference system, high renewable penetration scenarios tend to coincide with lower online thermal and nuclear capacity. Since the tripping contribution to the Monte Carlo imbalance distribution scales with the nominal power of online units, a smaller conventional fleet produces a lower aggregate trip risk, pulling the 99th percentile of the imbalance distribution downward even as the forecast uncertainty from renewables increases. The net effect is a slight reduction in Giglio FCR as renewable share rises, suggesting that in this system the conventional generation portfolio is the dominant driver of primary reserve requirements.

### 5.3.2. Secondary Reserve

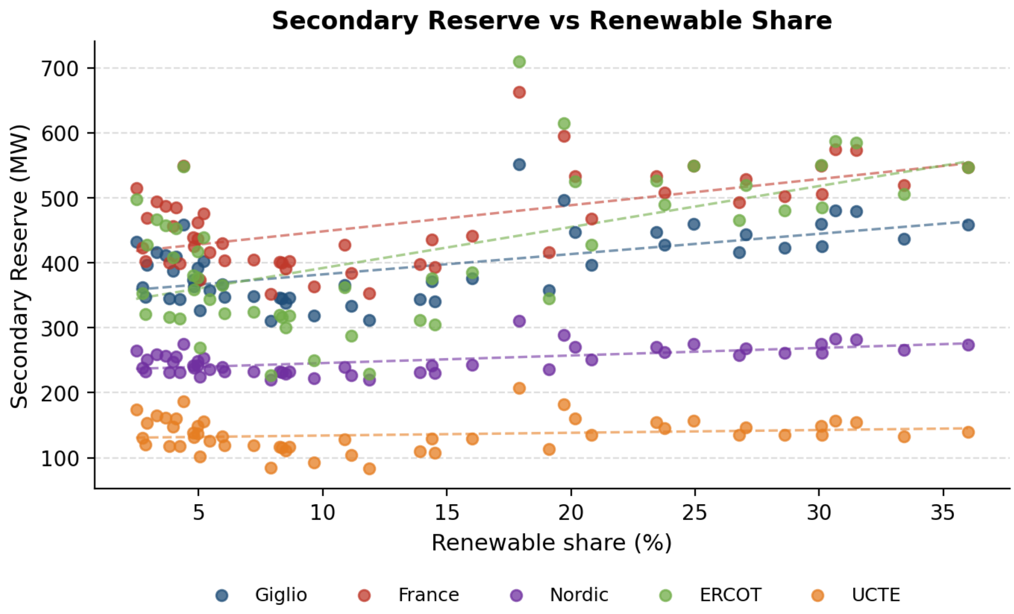


Figure 5.7: Secondary reserve as a function of renewable share.
For ERCOT, the value shown is Regulation Up.

Figure 5.7 shows a more differentiated picture. The France and Nordic aFRR both show a positive trend with renewable share, consistent with the expectation that higher renewable penetration increases the fast variability component of the imbalance signal that these methods target. The effect is modest in absolute terms (approximately 10 MW across the full renewable range for both methods).

The Giglio aFRR shows a strong positive trend with renewable share, driven by the same mechanism as with load: higher renewable penetration scenarios in the reference system tend to coincide with higher online conventional capacity, increasing the tripping contribution to the imbalance distribution. The variation in Giglio aFRR across the 51 scenarios is approximately 240 MW. The UCTE aFRR shows a negative trend, driven by the same mechanism as in Section 5.2.2: high renewable scenarios coincide with lower load, and the UCTE formula decreases with load. The ERCOT Regulation Up shows no meaningful trend, as the minute-to-minute variability it targets is not strongly correlated with the hourly renewable share metric used here.

### 5.3.3. Secondary + Tertiary Reserve

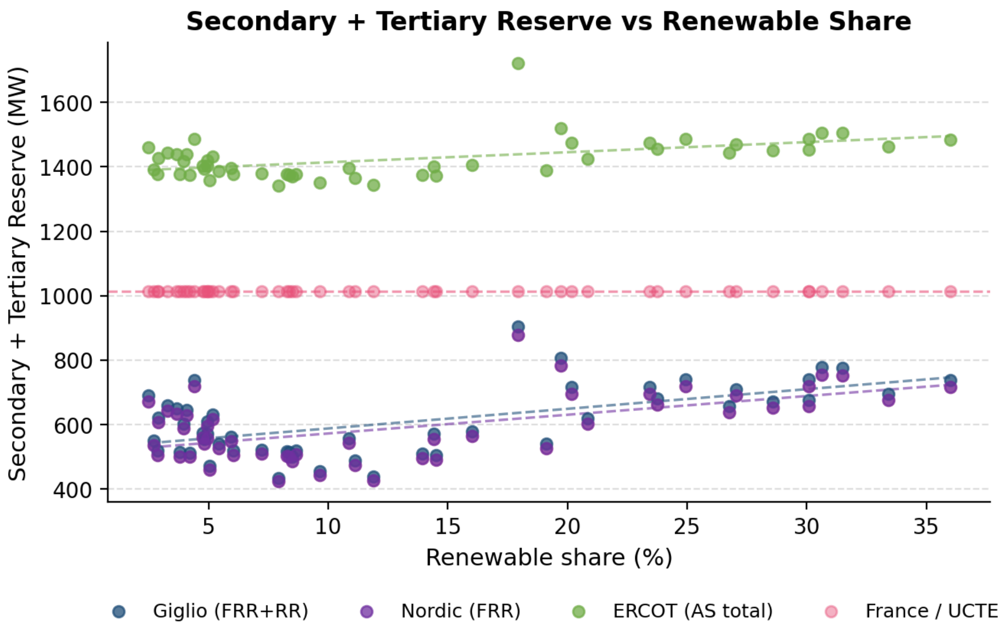


Figure 5.8: Secondary + Tertiary reserve (aFRR + mFRR + RR where applicable) as a function of renewable share.
For ERCOT, the total shown is Reg Up + RRS + ECRS + Non-Spin.

The Secondary plus Tertiary Reserve results in Figure 5.8 show that France, UCTE and ERCOT remain flat with renewable penetration, for the same structural reasons discussed in Section 5.2.3. Giglio and Nordic show a positive trend driven by the growth of both the aFRR and mFRR components with the online generation mix. The effect is moderate for Nordic, while for Giglio the variation across the renewable range is approximately 330 MW, reflecting the additional sensitivity of the aFRR component to the tripping contribution.

## 5.4. Combined Dependence on Load and Renewable Penetration

The analyses in Sections 5.2 and 5.3 examined the dependence of reserve requirements on system load and renewable penetration separately. In practice, the two variables are correlated: high-load scenarios tend to coincide with lower renewable shares, while high-renewable scenarios often occur at lower load levels. Examining both dimensions simultaneously provides a more complete picture of how each method responds to the operating conditions of the reference system.

Figures 5.9, 5.10 and 5.11 show the primary, secondary and tertiary reserve requirements as a function of system load, with the colour of each point encoding the renewable share of the corresponding scenario. Even within the same load level, points of different colour show visible spread in the reserve estimates, confirming that both load and renewable penetration contribute independently to the variability of reserve requirements across scenarios.

## 5.4.1. Primary Reserve

The colour pattern in Figure 5.9 reveals that the Giglio FCR is driven primarily by load: points of the same colour spread widely along the load axis, while points at the same load level show visible colour variation, indicating a secondary effect of renewable share. This confirms that the dominant source of variability in the Giglio FCR is the online thermal and nuclear fleet, which scales with load, while the forecast uncertainty introduced by renewables provides an additional contribution. The deterministic methods are fixed at $DI = 1013$ MW and show no response to either variable.

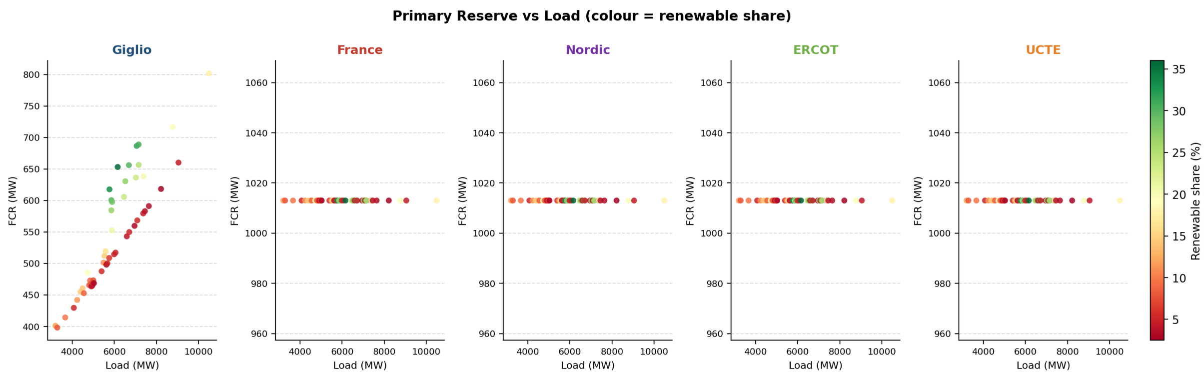


Figure 5.9: Primary reserve as a function of system load across the 51 operating scenarios. Point colour encodes the renewable share. Giglio and Nordic FCR-N vary with the generation mix; the remaining methods are fixed at $DI = 1013$ MW.

## 5.4.2. Secondary Reserve

Figure 5.10 shows a more differentiated picture for the secondary reserve. The Giglio and France panels show a clear positive gradient with load, and the colour pattern indicates that high-renewable scenarios (green points) tend to sit above the trend for a given load level, suggesting a secondary positive effect of renewable penetration on aFRR requirements. The Nordic panel shows a weaker but similar pattern. The UCTE panel shows the expected strong positive trend with load, with limited colour variation at any load level, reflecting the purely deterministic nature of the UCTE formula. The ERCOT Regulation Up panel is the most dispersed, reflecting the sensitivity of the minute-to-minute variability signal to both load and generation mix.

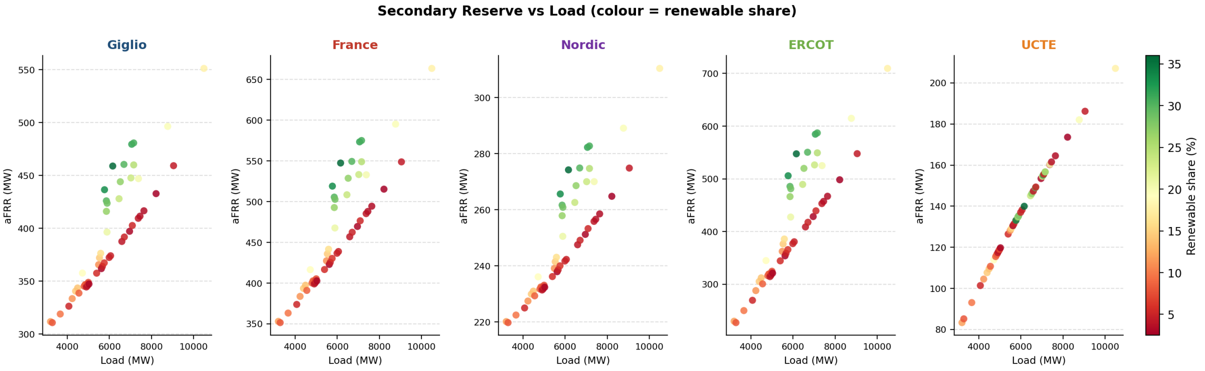


Figure 5.10: Secondary reserve as a function of system load across the 51 operating scenarios. Point colour encodes the renewable share. For ERCOT, the value shown is Regulation Up.

### 5.4.3. Tertiary Reserve

The tertiary reserve results in Figure 5.11 reflect the structural characteristics discussed in Section 5.1.4. For France and UCTE, the mFRR is determined by the residual $DI - \text{aFRR}$, so any increase in aFRR with load or renewable share is offset by a corresponding decrease in mFRR, leaving both panels flat in terms of colour gradient. For Giglio and Nordic, the mFRR grows with load and shows a secondary positive dependence on renewable share, consistent with the behaviour of the aFRR component.

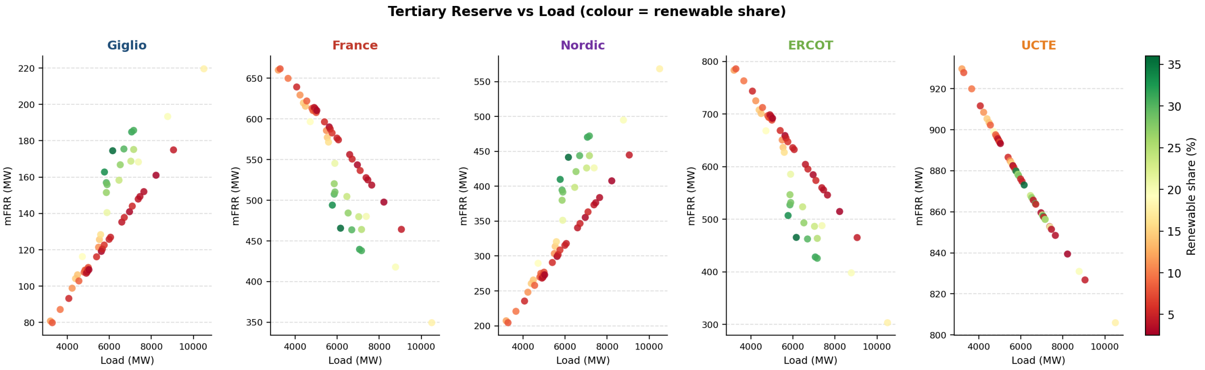


Figure 5.11: Tertiary reserve as a function of system load across the 51 operating scenarios. Point colour encodes the renewable share. For ERCOT, the value shown is RRS.

Taken together, the results of this chapter indicate that load level and renewable share both contribute to the variability of reserve requirements across scenarios, with load being the dominant driver for all probabilistic methods and renewable penetration providing a secondary positive effect on the secondary and tertiary reserves. The deterministic methods are by design insensitive to both variables. This finding has implications for procurement practice: methods anchored to the dimensioning incident will tend to over-procure reserve in low-load, low-uncertainty scenarios and may under-procure relative to the stochastic risk in high-load, high-renewable conditions.

# 6 | Conclusions and Future Developments

## 6.1. Main Findings

The comparative application of eight reserve sizing methodologies to a common system dataset produces a clear result: the choice of method matters. The spread between the lowest and highest estimates is not marginal. For primary reserve, the gap between the probabilistic total imbalance estimate and the deterministic threshold spans a factor of two under average operating conditions, reflecting the fact that the Monte Carlo simulation rarely generates imbalances approaching the full dimensioning incident in most scenarios. For secondary plus tertiary reserve, the range runs from approximately 424 MW to over 1700 MW depending on the method. These are not rounding differences or artefacts of parametrisation: they reflect genuine disagreement between methodological philosophies about what reserves are for and what risks they are meant to cover.

The most fundamental divide is between methods that anchor the reserve requirement to the dimensioning incident and those that derive it from the full distribution of system imbalances. While the direction of travel in both academic research and TSO practice is clearly towards probabilistic frameworks, this analysis shows that the transition is not uniform: several probabilistic methods retain the dimensioning incident as a binding floor, ensuring that the reserve is always sufficient to cover the loss of the largest unit online regardless of what the statistical distribution indicates, while others derive the requirement purely from the aggregate imbalance distribution without any contingency anchor. The practical consequence is that two methods can share the same probabilistic infrastructure and the same confidence level yet produce requirements that differ by a factor of two or more, depending solely on whether the dimensioning incident is treated as a constraint or as one input among many. This analysis demonstrates that the choice is consequential, and that treating probabilistic methodologies as interchangeable leads to reserve volumes that differ in ways that have direct implications for system security and procurement cost.

It should be noted that the magnitude of this divide depends on the relative size of the dimensioning incident with respect to the system. In the reference system, the dimensioning incident is large relative to total load due to the presence of large nuclear units, which amplifies the gap between contingency-anchored and purely statistical methods. In systems with a smaller dimensioning incident relative to system size, this divide would be less pronounced.

The decomposition of the Monte Carlo imbalance signal into its three constituent contributions (tripping, forecast error and variation of residual demand) reveals that the forecast error component is the dominant source of imbalance in the reference system across all 51 operating scenarios. The tripping contribution, however, grows strongly with system load as more large units are online, and it is this growth that drives the positive relationship between load level and the probabilistic FCR. At peak load, the tripping contribution approaches the magnitude of the forecast error component, explaining why the probabilistic FCR converges towards the deterministic threshold under the most demanding operating conditions.

The relationship between operating conditions and reserve requirements is substantial for the probabilistic methods. Load level is the dominant driver for the Giglio and Nordic frameworks, with FCR and mFRR growing strongly with the number of large units online. Renewable penetration provides a secondary positive effect on the secondary and tertiary reserves, reflecting the additional forecast uncertainty introduced by variable generation.

For the primary reserve, the purely contingency-based methods (France, Nordic FCR-D and ERCOT) are by design insensitive to both variables, as their FCR requirement is anchored to the dimensioning incident. For the secondary and tertiary reserves, however, this is no longer the case: France aFRR and mFRR vary substantially across scenarios as a function of the imbalance signal, and ERCOT Regulation Up and RRS show considerable scenario variability driven by the minute-to-minute dynamics of the imbalance distribution. The UCTE formula, while technically load-dependent through the term $\sqrt{aL_{\max} + b^2} - b$, was conceived to be applied to the annual peak load of a control area, producing a single static aFRR requirement for the whole year. In this implementation it is applied to each scenario individually, introducing a load dependence that is not present in the original operational usage. When considered in its intended application, UCTE is therefore equally insensitive to operating conditions for the secondary reserve as well.

This partial insensitivity has a direct implication for procurement practice: methods that anchor the primary reserve to the dimensioning incident will tend to over-procure FCR in low-load, low-uncertainty scenarios and may under-procure relative to the stochastic risk in high-load, high-renewable conditions. This result should not be interpreted as a general finding: it is likely specific to a system where the dimensioning incident dominates the reserve requirement, and the relationship between operating conditions and reserve requirements is an area where the choice of methodology is likely to matter more as systems continue to decarbonise.

## 6.2. Future Developments

The controlled comparative framework developed in this thesis establishes a basis from which several research directions can be pursued, both to address limitations of the present work and to extend the analysis towards broader questions that it has not been possible to treat here.

The most immediate extensions concern limitations that are specific to this study. Several parametric choices in this work are acknowledged approximations: the 50/50 split between spontaneous load variations and load forecast error in the Zima implementation, the percentile levels used to define each reserve product, and the forecast error standard deviations calibrated on the reference year dataset. A systematic sensitivity analysis quantifying the dependence of the results on these inputs would substantially strengthen the conclusions and identify which parameters the comparison is most sensitive to.

A related issue concerns the treatment of the variation of residual demand. In the framework developed in this thesis, VRD is treated as a fixed scalar parameter, derived from the 99.7th percentile of observed quarter-hourly residual demand changes and applied uniformly across all operating scenarios. In reality, the amplitude of intra-interval residual demand variations is likely to depend on the instantaneous renewable share, the forecast horizon, and the mix of technologies online. Developing a scenario-dependent formulation of VRD, in which the parameter varies across operating scenarios rather than remaining fixed at a single historical percentile, would improve the accuracy of the reserve estimates particularly at high renewable penetration. Given the central role that VRD plays in the Monte Carlo imbalance model, this extension could have a substantial effect on the results.

Beyond these specific limitations, the comparative framework opens three broader research directions. The first concerns the generalisability of the results. The findings of this thesis reflect the specific characteristics of the reference system, in which a large nuclear fleet produces a dimensioning incident that dominates the reserve requirement. The patterns observed, in particular the strong sensitivity of the probabilistic methods to load level and the partial insensitivity of the deterministic methods, may be specific to this system configuration. Applying the same framework to systems with different generation mixes, different dimensioning incidents relative to system size, or different levels of renewable penetration would allow separating findings that are genuinely methodological from those that are system-specific.

The second broader direction concerns long-term planning. The Giglio framework was originally designed to be embedded in a capacity expansion model, with reserve requirements treated as endogenous planning constraints rather than post-hoc corrections. The comparative analysis in this thesis has treated all eight methodologies as standalone sizing tools, without coupling them to an investment optimisation. Extending the comparison to the planning context, where the reserve requirement feeds back into technology selection and the optimal generation mix in turn affects the reserve requirement, would address the problem for which several of the methods reviewed here were specifically designed.

The third broader direction concerns the transition from static to dynamic reserve sizing. The most advanced TSOs reviewed in Chapter 2, including Elia and the German consortium, already dimension reserves on a day-ahead or intra-day basis, recomputing requirements for each scheduling interval using the forecast information available at that moment. All eight methodologies compared in this thesis produce static requirements, fixed for each operating scenario. Extending the framework to a dynamic setting, in which the reserve requirement varies with the forecast state of the system rather than with a small set of representative scenarios, would bring the academic comparison closer to the operational reality of the most advanced European TSOs and provide a more direct basis for regulatory recommendations.

Finally, a further simplification in this work is the treatment of the reference system as electrically isolated. In reality, reserve sharing mechanisms, such as the imbalance netting and cross-border activation platforms already in operation across Continental Europe, substantially reduce the domestic reserve volumes that individual TSOs need to hold. Introducing reserve sharing into the comparative framework is not a minor extension: it changes the fundamental structure of the sizing problem, shifting the unit of analysis from a single system to a network of interconnected areas whose imbalances can be partially offset against each other. How different sizing methodologies interact with sharing mechanisms, and whether the rankings observed in this thesis are preserved or reversed when sharing is accounted for, is a question that this work leaves open and that deserves dedicated investigation.

# Bibliography

[1] UCTE. Operation handbook — policy 1: Load-frequency control and performance, version 3.0. Technical report, Union for the Co-ordination of Transmission of Electricity, March 2009.

[2] Hannele Holttinen, Michael Milligan, Erik Ela, Nickie Menemenlis, Jan Dobschinski, Barry Rawn, Ricardo J. Bessa, Damian Flynn, Emilio Gomez-Lazaro, and Nina K. Detlefsen. Methodologies to determine operating reserves due to increased wind power. *IEEE Transactions on Sustainable Energy*, 3(4):713–723, 2012. doi: 10.1109/TSTE.2012.2208207.

[3] Miguel A. Ortega-Vazquez and Daniel S. Kirschen. Estimating the spinning reserve requirements in systems with significant wind power generation penetration. *IEEE Transactions on Power Systems*, 24(1):114–124, 2009. doi: 10.1109/TPWRS.2008.2004745.

[4] European Commission. Commission regulation (EU) 2017/1485 of 2 august 2017 establishing a guideline on electricity transmission system operation. Technical Report L 220, Official Journal of the European Union, 2017. System Operation Guideline (SO GL).

[5] ACER. Decision 08/2024 on the implementation framework for the European platform for the exchange of balancing energy from frequency restoration reserves with automatic activation (aFRRIF). annex IIa, consolidated version. Technical report, Agency for the Cooperation of Energy Regulators, July 2024. Consolidated version 5 July 2024.

[6] ACER. Decision 12/2020 — methodology pursuant to article 40 of the EB regulation on the sharing of reserves. Technical report, Agency for the Cooperation of Energy Regulators, July 2020.

[7] ENTSO-E. SAFA annex 1 — policy on load-frequency control and reserves. Continental Europe synchronous area framework agreement. Technical report, ENTSO-E, 2019. In force 14 April 2019, as subsequently amended.

[8] European Commission. Commission regulation (EU) 2017/2195 of 23 november 2017 establishing a guideline on electricity balancing. Technical Report L 312, Official Journal of the European Union, 2017. Electricity Balancing Guideline (EB GL).

[9] ENTSO-E. Synchronous area framework agreement (SAFA) for continental europe: FCR dimensioning methodology. Technical report, ENTSO-E, 2025. Approved by all National Regulatory Authorities, 15 January 2025.

[10] Elia Transmission Belgium. Report on balancing in accordance with article 60(1) of commission regulation (EU) 2017/2195 — 2022–2023. Technical report, Elia Transmission Belgium SA/NV, 2024.

[11] CREG. Decision (B)2025: Approval of Elia's FRR dimensioning methodology. Technical report, Commission de Régulation de l'Électricité et du Gaz, December 2019.

[12] TransnetBW, TenneT TSO GmbH, Amprion, 50Hertz Transmission, Energinet, and CREOS. Explanatory note on reserve capacity — biennial balancing report 2022–2023. Technical report, German TSOs / Energinet / CREOS, January 2025. Published in accordance with Article 60(1) of Commission Regulation (EU) 2017/2195.

[13] TenneT TSO B.V. Balancing report 2022. Technical report, TenneT TSO B.V., 2023. URL `https://www.tennet.eu`.

[14] Terna S.p.A. Report balancing Terna 2022–2023 (report ID: 8dd1eb707541092). Technical report, Terna S.p.A., 2023. URL `https://www.terna.it`.

[15] RTE. Report on balancing 2022–2023. Technical report, Réseau de Transport d'Électricité, 2024.

[16] ENTSO-E. SAFA article B-6-2-2-1-5 — recommended methodology for minimum aFRR sizing. Technical report, ENTSO-E, 2025.

[17] ENTSO-E. SAFA article B-2 — methodology description for FCR dimensioning. Technical report, ENTSO-E, 2025.

[18] Elia Transmission Belgium. LFC block operational agreement — belgium. Technical report, Elia Transmission Belgium SA/NV, 2024. Approved by CREG Decision (B)2025, December 2019; revised by CREG Decisions (B)2435 (July 2022) and (B)2748 (February 2024).

[19] CREG. Decision (B)2435: Amendment to Elia's FRR dimensioning methodology. Technical report, Commission de Régulation de l'Électricité et du Gaz, 2022.

[20] CREG. Decision (B)2748: Revision of Elia's FRR dimensioning methodology. Technical report, Commission de Régulation de l'Électricité et du Gaz, February 2024.

[21] Elia Transmission Belgium. Study on aFRR dimensioning methodology — assessment of replacement methodologies and proof of concept. Technical report, Elia Transmission Belgium SA/NV, September 2020.

[22] Bundesnetzagentur. Decision BK6-15-158 on dynamic dimensioning of aFRR and mFRR. Technical report, Bundesnetzagentur (BNetzA), December 2019.

[23] Bundesnetzagentur. Decision BK6-15-159 on dynamic dimensioning of aFRR and mFRR. Technical report, Bundesnetzagentur (BNetzA), December 2019.

[24] TenneT TSO B.V. Description of FRR dimensioning, version 1.0. Technical report, TenneT TSO B.V., September 2025.

[25] ARERA. Resolution 115/2023/r/eel — amendments to the italian network code on aFRR asymmetric offers and PICASSO platform participation. Technical report, Autorità di Regolazione per Energia Reti e Ambiente, July 2023. 4 July 2023.

[26] ARERA. Resolution 345/2023/r/EEL — approval of the testo integrato del dispacciamento elettrico (TIDE). Technical report, Autorità di Regolazione per Energia Reti e Ambiente, July 2023.

[27] ARERA. Resolution 202/2020/r/eel: Regulation of balancing services. Technical report, Autorità di Regolazione per Energia Reti e Ambiente, 2020.

[28] Terna S.p.A. Allegato A.22 — definizione del fabbisogno di riserva secondaria e terziaria, revision 12. Technical report, Terna S.p.A., August 2025.

[29] RTE. LFC block operational agreement (LFCBOA) for the France LFC block. Technical report, Réseau de Transport d'Électricité, 2026. Version in force 1 April 2026.

[30] RTE. Bilan Électrique 2023. Technical report, Réseau de Transport d'Électricité, 2024. URL `https://www.rte-france.com/analyses-tendances-et-prospectives/bilan-electrique-2023`.

[31] EirGrid and SONI Ltd. LFC block operational agreement for ireland and northern Ireland, version 2.1. Technical report, EirGrid / SONI, December 2024.

[32] EirGrid and SONI. Synchronous area operational agreement (SAOA) for synchronous area IE/NI. Technical report, EirGrid and System Operator for Northern Ireland, September 2022. URL `https://www.eirgridgroup.com/site-files/library/EirGrid/`

S1-SAOA-for-the-Ireland-and-Northern-Ireland-Synchronous-area-29.09.2022-(post-Title-2-approval).pdf. Schedule 1, Version 1.1 (post Title 2 approval).

[33] EirGrid and SONI. Operational constraints update. Technical report, EirGrid and System Operator for Northern Ireland, January 2021. URL https://www.readkong.com/page/operational-constraints-update-27-01-2021-eirgrid-2811568.

[34] EirGrid and SONI. Weekly operational constraints update, week 33 2024. Technical report, EirGrid and System Operator for Northern Ireland, August 2024. URL https://www.sem-o.com/sites/semo/files/documents/general-publications/Wk33_2024_Weekly_Operational_Constraints_Update.pdf.

[35] EirGrid and SONI. LFC block operational agreement (LFCBOA) for Ireland and Northern Ireland. Technical report, EirGrid and System Operator for Northern Ireland, September 2022. URL https://cms.eirgrid.ie/sites/default/files/publications/S2-LFC-Block-Operational-Agreement-for-Ireland-and-Northern-Ireland-29.09.2022.pdf. Schedule 2, Version 1.1 (post Title 2 approval).

[36] EirGrid and SONI Ltd. Future arrangements for system services (FASS) — phased implementation roadmap, version 1.0. Technical report, EirGrid / SONI, March 2024.

[37] EirGrid and SONI Ltd. Future arrangements for system services (FASS) — phased implementation roadmap, version 2.0. Technical report, EirGrid / SONI, September 2024.

[38] Statnett, Svenska kraftnät, Fingrid, and Energinet. Nordic system operation agreement (SOA) — annex electricity balancing (EB), version 3. Technical report, Nordic TSOs, December 2024. URL https://www.entsoe.eu/Documents/SOC%20documents/Nordic/2025/Annex_EB_v3.pdf. Approved 11 December 2024, in force 4 March 2025 (update for mFRR EAM). SOA main agreement in force since 14 August 2019.

[39] Statnett SF. Balancing report 2026. Technical report, Statnett SF, 2026. URL https://www.statnett.no.

[40] ENTSO-E. ENTSO-E statistical factsheet 2022. Technical report, European Network of Transmission System Operators for Electricity, 2023. URL https://www.entsoe.eu/data/statistics/.

[41] ENTSO-E. ENTSO-E statistical factsheet 2023. Technical report, European Network of Transmission System Operators for Electricity, 2024. URL https://www.entsoe.eu/data/statistics/.

[42] ENTSO-E. ENTSO-E statistical factsheet 2024. Technical report, European Network of Transmission System Operators for Electricity, 2025. URL https://www.entsoe.eu/data/statistics/.

[43] Statnett, Svenska kraftnät, Fingrid, and Energinet. Nordic FCR dimensioning methodology. Technical report, Nordic TSOs, February 2023.

[44] Statnett, Svenska kraftnät, Fingrid, and Energinet. Common nordic LFC block methodology for FRR dimensioning in accordance with article 157(1) of the SO GL. Technical report, Nordic TSOs, April 2023. Approved by Nordic National Regulatory Authorities, April 2023.

[45] AEMO. Power system security guidelines. document ref: SO_OP_3715, version 105. Technical report, Australian Energy Market Operator, 2024. Effective 3 June 2024.

[46] AEMO. FCAS model in NEMDE, version 3.0. Technical report, Australian Energy Market Operator, 2024. URL https://www.aemo.com.au.

[47] AEMO. Quarterly energy dynamics, 2023–2024. Technical report, Australian Energy Market Operator, 2024. URL https://www.aemo.com.au/energy-systems/electricity/national-electricity-market-nem/data-nem/quarterly-energy-dynamics-qed.

[48] AEMO. Frequency monitoring — quarter 4 2023. Technical report, Australian Energy Market Operator, February 2024.

[49] AEMO. Frequency monitoring — quarter 1 2024. Technical report, Australian Energy Market Operator, May 2024.

[50] AEMO. Quarterly frequency monitoring reports, 2023–2025. Technical report, Australian Energy Market Operator, 2025. URL https://www.aemo.com.au.

[51] Australian Energy Regulator. State of the energy market 2025. Technical report, Australian Energy Regulator, 2025. URL https://www.aer.gov.au.

[52] AEMO. Market ancillary service specification (MASS), version 8.2. Technical report, Australian Energy Market Operator, 2024. URL https://www.aemo.com.au.

[53] AEMO. Guide to ancillary services in the national electricity market, version 3.0.

Technical report, Australian Energy Market Operator, 2024. URL https://www.aemo.com.au.

[54] AEMO. Reserve level declaration guidelines, version 3.0. Technical report, Australian Energy Market Operator, June 2024. Effective 26 June 2024.

[55] AEMO. Procedure for the exercise of the reliability and emergency reserve trader. document ref: SO_OP_3717, version 6.2. Technical report, Australian Energy Market Operator, 2024. Effective 3 June 2024.

[56] AEMO. Updated amended panel RERT guidelines. Technical report, Australian Energy Market Operator, August 2020. Final, 18 August 2020.

[57] AEMC. Final determination — review of the frequency operating standard. Technical report, Australian Energy Market Commission, April 2023. 6 April 2023.

[58] AEMO. 2025 electricity statement of opportunities. Technical report, Australian Energy Market Operator, 2025. URL https://www.aemo.com.au.

[59] AEMO. WEM procedure: Essential System Services quantities, version 2.0. Technical report, Australian Energy Market Operator, 2024. URL https://www.aemo.com.au/energy-systems/electricity/wholesale-electricity-market-wem.

[60] NERC. BAL-001-2: Real power balancing control performance. Technical report, North American Electric Reliability Corporation, 2015. URL https://www.nerc.com/pa/Stand/Pages/ReliabilityStandards.aspx.

[61] NERC. BAL-002-3: Disturbance control standard — contingency reserve for recovery from a balancing contingency event. Technical report, North American Electric Reliability Corporation, 2018. URL https://www.nerc.com/pa/Stand/Pages/ReliabilityStandards.aspx.

[62] NERC. BAL-003-2: Frequency response and frequency bias setting. Technical report, North American Electric Reliability Corporation, 2020. URL https://www.nerc.com/pa/Stand/Pages/ReliabilityStandards.aspx.

[63] NERC. Operating reserve management. reliability guideline, version 3. Technical report, North American Electric Reliability Corporation, June 2021. URL https://www.nerc.com/comm/OC/Documents/Operating_Reserve_Management_Reliability_Guideline.pdf.

[64] NERC. Frequency response annual analysis (FRAA) 2025. operating year 2020–

2024. Technical report, North American Electric Reliability Corporation, 2025. URL https://www.nerc.com/comm/OC/Pages/Frequency-Response.aspx.

[65] FERC. Order no. 842: Essential reliability services and the evolving bulk-power system — primary frequency response. Technical report, Federal Energy Regulatory Commission, February 2018. Docket No. RM16-6-000.

[66] NERC. Primary frequency control. reliability guideline, version 4.0. Technical report, North American Electric Reliability Corporation, September 2023. URL https://www.nerc.com/comm/PC/Documents/Primary_Frequency_Control_Guideline.pdf.

[67] ERCOT. Ancillary services study white paper. Technical report, Electric Reliability Council of Texas, October 2024. URL https://ercot.com/mktrules/issues/ancillary. Justifies ancillary service quantities for calendar year 2025.

[68] ERCOT. Market information system (MIS) — ancillary service requirement methodology. report ID 13036. Technical report, Electric Reliability Council of Texas, 2024. URL https://mis.ercot.com. Hourly and monthly AS requirement quantities for Regulation Up/Down, RRS, ECRS, and Non-Spinning Reserve. Accessed December 2025 for calendar years 2023–2024.

[69] ERCOT. ERCOT sets new all-time record peak demand. Press release, August 2023. Reports all-time record demand of 85,508 MW on 20 August 2023.

[70] ERCOT. ERCOT records preliminary peak demand of 85,559 MW. Press release / Utility Dive report, August 2024. Preliminary figure for 20 August 2024, pending final market settlement.

[71] LCG Consulting and ERCOT. 2025 ERCOT electricity market outlook. Technical report, LCG Consulting, 2025. Source for wind and solar generation shares 2022–2023.

[72] U.S. Energy Information Administration. Electric power monthly / electricity data browser. annual generation data for the ERCOT region, 2024. Technical report, U.S. Energy Information Administration, 2024. URL https://eia.gov/electricity/data/browser.

[73] ERCOT. Methodologies for determining minimum ancillary service requirements — 2024. Technical report, Electric Reliability Council of Texas, December 2023. URL https://mis.ercot.com. Approved by ERCOT Board of Directors, 19 December 2023. Sets uniform RRS minimum of 2,300 MW.

[74] ERCOT. Methodologies for determining minimum ancillary service requirements — 2023. Technical report, Electric Reliability Council of Texas, December 2022. Approved by ERCOT Board of Directors, December 2022. Defines minimum quantities for RRS, Non-Spin, Regulation Up/Down, and FFR cap for calendar year 2023.

[75] ERCOT. Nodal protocol revision request 863 (NPRR863): Addition of fast frequency response (FFR) and contingency reserve service (ECRS). Technical report, Electric Reliability Council of Texas, 2023. URL https://ercot.com/mktrules/nprr. Implemented 10 June 2023. Establishes the ECRS product and formalises FFR within RRS.

[76] WECC and NERC. Contingency reserve — Western Interconnection. reliability standard BAL-002-WECC-3. Technical report, Western Electricity Coordinating Council / North American Electric Reliability Corporation, 2021. URL https://www.nerc.com/pa/Stand/Pages/BAL.aspx. Approved by FERC 2021.

[77] California ISO. Contingency reserve cost allocation – FERC order 789, 2014. URL https://www.caiso.com/documents/fercorder789contingencyreservecostallocation.pdf. Accessed 2025.

[78] ENTSO-E. ENTSO-E balancing report 2024. Technical report, European Network of Transmission System Operators for Electricity, June 2024. URL https://www.entsoe.eu.

[79] Jethro Dowell, Graeme Hawker, Keith Bell, and Simon Gill. A review of probabilistic methods for defining reserve requirements. *IEEE Power and Energy Society General Meeting*, 2016. University of Strathclyde, Glasgow.

[80] Erik Ela, Michael Milligan, and Brendan Kirby. Operating reserves and variable generation: A comprehensive review of current strategies, studies, and fundamental research on the impact that increased penetration of variable renewable generation has on power system operating reserves. Technical Report NREL/TP-5500-51978, National Renewable Energy Laboratory, August 2011.

[81] Enrico Giglio, Davide Fioriti, Munyaradzi Justice Chihota, Davide Poli, Bernard Bekker, and Giuliana Mattiazzo. Integrated stochastic reserve estimation and MILP energy planning for high renewable penetration: Application to 2050 South African energy system. *Sustainable Energy, Grids and Networks*, 42:101650, 2025. doi: 10.1016/j.segan.2025.101650.

[82] Marek Zima, Stephan Koch, and Göran Andersson. Dimensioning of control reserves:

Approach based on probabilistic methods. *ETH Zurich, EEH – Power Systems Laboratory*, November 2008.

[83] Dominik Jost, Axel Braun, Rafael Fritz, and Scott Otterson. Dynamic sizing of automatic and manual frequency restoration reserves for different product lengths. 2015.

[84] Abolfazl Khodadadi, Henrik Nordström, Robert Eriksson, and Lennart Söder. Investigating reserve dimensioning approaches for multi-area reserve capacity markets: A nordic case study. *IEEE Transactions on Power Systems*, 2023. KTH Royal Institute of Technology.

[85] Filippo Bovera, Giuliano Rancilio, Davide Falabretti, and Marco Merlo. Data-driven evaluation of secondary- and tertiary-reserve needs with high renewables penetration: The Italian case. *Energies*, 14(8):2157, 2021. doi: 10.3390/en14082157.

[86] N-SIDE. Study on outages on generation units and DC-links. Technical report, N-SIDE, 2022. Prepared for Elia; used in Elia Adequacy & Flexibility Study 2023–2034.

[87] E. Leahy and R.S.J. Tol. An estimate of the value of lost load for Ireland. *Energy Policy*, 39(3):1514–1520, 2011. doi: 10.1016/j.enpol.2010.12.025. Forced outage rate data used for hydro: FOR = 2%, MTTR = 120 h.

[88] J. Carroll, A. McDonald, and D. McMillan. Failure rate, repair time and unscheduled o&m cost analysis of offshore wind turbines. *Wind Energy*, 19(6):1107–1119, 2016. doi: 10.1002/we.1887. Forced outage rate data used for offshore wind: FOR = 5%, MTTR = 200 h.

# A | Operating Scenarios

Table A.1: Operating scenarios S01–S26: unit commitment and renewable conditions.

| ID | Units online ($n$) | | | | | | | | | | | | | CF (%) | | | [MW] | (%) | (h) |
|---|---|---|---|---|---|---|---|---|---|---|---|---|---|---|---|---|---|---|---|
| | **CCGT** | **OCGT** | **CHP1** | **CHP2** | **CHP3** | **NU1** | **NU2** | **HYD** | **PSP1** | **PSP2** | **BESS** | **TJ** | **WST** | **Off** | **On** | **Sol** | **Load** | **RES** | $w_t$ |
| S01 | 1 | 0 | 2 | 13 | 6 | 3 | 0 | 6 | 0 | 0 | 1 | 0 | 5 | 15.4 | 8.3 | 5.8 | 3193 | 11.9 | 75 |
| S02 | 0 | 0 | 2 | 13 | 6 | 3 | 0 | 6 | 0 | 0 | 1 | 0 | 5 | 8.9 | 5.3 | 42.5 | 3280 | 7.9 | 132 |
| S03 | 0 | 0 | 2 | 13 | 6 | 3 | 0 | 6 | 0 | 0 | 1 | 0 | 5 | 11.6 | 5.4 | 75.4 | 3658 | 9.7 | 144 |
| S04 | 1 | 0 | 2 | 13 | 6 | 3 | 0 | 6 | 0 | 0 | 1 | 0 | 5 | 8.2 | 5.6 | 2.3 | 4068 | 5.0 | 538 |
| S05 | 0 | 0 | 2 | 13 | 6 | 3 | 0 | 6 | 0 | 0 | 1 | 0 | 5 | 18.3 | 9.3 | 28.8 | 4227 | 11.1 | 281 |
| S06 | 0 | 0 | 2 | 13 | 6 | 3 | 0 | 6 | 0 | 0 | 1 | 0 | 5 | 24.4 | 10.7 | 52.4 | 4388 | 14.5 | 174 |
| S07 | 0 | 0 | 2 | 13 | 6 | 3 | 0 | 6 | 0 | 0 | 1 | 0 | 5 | 25.7 | 13.5 | 2.0 | 4485 | 13.9 | 242 |
| S08 | 1 | 0 | 2 | 13 | 6 | 3 | 0 | 6 | 1 | 0 | 1 | 0 | 5 | 14.5 | 5.1 | 43.2 | 4548 | 8.5 | 78 |
| S09 | 0 | 0 | 2 | 13 | 6 | 3 | 0 | 6 | 0 | 0 | 1 | 0 | 5 | 37.0 | 20.1 | 2.4 | 4713 | 19.1 | 307 |
| S10 | 2 | 0 | 2 | 13 | 6 | 3 | 0 | 6 | 1 | 0 | 1 | 0 | 5 | 16.6 | 7.6 | 2.9 | 4797 | 8.4 | 88 |
| S11 | 6 | 0 | 2 | 13 | 6 | 3 | 0 | 6 | 0 | 0 | 1 | 0 | 5 | 17.3 | 6.5 | 8.5 | 4842 | 8.7 | 73 |
| S12 | 1 | 0 | 2 | 13 | 6 | 3 | 0 | 6 | 0 | 2 | 1 | 0 | 5 | 16.4 | 8.7 | 5.1 | 4864 | 8.3 | 122 |
| S13 | 0 | 0 | 2 | 13 | 6 | 3 | 2 | 6 | 0 | 0 | 1 | 0 | 5 | 6.5 | 3.4 | 50.2 | 4901 | 4.2 | 286 |
| S14 | 0 | 0 | 2 | 13 | 6 | 3 | 1 | 6 | 0 | 0 | 1 | 0 | 5 | 6.6 | 4.3 | 26.4 | 4949 | 3.8 | 307 |
| S15 | 1 | 0 | 2 | 13 | 6 | 3 | 0 | 6 | 2 | 2 | 1 | 0 | 5 | 12.2 | 7.0 | 3.2 | 4976 | 6.0 | 171 |
| S16 | 3 | 0 | 2 | 13 | 6 | 3 | 0 | 6 | 1 | 0 | 1 | 0 | 5 | 14.2 | 8.3 | 13.8 | 4996 | 7.2 | 118 |
| S17 | 0 | 0 | 2 | 13 | 6 | 3 | 2 | 6 | 0 | 0 | 1 | 0 | 5 | 5.7 | 4.3 | 1.8 | 5026 | 2.9 | 669 |
| S18 | 1 | 0 | 2 | 13 | 6 | 3 | 2 | 6 | 1 | 0 | 1 | 0 | 5 | 12.0 | 6.1 | 3.4 | 5391 | 5.4 | 229 |
| S19 | 2 | 0 | 2 | 13 | 6 | 3 | 0 | 6 | 0 | 3 | 1 | 0 | 5 | 24.6 | 11.2 | 5.8 | 5485 | 10.9 | 93 |
| S20 | 0 | 0 | 2 | 13 | 6 | 3 | 2 | 6 | 0 | 0 | 1 | 0 | 5 | 32.6 | 18.4 | 2.4 | 5526 | 14.4 | 265 |
| S21 | 0 | 0 | 2 | 13 | 6 | 3 | 2 | 6 | 0 | 0 | 1 | 0 | 5 | 36.2 | 12.3 | 38.0 | 5584 | 16.0 | 133 |
| S22 | 5 | 0 | 2 | 13 | 6 | 3 | 0 | 6 | 0 | 0 | 1 | 0 | 5 | 6.1 | 4.1 | 2.6 | 5618 | 2.7 | 229 |
| S23 | 2 | 0 | 2 | 13 | 6 | 3 | 2 | 6 | 2 | 0 | 1 | 0 | 5 | 11.0 | 5.2 | 8.4 | 5665 | 4.8 | 168 |
| S24 | 6 | 0 | 2 | 13 | 6 | 3 | 0 | 6 | 0 | 3 | 1 | 0 | 5 | 14.1 | 6.7 | 3.3 | 5754 | 6.0 | 53 |
| S25 | 0 | 0 | 2 | 13 | 6 | 3 | 0 | 6 | 0 | 0 | 1 | 0 | 5 | 80.8 | 31.6 | 2.5 | 5766 | 33.4 | 313 |
| S26 | 0 | 0 | 2 | 13 | 6 | 3 | 0 | 6 | 0 | 0 | 1 | 0 | 5 | 72.8 | 26.8 | 34.2 | 5854 | 30.1 | 136 |

Table A.2: Operating scenarios S27–S51: unit commitment and renewable conditions.

| ID | Units online ($n$) | | | | | | | | | | | | | CF (%) | | | [MW] | (%) | (h) |
|---|---|---|---|---|---|---|---|---|---|---|---|---|---|---|---|---|---|---|---|
| | **CCGT** | **OCGT** | **CHP1** | **CHP2** | **CHP3** | **NU1** | **NU2** | **HYD** | **PSP1** | **PSP2** | **BESS** | **TJ** | **WST** | **Off** | **On** | **Sol** | **Load** | **RES** | $w_t$ |
| S27 | 0 | 0 | 2 | 13 | 6 | 3 | 0 | 6 | 1 | 2 | 1 | 0 | 5 | 65.8 | 25.3 | 3.0 | 5856 | 26.8 | 133 |
| S28 | 0 | 0 | 2 | 13 | 6 | 3 | 1 | 6 | 1 | 0 | 1 | 0 | 5 | 49.5 | 32.7 | 7.0 | 5885 | 20.8 | 86 |
| S29 | 1 | 0 | 2 | 13 | 6 | 3 | 0 | 6 | 2 | 0 | 1 | 0 | 5 | 70.7 | 27.1 | 3.5 | 5891 | 28.6 | 94 |
| S30 | 2 | 0 | 2 | 13 | 6 | 3 | 2 | 6 | 2 | 2 | 1 | 0 | 5 | 12.2 | 5.8 | 3.3 | 5987 | 5.0 | 248 |
| S31 | 2 | 0 | 2 | 13 | 6 | 3 | 2 | 6 | 2 | 2 | 1 | 0 | 5 | 11.8 | 5.1 | 6.6 | 6056 | 4.8 | 142 |
| S32 | 0 | 0 | 2 | 13 | 6 | 3 | 0 | 6 | 0 | 0 | 1 | 0 | 5 | 89.5 | 61.6 | 3.5 | 6157 | 36.0 | 121 |
| S33 | 1 | 0 | 2 | 13 | 6 | 3 | 2 | 6 | 0 | 0 | 1 | 0 | 5 | 64.7 | 21.2 | 6.9 | 6458 | 23.8 | 147 |
| S34 | 0 | 0 | 2 | 13 | 6 | 3 | 2 | 6 | 0 | 0 | 1 | 0 | 5 | 75.3 | 18.2 | 5.4 | 6518 | 27.1 | 223 |
| S35 | 6 | 0 | 2 | 13 | 6 | 3 | 1 | 6 | 0 | 0 | 1 | 0 | 5 | 9.6 | 3.8 | 33.6 | 6591 | 4.0 | 83 |
| S36 | 0 | 0 | 2 | 13 | 6 | 3 | 1 | 6 | 0 | 0 | 1 | 0 | 5 | 83.6 | 38.9 | 4.2 | 6691 | 30.1 | 219 |
| S37 | 5 | 0 | 2 | 13 | 6 | 3 | 2 | 6 | 0 | 0 | 1 | 0 | 5 | 13.8 | 6.0 | 2.3 | 6710 | 5.0 | 274 |
| S38 | 8 | 0 | 2 | 13 | 6 | 3 | 0 | 6 | 1 | 0 | 1 | 0 | 5 | 8.2 | 4.1 | 5.0 | 6959 | 2.9 | 183 |
| S39 | 1 | 0 | 2 | 13 | 6 | 3 | 1 | 6 | 0 | 3 | 1 | 0 | 5 | 69.5 | 23.7 | 2.8 | 7023 | 23.4 | 67 |
| S40 | 0 | 0 | 2 | 13 | 6 | 3 | 2 | 6 | 1 | 0 | 1 | 0 | 5 | 90.3 | 58.8 | 2.3 | 7061 | 31.5 | 229 |
| S41 | 8 | 0 | 2 | 13 | 6 | 3 | 0 | 6 | 1 | 0 | 1 | 0 | 5 | 15.2 | 7.0 | 2.9 | 7090 | 5.2 | 144 |
| S42 | 1 | 0 | 2 | 13 | 6 | 3 | 1 | 6 | 2 | 2 | 1 | 0 | 5 | 89.9 | 51.8 | 1.3 | 7155 | 30.6 | 87 |
| S43 | 1 | 0 | 2 | 13 | 6 | 3 | 2 | 6 | 2 | 2 | 1 | 0 | 5 | 76.2 | 19.5 | 1.8 | 7156 | 24.9 | 111 |
| S44 | 7 | 0 | 2 | 13 | 6 | 3 | 1 | 6 | 1 | 0 | 1 | 0 | 5 | 12.2 | 7.3 | 3.8 | 7373 | 4.1 | 93 |
| S45 | 5 | 0 | 2 | 13 | 6 | 3 | 0 | 6 | 1 | 0 | 1 | 0 | 5 | 62.0 | 26.7 | 4.7 | 7381 | 20.2 | 94 |
| S46 | 8 | 0 | 2 | 13 | 6 | 3 | 0 | 6 | 2 | 2 | 1 | 0 | 5 | 11.3 | 4.9 | 2.4 | 7456 | 3.7 | 130 |
| S47 | 8 | 0 | 2 | 13 | 6 | 3 | 0 | 6 | 1 | 2 | 1 | 0 | 5 | 10.2 | 6.2 | 2.4 | 7642 | 3.3 | 78 |
| S48 | 10 | 0 | 2 | 13 | 6 | 3 | 2 | 6 | 1 | 0 | 1 | 0 | 5 | 8.4 | 3.3 | 4.2 | 8221 | 2.5 | 202 |
| S49 | 7 | 0 | 2 | 13 | 6 | 3 | 1 | 6 | 0 | 1 | 1 | 0 | 5 | 72.9 | 25.8 | 3.9 | 8776 | 19.7 | 74 |
| S50 | 10 | 0 | 2 | 13 | 6 | 3 | 2 | 6 | 2 | 2 | 1 | 0 | 5 | 16.7 | 6.2 | 1.2 | 9054 | 4.4 | 74 |
| S51 | 10 | 0 | 2 | 13 | 6 | 3 | 2 | 6 | 0 | 3 | 1 | 0 | 5 | 78.8 | 32.8 | 0.0 | 10500 | 17.9 | 6 |

# B | Reserve Sizing Results

Table B.1: Reserve sizing results (Giglio, France, Nordic), scenarios S01–S26 (MW).

| ID | Load (MW) | Giglio | | | | France | | | Nordic | | | |
|---|---|---|---|---|---|---|---|---|---|---|---|---|
| | | FCR | aFRR | mFRR | RR | FCR | aFRR | mFRR | FCR-D | FCR-N | aFRR | mFRR |
| S01 | 3193 | 401.0 | 311.7 | 80.8 | 45.2 | 1013.0 | 353.0 | 74.2 | 1013.0 | 401.0 | 220.1 | 207.1 |
| S02 | 3280 | 398.1 | 310.7 | 79.9 | 44.5 | 1013.0 | 351.5 | 72.7 | 1013.0 | 398.1 | 219.7 | 204.4 |
| S03 | 3658 | 414.2 | 318.9 | 87.1 | 49.1 | 1013.0 | 363.2 | 79.9 | 1013.0 | 414.2 | 222.4 | 220.7 |
| S04 | 4068 | 429.5 | 326.3 | 93.2 | 53.1 | 1013.0 | 373.8 | 86.6 | 1013.0 | 429.5 | 225.0 | 235.4 |
| S05 | 4227 | 442.1 | 333.5 | 98.9 | 56.6 | 1013.0 | 383.7 | 91.9 | 1013.0 | 442.1 | 227.4 | 248.1 |
| S06 | 4388 | 455.0 | 340.5 | 104.1 | 60.0 | 1013.0 | 393.4 | 97.0 | 1013.0 | 455.0 | 229.9 | 260.5 |
| S07 | 4485 | 460.4 | 343.5 | 106.2 | 61.3 | 1013.0 | 397.4 | 99.1 | 1013.0 | 460.4 | 231.0 | 265.6 |
| S08 | 4548 | 452.8 | 338.7 | 102.9 | 59.1 | 1013.0 | 391.0 | 96.2 | 1013.0 | 452.8 | 229.3 | 257.9 |
| S09 | 4713 | 485.6 | 357.6 | 116.2 | 67.4 | 1013.0 | 416.5 | 109.1 | 1013.0 | 485.6 | 236.1 | 289.5 |
| S10 | 4797 | 465.6 | 345.2 | 107.7 | 62.1 | 1013.0 | 400.1 | 101.4 | 1013.0 | 465.6 | 231.7 | 269.8 |
| S11 | 4842 | 472.9 | 346.7 | 108.9 | 63.2 | 1013.0 | 402.8 | 104.8 | 1013.0 | 472.9 | 232.5 | 275.1 |
| S12 | 4864 | 467.1 | 346.6 | 108.6 | 62.6 | 1013.0 | 401.9 | 102.0 | 1013.0 | 467.1 | 232.2 | 271.7 |
| S13 | 4901 | 463.6 | 344.5 | 107.1 | 61.8 | 1013.0 | 399.0 | 100.7 | 1013.0 | 463.6 | 231.4 | 268.3 |
| S14 | 4949 | 464.7 | 345.5 | 107.9 | 62.3 | 1013.0 | 400.3 | 101.1 | 1013.0 | 464.7 | 231.7 | 269.7 |
| S15 | 4976 | 468.9 | 347.6 | 109.3 | 63.1 | 1013.0 | 403.2 | 102.6 | 1013.0 | 468.9 | 232.5 | 273.3 |
| S16 | 4996 | 473.2 | 348.9 | 110.3 | 63.9 | 1013.0 | 405.2 | 104.6 | 1013.0 | 473.2 | 233.1 | 276.8 |
| S17 | 5026 | 468.6 | 347.2 | 109.0 | 63.0 | 1013.0 | 402.7 | 102.6 | 1013.0 | 468.6 | 232.4 | 273.0 |
| S18 | 5391 | 487.6 | 357.5 | 116.1 | 67.5 | 1013.0 | 416.7 | 110.2 | 1013.0 | 487.6 | 236.2 | 290.6 |
| S19 | 5485 | 501.4 | 365.5 | 121.4 | 70.8 | 1013.0 | 427.3 | 115.2 | 1013.0 | 501.4 | 239.1 | 303.5 |
| S20 | 5526 | 512.1 | 372.1 | 125.6 | 73.6 | 1013.0 | 435.9 | 119.3 | 1013.0 | 512.1 | 241.5 | 313.7 |
| S21 | 5584 | 519.4 | 376.3 | 128.3 | 75.2 | 1013.0 | 441.5 | 122.0 | 1013.0 | 519.4 | 243.1 | 320.5 |
| S22 | 5618 | 498.1 | 361.8 | 119.1 | 69.5 | 1013.0 | 422.9 | 114.4 | 1013.0 | 498.1 | 237.9 | 299.4 |
| S23 | 5665 | 500.1 | 364.0 | 120.4 | 70.2 | 1013.0 | 425.5 | 115.0 | 1013.0 | 500.1 | 238.6 | 301.8 |
| S24 | 5754 | 508.7 | 367.3 | 122.6 | 71.8 | 1013.0 | 430.3 | 118.3 | 1013.0 | 508.7 | 240.0 | 308.6 |
| S25 | 5766 | 617.7 | 436.5 | 162.8 | 97.1 | 1013.0 | 519.0 | 156.4 | 1013.0 | 617.7 | 265.6 | 409.7 |
| S26 | 5854 | 600.6 | 426.0 | 156.9 | 93.7 | 1013.0 | 505.6 | 150.6 | 1013.0 | 600.6 | 261.7 | 394.5 |

Table B.2: Reserve sizing results (Giglio, France, Nordic), scenarios S27–S51 (MW).

| ID | Load (MW) | Giglio | | | | France | | | Nordic | | | |
|---|---|---|---|---|---|---|---|---|---|---|---|---|
| | | FCR | aFRR | mFRR | RR | FCR | aFRR | mFRR | FCR-D | FCR-N | aFRR | mFRR |
| S27 | 5856 | 584.4 | 416.0 | 151.5 | 90.1 | 1013.0 | 492.7 | 145.0 | 1013.0 | 584.4 | 257.9 | 379.9 |
| S28 | 5885 | 552.7 | 396.4 | 140.5 | 83.0 | 1013.0 | 467.7 | 134.0 | 1013.0 | 552.7 | 250.5 | 351.2 |
| S29 | 5891 | 597.7 | 423.7 | 155.9 | 92.7 | 1013.0 | 502.8 | 149.6 | 1013.0 | 597.7 | 260.9 | 391.6 |
| S30 | 5987 | 514.5 | 372.4 | 125.8 | 73.6 | 1013.0 | 436.6 | 120.3 | 1013.0 | 514.5 | 241.7 | 315.2 |
| S31 | 6056 | 517.3 | 374.0 | 126.9 | 74.3 | 1013.0 | 438.8 | 121.4 | 1013.0 | 517.3 | 242.3 | 317.9 |
| S32 | 6157 | 653.3 | 458.9 | 174.5 | 104.7 | 1013.0 | 547.4 | 168.3 | 1013.0 | 653.3 | 274.2 | 441.5 |
| S33 | 6458 | 605.7 | 428.0 | 158.3 | 94.2 | 1013.0 | 508.4 | 152.5 | 1013.0 | 605.7 | 262.6 | 398.3 |
| S34 | 6518 | 630.5 | 444.0 | 166.8 | 99.5 | 1013.0 | 528.7 | 160.8 | 1013.0 | 630.5 | 268.6 | 420.9 |
| S35 | 6591 | 543.0 | 387.5 | 135.2 | 79.9 | 1013.0 | 456.9 | 131.0 | 1013.0 | 543.0 | 247.5 | 340.4 |
| S36 | 6691 | 656.2 | 460.4 | 175.5 | 105.1 | 1013.0 | 549.4 | 169.3 | 1013.0 | 656.2 | 274.9 | 443.8 |
| S37 | 6710 | 549.9 | 391.7 | 137.8 | 81.4 | 1013.0 | 462.4 | 133.3 | 1013.0 | 549.9 | 249.1 | 346.6 |
| S38 | 6959 | 559.8 | 397.1 | 140.9 | 83.4 | 1013.0 | 469.5 | 137.0 | 1013.0 | 559.8 | 251.2 | 355.3 |
| S39 | 7023 | 636.5 | 447.6 | 168.8 | 100.9 | 1013.0 | 533.2 | 162.9 | 1013.0 | 636.5 | 270.0 | 426.1 |
| S40 | 7061 | 686.7 | 479.5 | 184.8 | 111.5 | 1013.0 | 573.4 | 179.1 | 1013.0 | 686.7 | 282.3 | 470.2 |
| S41 | 7090 | 568.5 | 402.6 | 144.0 | 85.4 | 1013.0 | 476.5 | 140.0 | 1013.0 | 568.5 | 253.3 | 363.2 |
| S42 | 7155 | 689.0 | 480.7 | 185.7 | 111.7 | 1013.0 | 575.1 | 179.8 | 1013.0 | 689.0 | 282.8 | 472.0 |
| S43 | 7156 | 656.6 | 459.9 | 175.2 | 105.0 | 1013.0 | 549.0 | 169.5 | 1013.0 | 656.6 | 274.7 | 443.8 |
| S44 | 7373 | 579.5 | 409.4 | 147.9 | 87.7 | 1013.0 | 485.3 | 143.9 | 1013.0 | 579.5 | 255.9 | 373.3 |
| S45 | 7381 | 638.5 | 446.9 | 168.3 | 101.0 | 1013.0 | 532.9 | 163.3 | 1013.0 | 638.5 | 270.0 | 426.2 |
| S46 | 7456 | 583.1 | 411.5 | 149.3 | 88.4 | 1013.0 | 488.0 | 145.0 | 1013.0 | 583.1 | 256.6 | 376.4 |
| S47 | 7642 | 591.2 | 416.6 | 152.0 | 90.5 | 1013.0 | 494.4 | 147.9 | 1013.0 | 591.2 | 258.5 | 383.8 |
| S48 | 8221 | 618.4 | 432.8 | 161.0 | 96.2 | 1013.0 | 515.3 | 157.2 | 1013.0 | 618.4 | 264.8 | 407.7 |
| S49 | 8776 | 716.9 | 496.4 | 193.3 | 116.8 | 1013.0 | 595.2 | 188.8 | 1013.0 | 716.9 | 289.1 | 494.8 |
| S50 | 9054 | 660.2 | 459.2 | 175.0 | 104.7 | 1013.0 | 548.8 | 170.8 | 1013.0 | 660.2 | 274.9 | 444.7 |
| S51 | 10500 | 801.8 | 551.2 | 219.6 | 133.1 | 1013.0 | 663.6 | 215.1 | 1013.0 | 801.8 | 310.4 | 568.3 |

Table B.3: Reserve sizing results (ERCOT, UCTE, N-sigma), scenarios S01–S26 (MW).

| ID | Load (MW) | ERCOT | | | | | | UCTE | | | N-sigma | | |
|---|---|---|---|---|---|---|---|---|---|---|---|---|---|
| | | PFR | Reg Up | Reg Dn | RRS | ECRS | Non-Spin | FCR | aFRR | mFRR | aFRR | mFRR | RR |
| S01 | 3193 | 1013.0 | 229.6 | 501.3 | 783.4 | 330.4 | 0.0 | 1013.0 | 83.3 | 929.7 | 361.8 | 149.8 | 258.2 |
| S02 | 3280 | 1013.0 | 226.9 | 502.5 | 786.1 | 329.4 | 0.0 | 1013.0 | 85.2 | 927.8 | 359.8 | 149.0 | 256.8 |
| S03 | 3658 | 1013.0 | 249.8 | 492.9 | 763.2 | 337.2 | 0.0 | 1013.0 | 93.1 | 919.9 | 360.5 | 149.3 | 257.3 |
| S04 | 4068 | 1013.0 | 269.3 | 485.4 | 743.7 | 344.3 | 0.0 | 1013.0 | 101.4 | 911.6 | 359.7 | 148.9 | 256.7 |
| S05 | 4227 | 1013.0 | 287.7 | 479.3 | 725.3 | 351.4 | 0.0 | 1013.0 | 104.5 | 908.5 | 363.0 | 150.3 | 259.1 |
| S06 | 4388 | 1013.0 | 305.0 | 475.4 | 708.0 | 358.2 | 0.0 | 1013.0 | 107.6 | 905.4 | 366.3 | 151.6 | 261.4 |
| S07 | 4485 | 1013.0 | 311.9 | 474.5 | 701.1 | 361.1 | 0.0 | 1013.0 | 109.5 | 903.5 | 367.1 | 152.0 | 262.0 |
| S08 | 4548 | 1013.0 | 300.5 | 476.3 | 712.5 | 356.4 | 0.0 | 1013.0 | 110.7 | 902.3 | 361.5 | 149.6 | 258.0 |
| S09 | 4713 | 1013.0 | 344.7 | 476.7 | 668.3 | 374.8 | 0.0 | 1013.0 | 113.9 | 899.1 | 375.7 | 155.5 | 268.1 |
| S10 | 4797 | 1013.0 | 316.0 | 474.4 | 697.0 | 362.8 | 0.0 | 1013.0 | 115.5 | 897.5 | 362.3 | 150.0 | 258.5 |
| S11 | 4842 | 1013.0 | 319.1 | 474.2 | 693.9 | 364.2 | 0.0 | 1013.0 | 116.3 | 896.7 | 362.6 | 150.1 | 258.8 |
| S12 | 4864 | 1013.0 | 319.4 | 474.2 | 693.6 | 364.2 | 0.0 | 1013.0 | 116.7 | 896.3 | 362.2 | 149.9 | 258.5 |
| S13 | 4901 | 1013.0 | 314.3 | 474.4 | 698.7 | 362.0 | 0.0 | 1013.0 | 117.4 | 895.6 | 359.4 | 148.8 | 256.5 |
| S14 | 4949 | 1013.0 | 316.9 | 474.2 | 696.1 | 363.1 | 0.0 | 1013.0 | 118.3 | 894.7 | 359.4 | 148.8 | 256.5 |
| S15 | 4976 | 1013.0 | 321.7 | 474.2 | 691.3 | 365.1 | 0.0 | 1013.0 | 118.8 | 894.2 | 360.7 | 149.3 | 257.4 |
| S16 | 4996 | 1013.0 | 324.4 | 474.4 | 688.6 | 366.3 | 0.0 | 1013.0 | 119.2 | 893.8 | 361.4 | 149.6 | 257.9 |
| S17 | 5026 | 1013.0 | 320.8 | 474.1 | 692.2 | 364.7 | 0.0 | 1013.0 | 119.7 | 893.3 | 359.2 | 148.7 | 256.4 |
| S18 | 5391 | 1013.0 | 344.2 | 476.7 | 668.8 | 374.7 | 0.0 | 1013.0 | 126.4 | 886.6 | 360.6 | 149.3 | 257.4 |
| S19 | 5485 | 1013.0 | 362.1 | 481.5 | 650.9 | 382.5 | 0.0 | 1013.0 | 128.1 | 884.9 | 366.4 | 151.7 | 261.5 |
| S20 | 5526 | 1013.0 | 376.3 | 487.0 | 636.7 | 388.8 | 0.0 | 1013.0 | 128.9 | 884.1 | 372.0 | 154.0 | 265.5 |
| S21 | 5584 | 1013.0 | 385.7 | 491.1 | 627.3 | 393.0 | 0.0 | 1013.0 | 129.9 | 883.1 | 375.0 | 155.2 | 267.6 |
| S22 | 5618 | 1013.0 | 353.7 | 479.0 | 659.3 | 378.9 | 0.0 | 1013.0 | 130.5 | 882.5 | 359.3 | 148.7 | 256.4 |
| S23 | 5665 | 1013.0 | 358.5 | 480.4 | 654.5 | 381.0 | 0.0 | 1013.0 | 131.3 | 881.7 | 360.3 | 149.2 | 257.2 |
| S24 | 5754 | 1013.0 | 365.6 | 482.9 | 647.4 | 384.2 | 0.0 | 1013.0 | 132.9 | 880.1 | 361.3 | 149.6 | 257.9 |
| S25 | 5766 | 1013.0 | 505.8 | 570.3 | 507.2 | 450.6 | 0.0 | 1013.0 | 133.1 | 879.9 | 433.5 | 179.4 | 309.4 |
| S26 | 5854 | 1013.0 | 485.6 | 555.0 | 527.4 | 440.5 | 0.0 | 1013.0 | 134.7 | 878.3 | 420.4 | 174.0 | 300.1 |

Table B.4: Reserve sizing results (ERCOT, UCTE, N-sigma), scenarios S27–S51 (MW).

| ID | Load (MW) | ERCOT | | | | | | UCTE | | | N-sigma | | |
|---|---|---|---|---|---|---|---|---|---|---|---|---|---|
| | | PFR | Reg Up | Reg Dn | RRS | ECRS | Non-Spin | FCR | aFRR | mFRR | aFRR | mFRR | RR |
| S27 | 5856 | 1013.0 | 466.2 | 540.7 | 546.8 | 431.0 | 0.0 | 1013.0 | 134.7 | 878.3 | 409.8 | 169.7 | 292.5 |
| S28 | 5885 | 1013.0 | 427.4 | 514.5 | 585.6 | 412.2 | 0.0 | 1013.0 | 135.2 | 877.8 | 388.6 | 160.9 | 277.3 |
| S29 | 5891 | 1013.0 | 481.1 | 551.6 | 531.9 | 438.4 | 0.0 | 1013.0 | 135.3 | 877.7 | 417.2 | 172.7 | 297.7 |
| S30 | 5987 | 1013.0 | 376.9 | 487.2 | 636.1 | 389.1 | 0.0 | 1013.0 | 137.0 | 876.0 | 360.7 | 149.3 | 257.4 |
| S31 | 6056 | 1013.0 | 380.4 | 488.9 | 632.6 | 390.7 | 0.0 | 1013.0 | 138.2 | 874.8 | 360.6 | 149.3 | 257.3 |
| S32 | 6157 | 1013.0 | 547.4 | 603.7 | 465.6 | 471.9 | 0.0 | 1013.0 | 139.9 | 873.1 | 449.0 | 185.9 | 320.4 |
| S33 | 6458 | 1013.0 | 489.3 | 557.7 | 523.7 | 442.5 | 0.0 | 1013.0 | 145.1 | 867.9 | 408.2 | 169.0 | 291.3 |
| S34 | 6518 | 1013.0 | 519.8 | 581.2 | 493.2 | 457.8 | 0.0 | 1013.0 | 146.1 | 866.9 | 424.3 | 175.7 | 302.8 |
| S35 | 6591 | 1013.0 | 408.6 | 503.2 | 604.4 | 403.7 | 0.0 | 1013.0 | 147.3 | 865.7 | 360.0 | 149.0 | 256.9 |
| S36 | 6691 | 1013.0 | 550.4 | 605.8 | 462.6 | 473.4 | 0.0 | 1013.0 | 149.0 | 864.0 | 438.3 | 181.5 | 312.8 |
| S37 | 6710 | 1013.0 | 417.5 | 508.4 | 595.5 | 407.9 | 0.0 | 1013.0 | 149.3 | 863.7 | 361.2 | 149.5 | 257.8 |
| S38 | 6959 | 1013.0 | 428.3 | 515.2 | 584.7 | 413.1 | 0.0 | 1013.0 | 153.5 | 859.5 | 359.7 | 148.9 | 256.7 |
| S39 | 7023 | 1013.0 | 526.4 | 586.5 | 486.6 | 461.2 | 0.0 | 1013.0 | 154.5 | 858.5 | 415.3 | 171.9 | 296.4 |
| S40 | 7061 | 1013.0 | 584.7 | 634.7 | 428.3 | 491.5 | 0.0 | 1013.0 | 155.1 | 857.9 | 450.4 | 186.4 | 321.4 |
| S41 | 7090 | 1013.0 | 439.2 | 522.1 | 573.8 | 418.2 | 0.0 | 1013.0 | 155.6 | 857.4 | 361.7 | 149.7 | 258.1 |
| S42 | 7155 | 1013.0 | 587.1 | 636.8 | 425.9 | 492.7 | 0.0 | 1013.0 | 156.7 | 856.3 | 449.6 | 186.1 | 320.8 |
| S43 | 7156 | 1013.0 | 549.3 | 605.1 | 463.7 | 473.0 | 0.0 | 1013.0 | 156.7 | 856.3 | 425.8 | 176.3 | 303.9 |
| S44 | 7373 | 1013.0 | 453.0 | 531.3 | 560.0 | 424.8 | 0.0 | 1013.0 | 160.2 | 852.8 | 360.7 | 149.3 | 257.4 |
| S45 | 7381 | 1013.0 | 525.0 | 585.5 | 488.0 | 460.6 | 0.0 | 1013.0 | 160.3 | 852.7 | 404.5 | 167.4 | 288.7 |
| S46 | 7456 | 1013.0 | 457.2 | 534.2 | 555.8 | 426.8 | 0.0 | 1013.0 | 161.5 | 851.5 | 360.4 | 149.2 | 257.2 |
| S47 | 7642 | 1013.0 | 466.9 | 541.2 | 546.1 | 431.5 | 0.0 | 1013.0 | 164.5 | 848.5 | 360.1 | 149.1 | 257.0 |
| S48 | 8221 | 1013.0 | 498.2 | 564.5 | 514.8 | 447.1 | 0.0 | 1013.0 | 173.6 | 839.4 | 359.7 | 148.9 | 256.7 |
| S49 | 8776 | 1013.0 | 614.8 | 660.5 | 398.2 | 507.7 | 0.0 | 1013.0 | 182.1 | 830.9 | 420.6 | 174.1 | 300.2 |
| S50 | 9054 | 1013.0 | 547.7 | 603.8 | 465.3 | 472.3 | 0.0 | 1013.0 | 186.2 | 826.8 | 362.3 | 150.0 | 258.6 |
| S51 | 10500 | 1013.0 | 709.6 | 745.1 | 303.4 | 560.0 | 147.5 | 1013.0 | 207.1 | 805.9 | 430.1 | 178.1 | 307.0 |

# List of Figures

# List of Tables